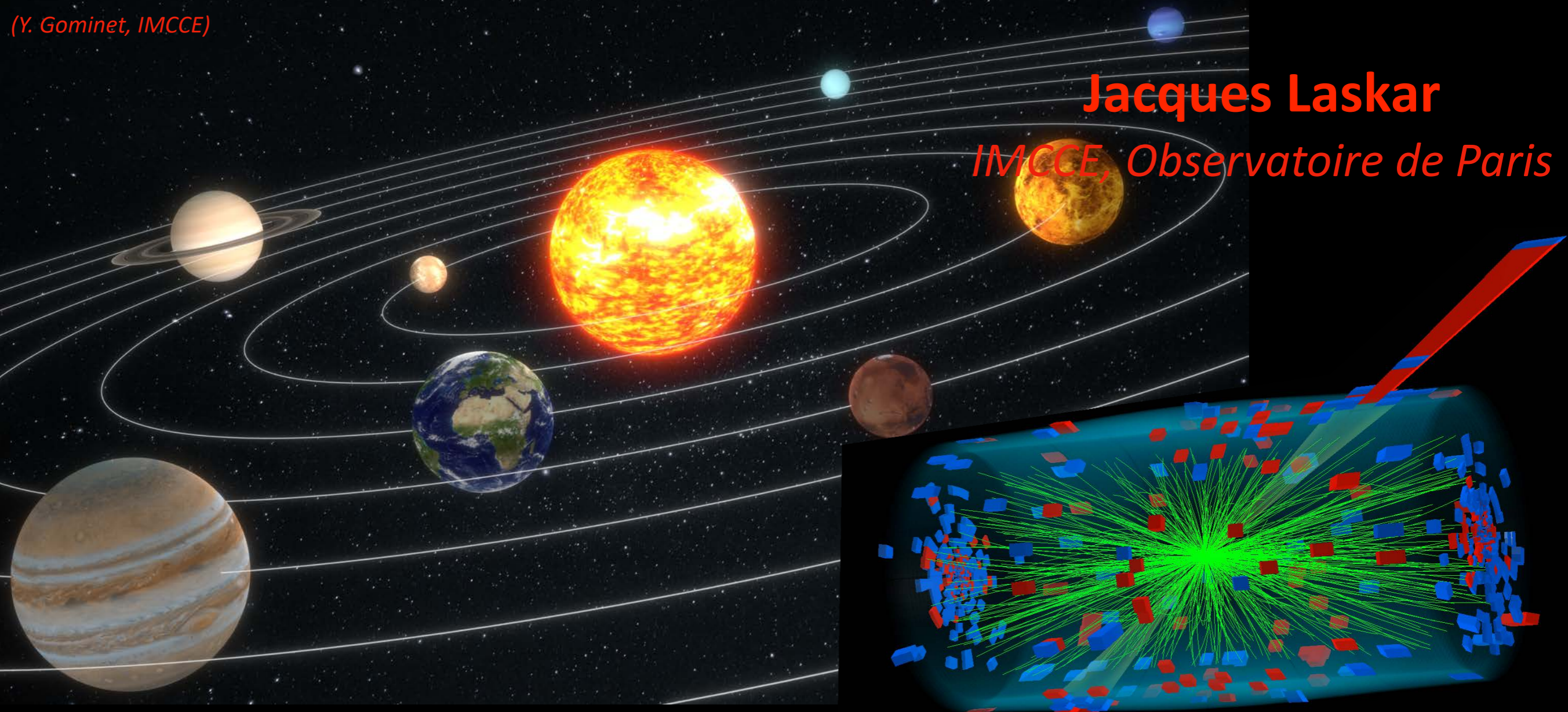


**Jacques Laskar**  
*IMCCE, Observatoire de Paris*

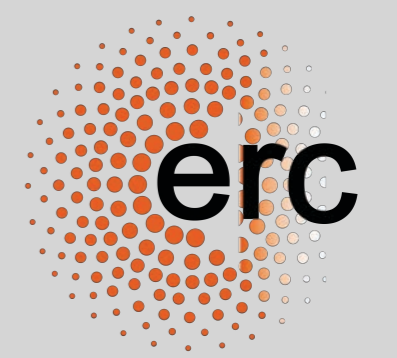


CMS-LHC

# From chaos in planetary motions to the HL-LHC design



*Rencontres du Vietnam, 2-12 August 2023*





# Is the Solar System Stable?

Jürgen Moser (*July 1928 - december 1999*)



*In 1954 Kolmogorov indicated that, for certain mechanical systems, in some sense the “majority” of solutions are quasi-periodic. He indicated a possible method of solution but the actual proof was first provided by Arnold 8 years later, and, in a special case, by the author. In accordance with the modern usage this theory became known by the acronym KAM.*

# Is the Solar System Stable?

Jürgen Moser (July 1928 - december 1999)



*The mathematical theorems of KAM deal not only with the planetary system but also with general Hamiltonian systems.... One of these applications is the stability problem of proton accelerators, which since the 1950's have been built in every greater number and size.*

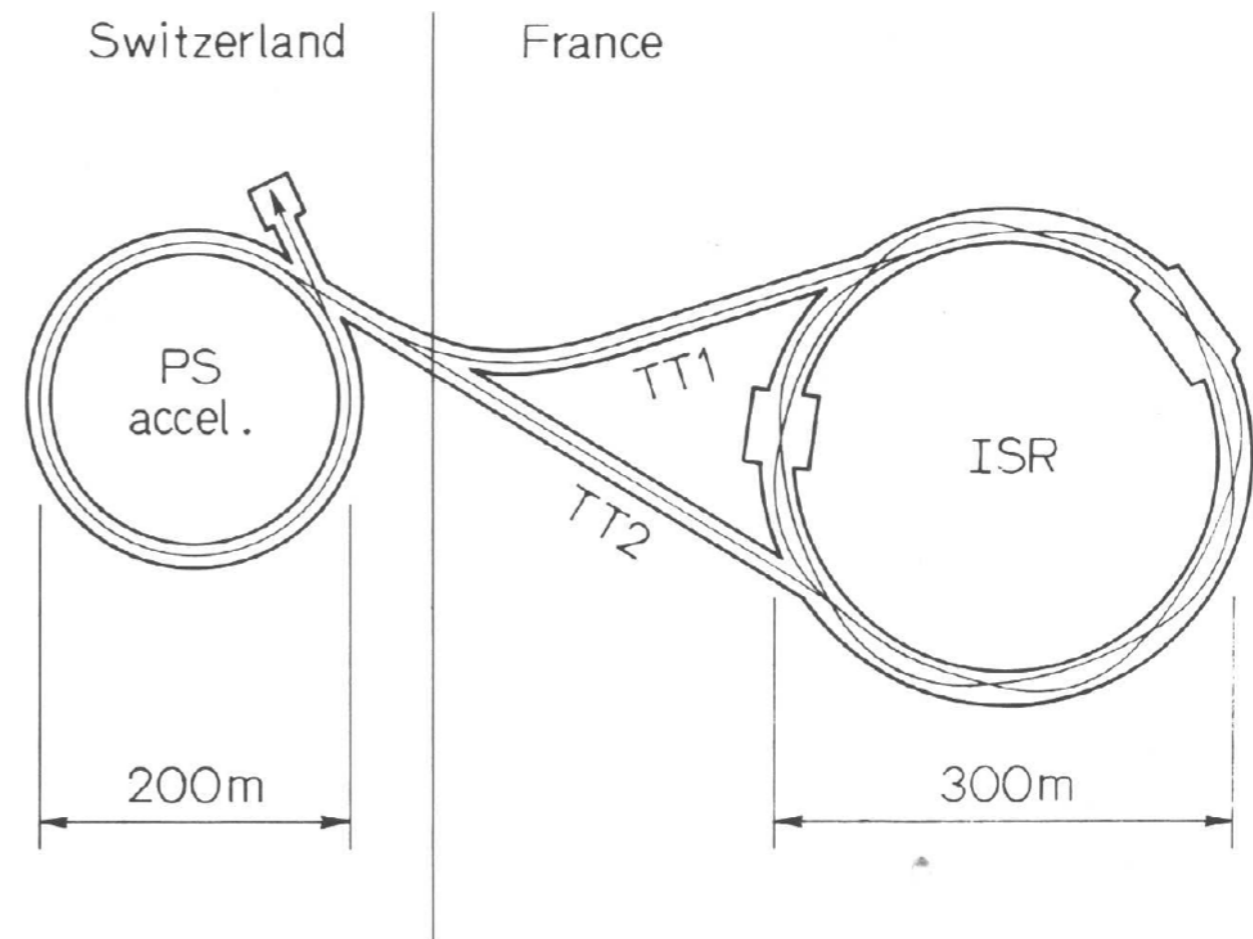


Figure 4 a. Cross-section of the vacuum chamber at the position of the beam inflector, with indication of the stacking process

Is the Solar System Stable ?

# Is the Solar System Stable ?

- Question raised since Newton (1704)

# Is the Solar System Stable ?

- Question raised since Newton (1704)
- Positive answer by Lagrange and Laplace (1772-76)

# Is the Solar System Stable ?

- Question raised since Newton (1704)
- Positive answer by Lagrange and Laplace (1772-76)
- Questioned by Poincaré (1892)

# Is the Solar System Stable ?

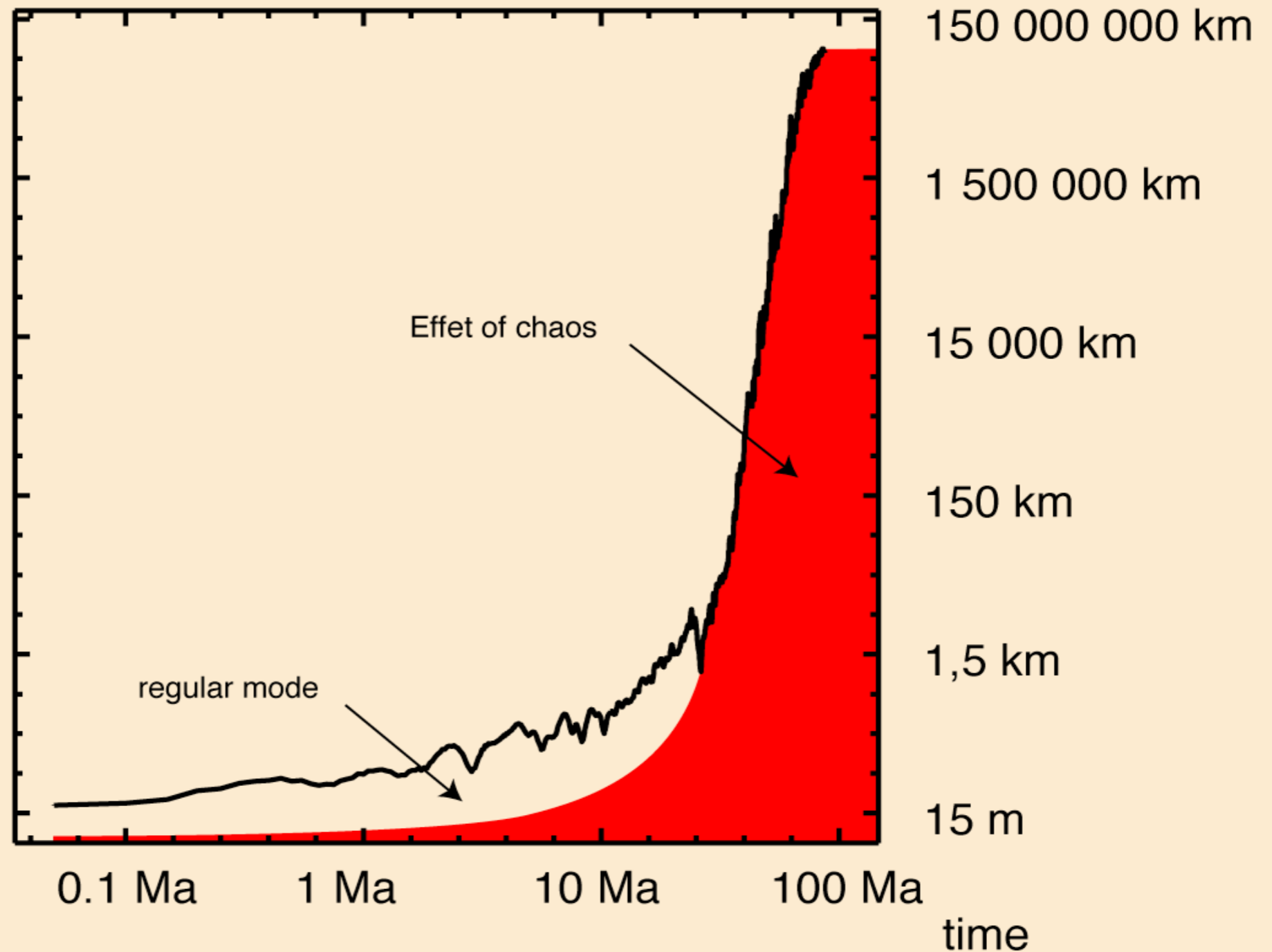
- Question raised since Newton (1704)
- Positive answer by Lagrange and Laplace (1772-76)
- Questioned by Poincaré (1892)
- Positive answer by Arnold (KAM) (1963)



# Chaotic motion of the Solar System

Secular equations : 200 Ma : *J. Laskar (1989, 1990)*

Direct integration : 100 Ma : *J.G. Sussman & J. Wisdom (1992)*



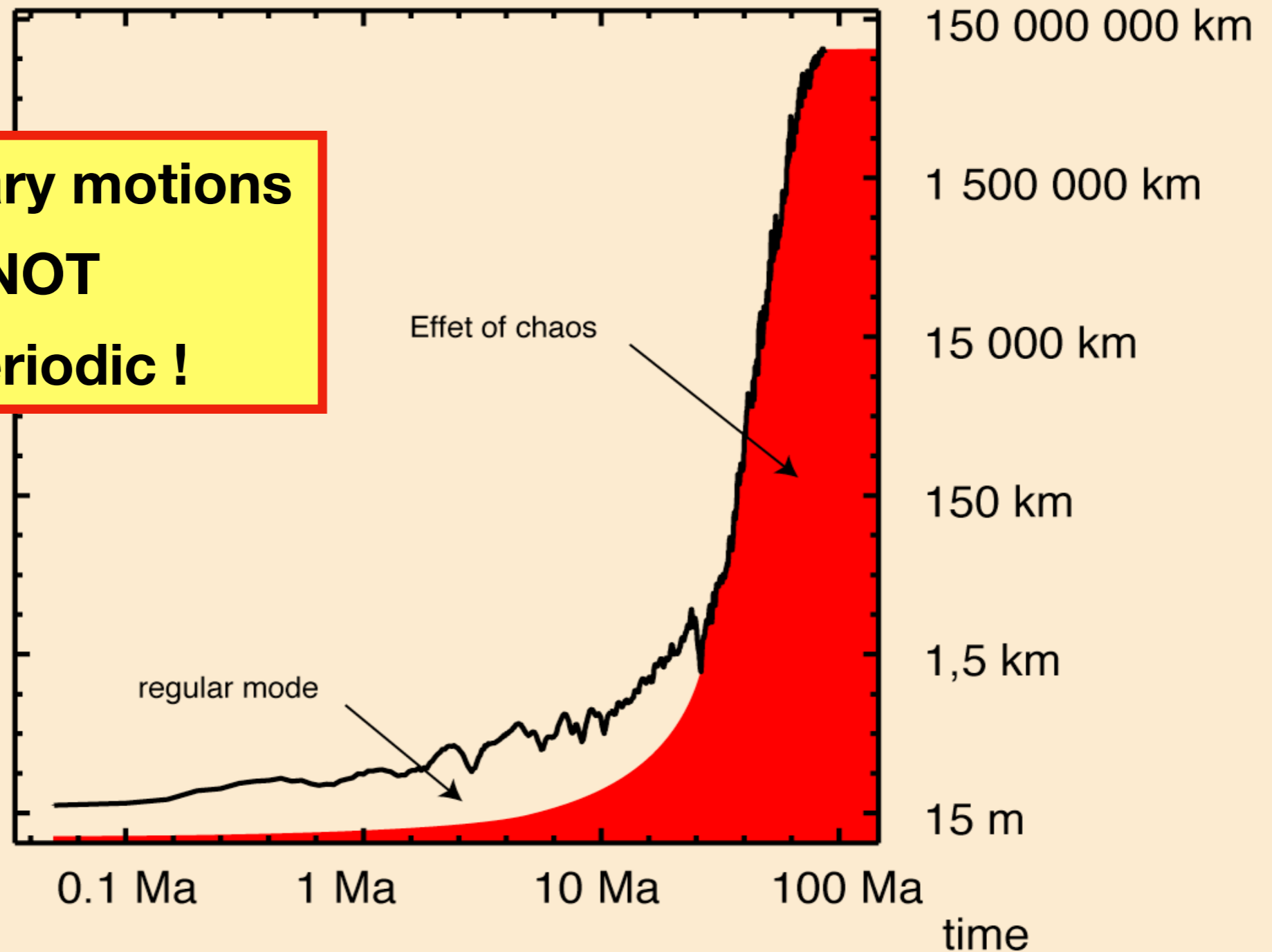
$$d(T) \approx d_0 10^{T/10}$$

# Chaotic motion of the Solar System

Secular equations : 200 Ma : *J. Laskar (1989, 1990)*

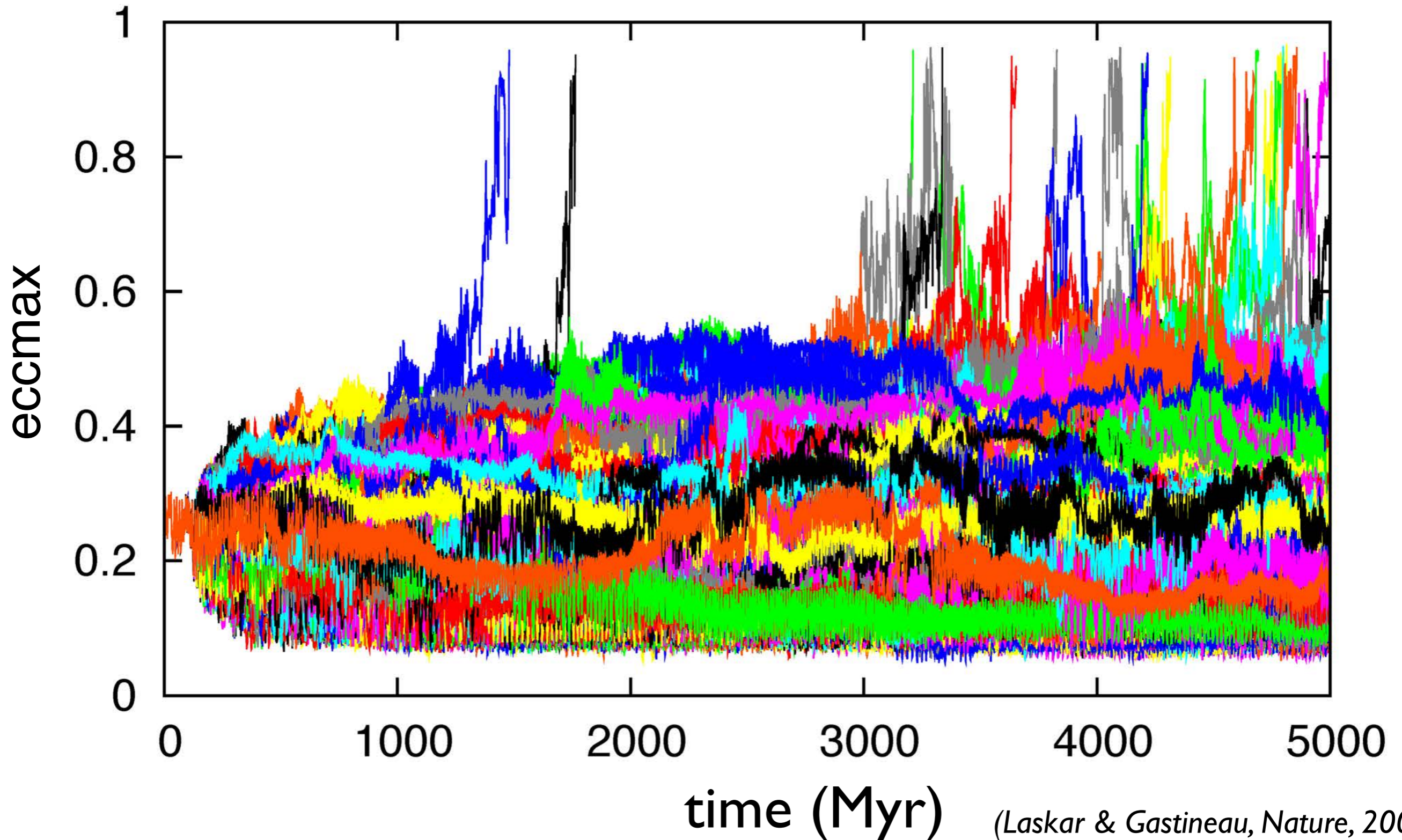
Direct integration : 100 Ma : *J.G. Sussman & J. Wisdom (1992)*

**The planetary motions  
are NOT  
quasiperiodic !**



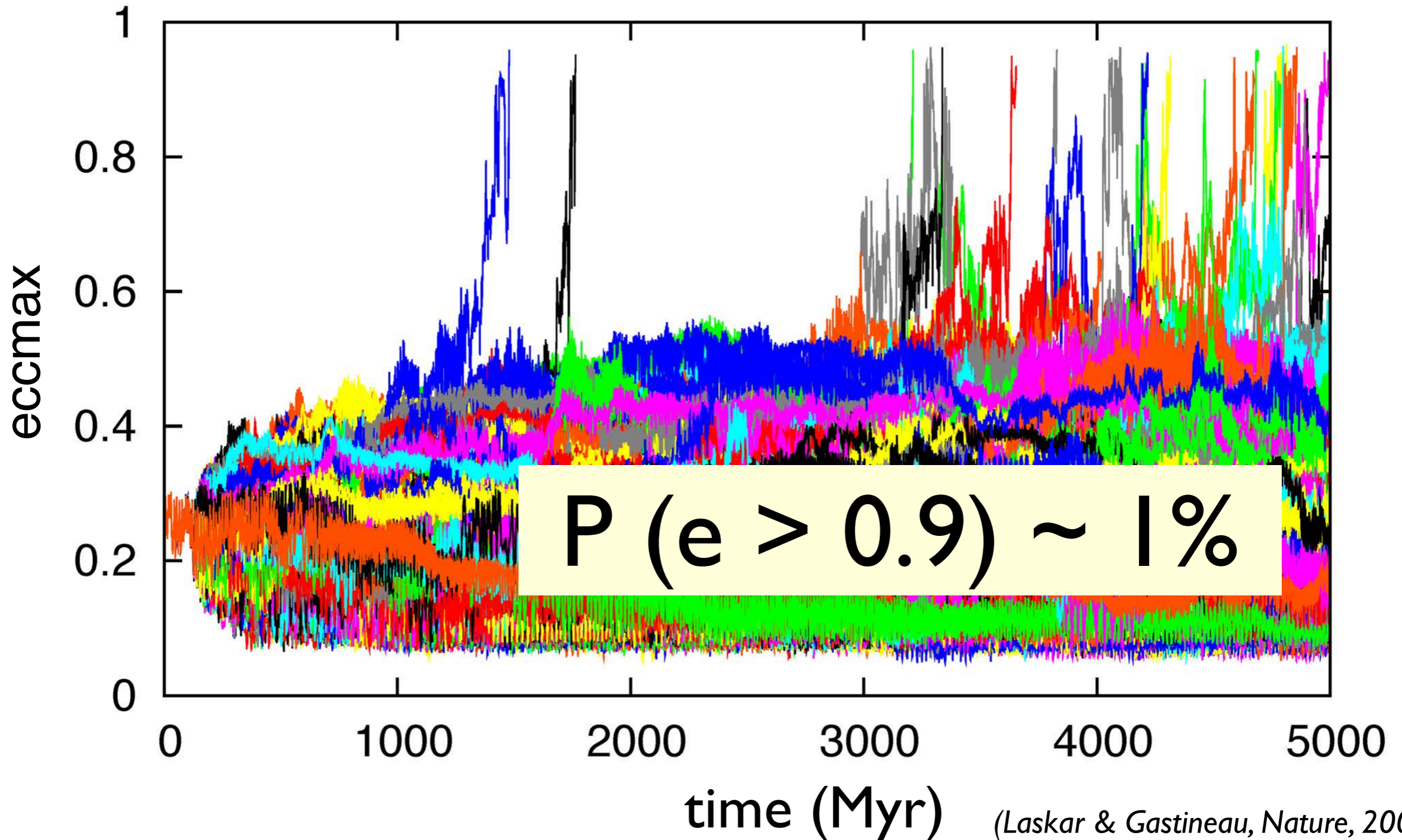
$$d(T) \approx d_0 10^{T/10}$$

Max eccentricity of Mercury **WITH** relativity  
direct equations (2501 sol)  
(0.38 mm)



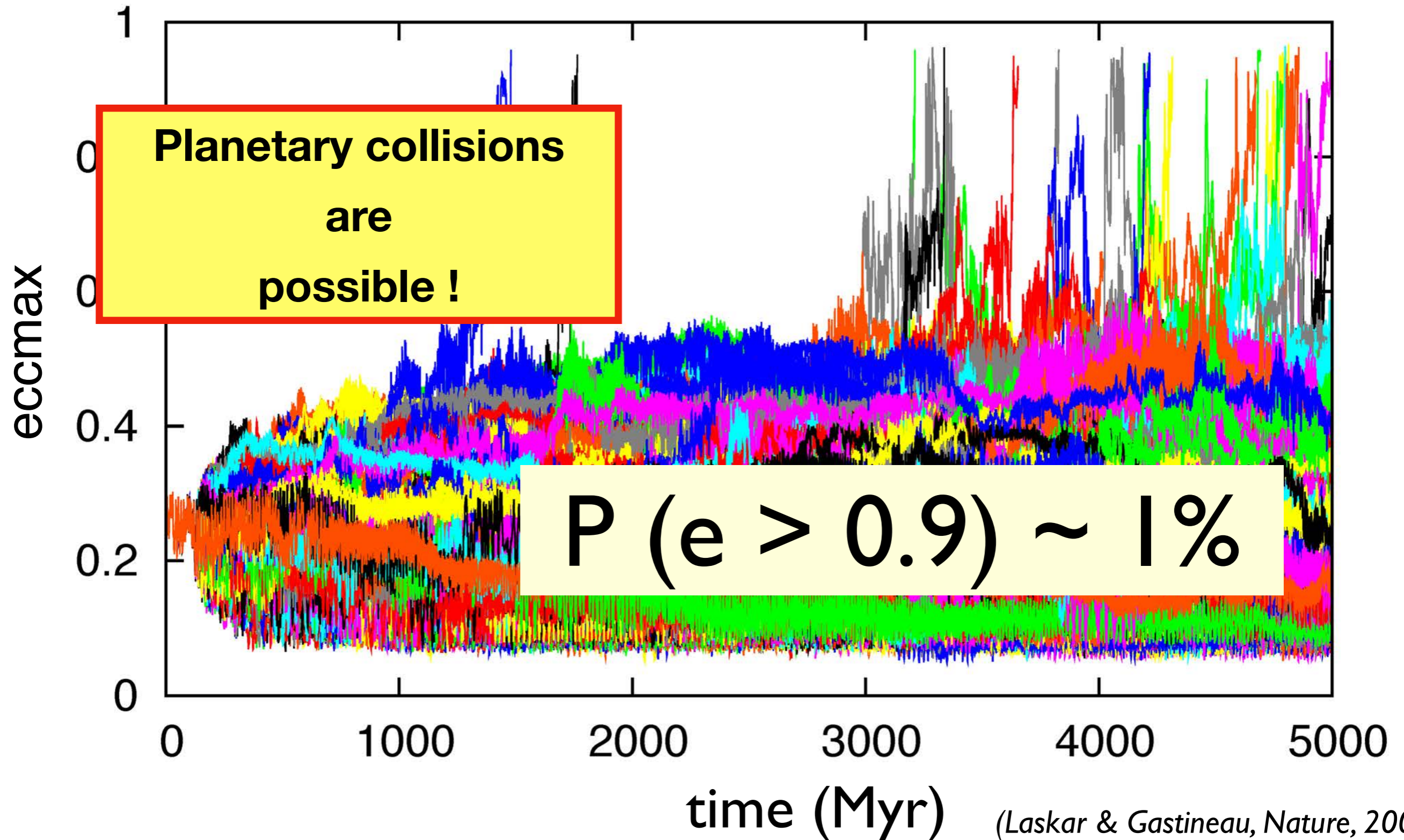


Max eccentricity of Mercury **WITH relativity**  
direct equations (2501 sol)  
(0.38 mm)





Max eccentricity of Mercury **WITH relativity**  
direct equations (2501 sol)  
(0.38 mm)





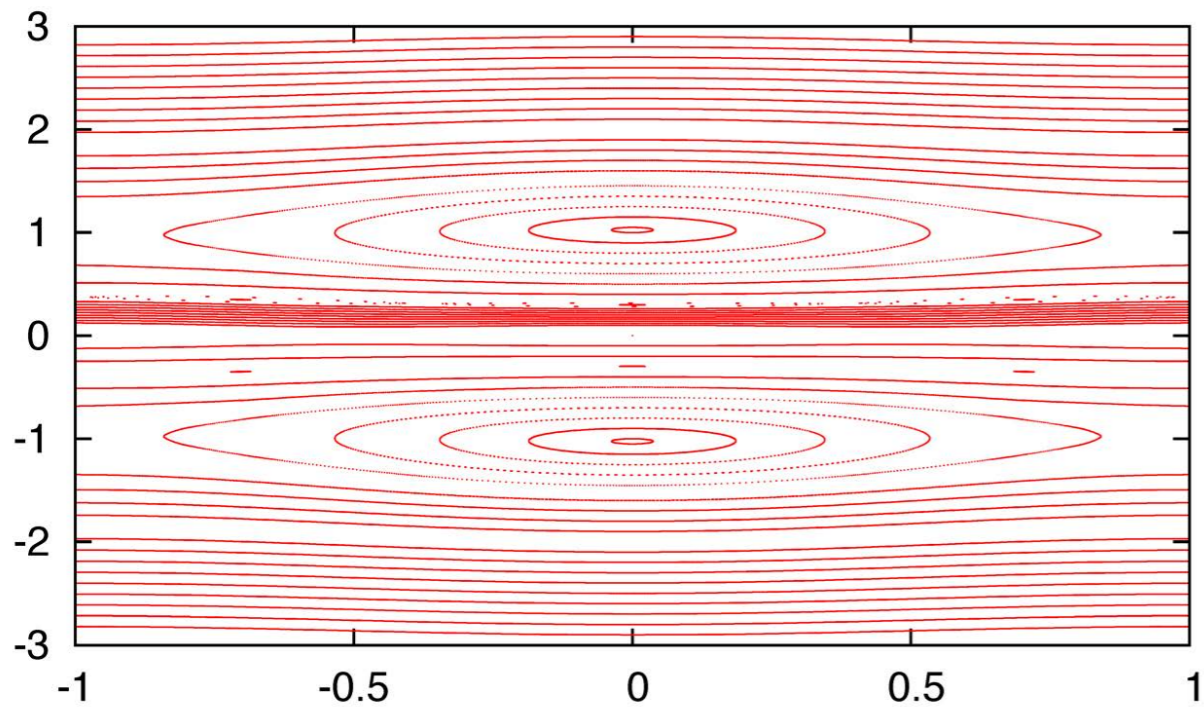
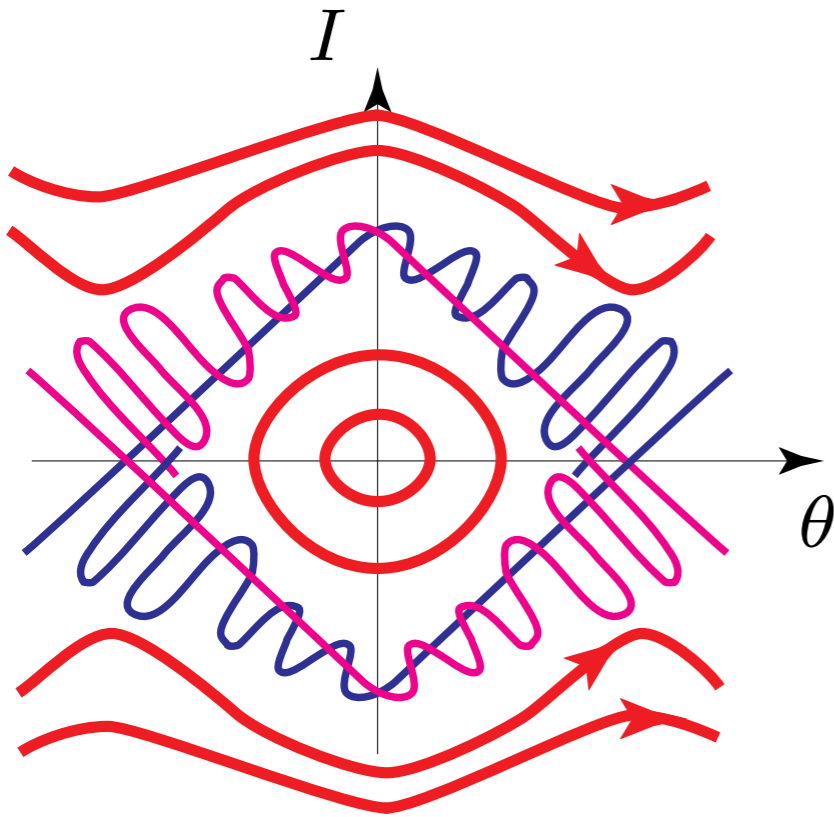
# Origin of CHAOS

## Resonance overlap

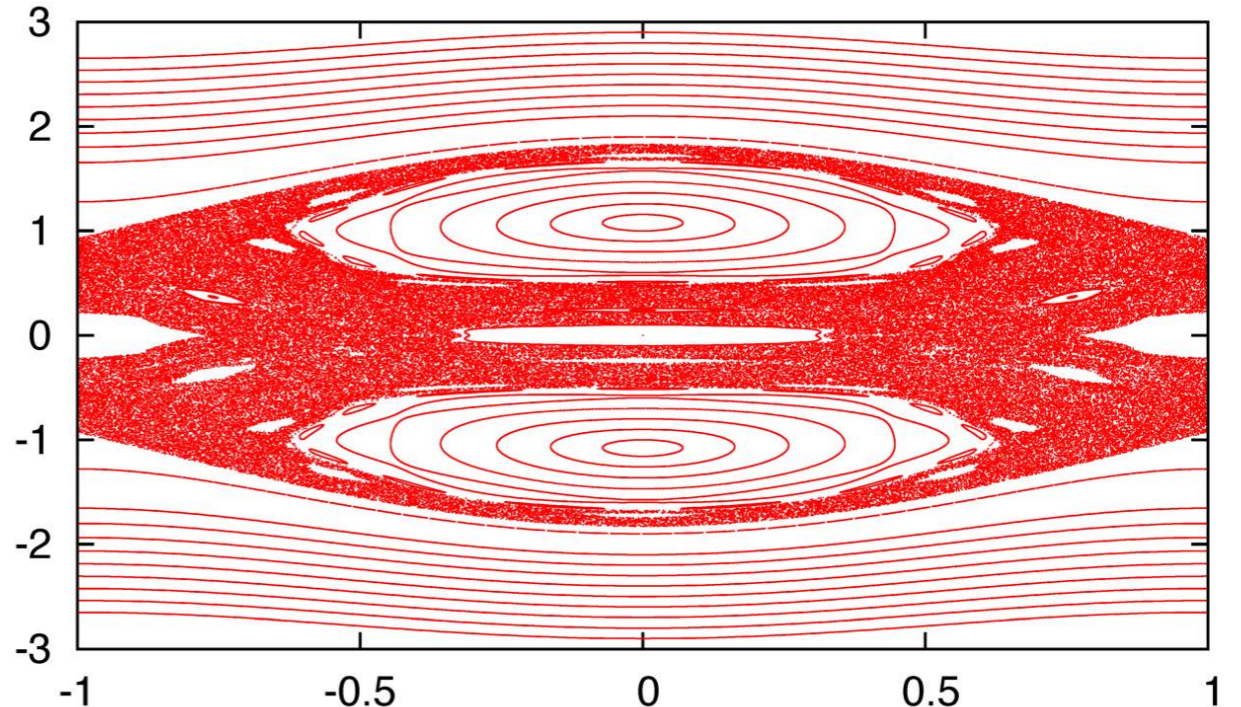
Chirikov (1972)

$$H = \frac{I^2}{2} + a \cos(\theta - t) + a \cos(\theta + t)$$

$$\Delta\omega = 4\sqrt{a}$$



$a=0.05$



$a=0.15$

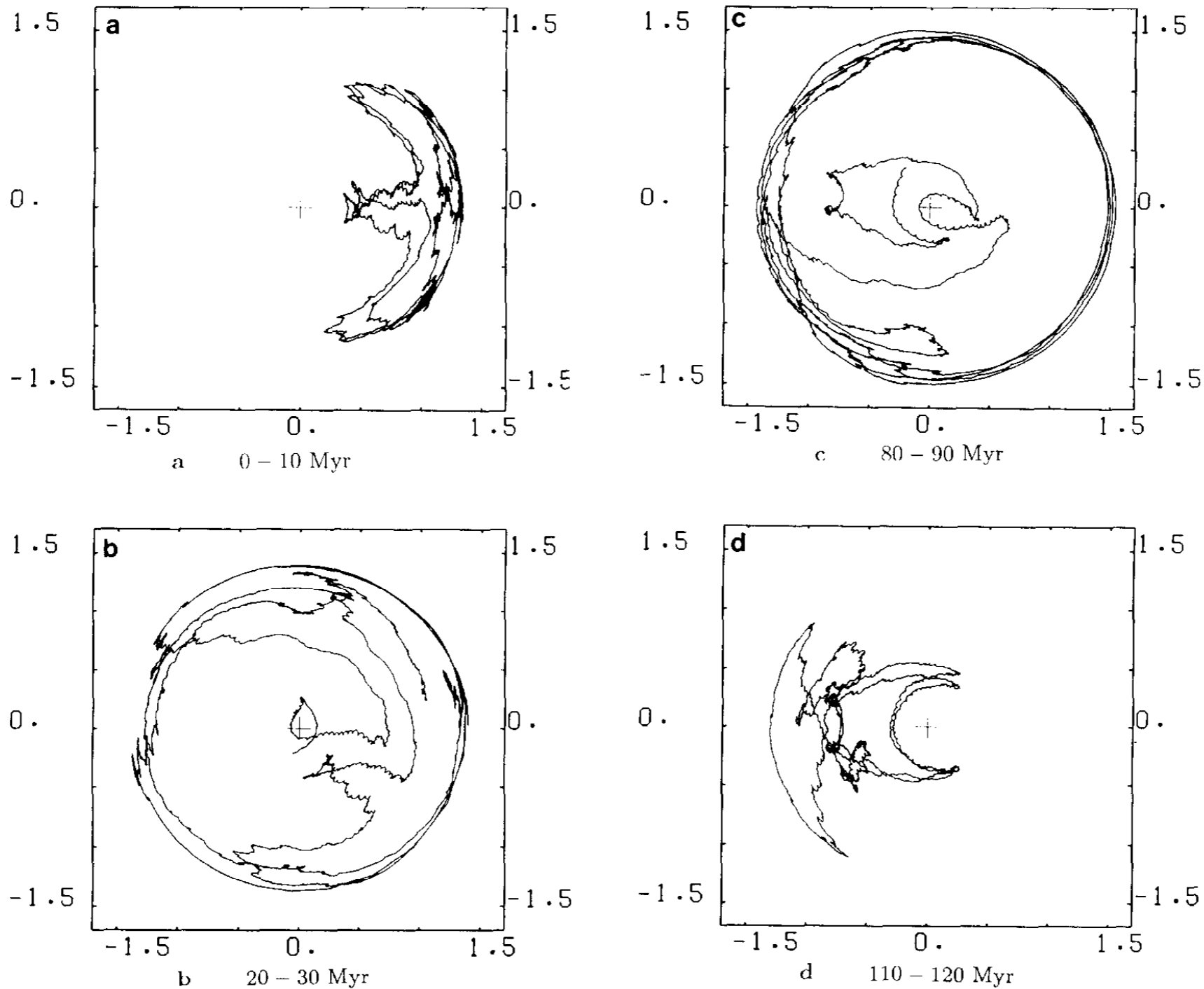


FIG. 3. (a–d) Examples of transition from libration around  $0^\circ$  (a) to circulation (b), and from circulation (c) to libration around  $180^\circ$  for the argument  $2(\varpi_4 - \varpi_3) - (\Omega_4 - \Omega_3)$ . The quantity which is actually plotted in the complex plane is  $z_{04} \exp i(2(\varpi_4 - \varpi_3) - (\Omega_4 - \Omega_3))$  (Eq. (26)).

$$2(g_4 - g_3) - (s_4 - s_3)$$

## The origin of chaos in the Solar System through computer algebra

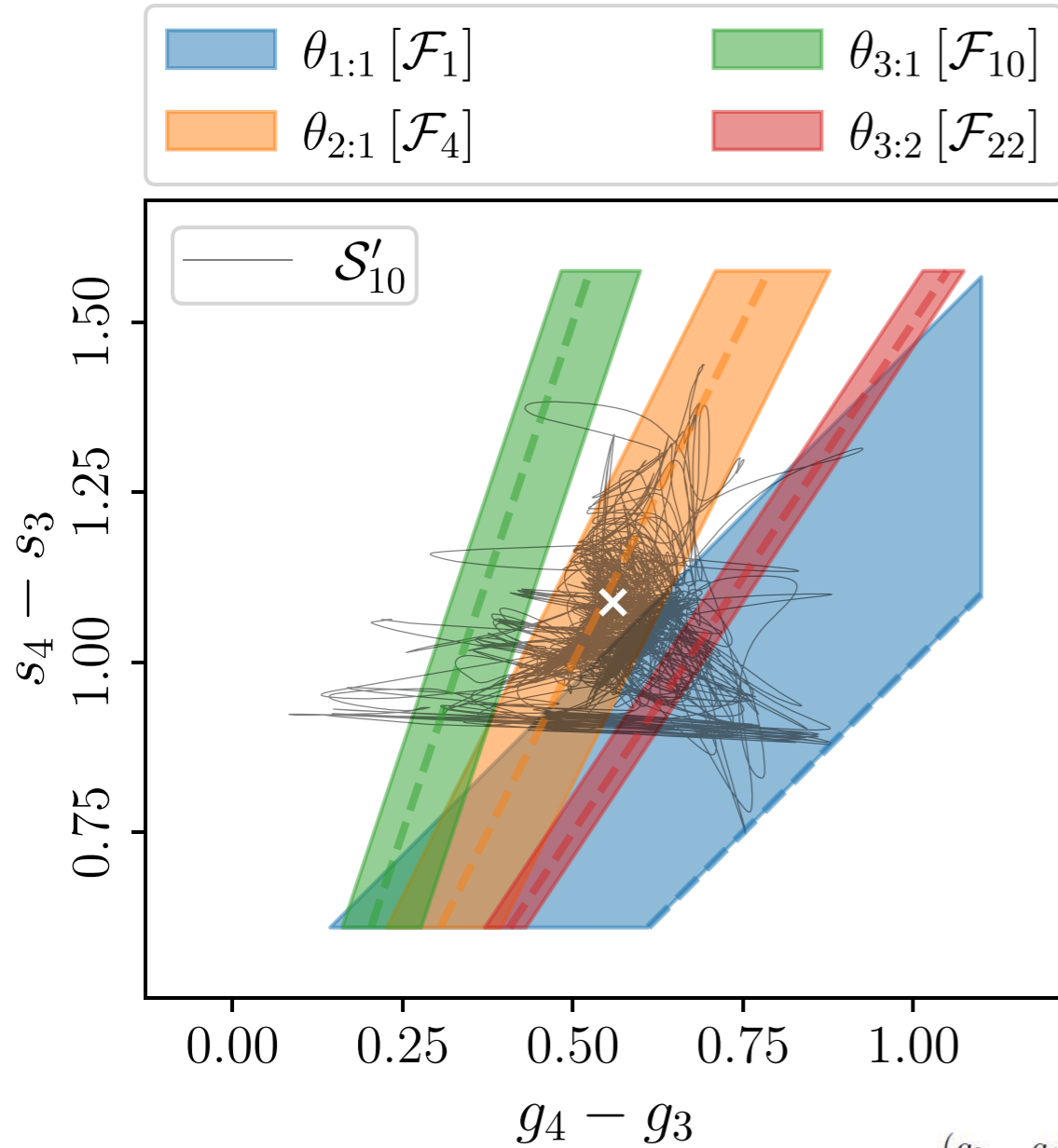
Federico Mogavero and Jacques Laskar

Deg	2	4	6	8	10
N monomials	8	6304	188024	3 394 892	42 817 100

$i$		Fourier harmonic [ $\mathcal{F}_i$ ]	$\omega_{\text{hyp}}$	$\tau_{\text{res}}$	$\omega_{\text{ell}}$	$\tau_{\text{libr}}$	$\Delta\omega$
1	★	$g_3 - g_4 - s_3 + s_4$	$0.31_{0.08}^{0.67}$	12%	$0.65_{0.26}^{1.56}$	18%	$0.33_{0.09}^{0.53}$
2	†	$g_1 - g_2 + s_1 - s_2$	$0.38_{0.12}^{0.79}$	19%	$0.89_{0.26}^{1.34}$	26%	$0.30_{0.15}^{0.61}$
3	†	$g_2 - g_5 - 2s_1 + 2s_2$	$0.22_{0.07}^{0.33}$	23%	$0.33_{0.16}^{0.45}$	56%	$0.11_{0.04}^{0.22}$
4	★	$2g_3 - 2g_4 - s_3 + s_4$	$0.14_{0.04}^{0.36}$	70%	$0.43_{0.23}^{0.73}$	74%	$0.08_{0.02}^{0.16}$
5	†	$g_1 - g_5 - s_1 + s_2$	$0.08_{0.05}^{0.10}$	10%	$0.22_{0.14}^{0.28}$	63%	$0.07_{0.06}^{0.18}$
6		$g_2 - g_4 + s_2 - s_4$	$0.07_{0.04}^{0.09}$	6%	$0.07_{0.05}^{0.09}$	70%	$0.07_{0.03}^{0.10}$
7		$g_1 - 2g_2 + g_4 + s_1 - 2s_2 + s_4$	$0.11_{0.10}^{0.13}$	5%	$0.12_{0.11}^{0.13}$	69%	$0.06_{0.05}^{0.07}$
8		$g_1 - g_3 + s_2 - s_3$	$0.06_{0.03}^{0.09}$	17%	$0.06_{0.04}^{0.10}$	60%	$0.06_{0.03}^{0.09}$
9		$g_1 + g_3 - 2g_4 + s_2 - s_3$	$0.08_{0.06}^{0.09}$	5%	$0.08_{0.07}^{0.09}$	55%	$0.05_{0.04}^{0.06}$
10	★	$3g_3 - 3g_4 - s_3 + s_4$	$0.11_{0.01}^{0.34}$	9%	$0.14_{0.06}^{0.24}$	40%	$0.05_{0.01}^{0.14}$
11		$g_2 - g_3 - s_1 + 2s_2 - s_3$	$0.06_{0.04}^{0.07}$	5%	$0.06_{0.05}^{0.07}$	50%	$0.04_{0.03}^{0.05}$
12		$g_1 - 2g_3 + g_4 + s_2 - s_4$	$0.06_{0.03}^{0.12}$	36%	$0.06_{0.03}^{0.12}$	51%	$0.04_{0.02}^{0.08}$
13		$2g_1 - g_3 - g_5 + s_2 - s_4$	$0.05_{0.04}^{0.06}$	5%	$0.05_{0.04}^{0.06}$	52%	$0.04_{0.03}^{0.04}$
14		$g_1 - g_2 - s_1 + s_2$	$0.05_{0.05}^{0.05}$	2%	$0.05_{0.05}^{0.05}$	56%	$0.02_{0.04}^{0.04}$



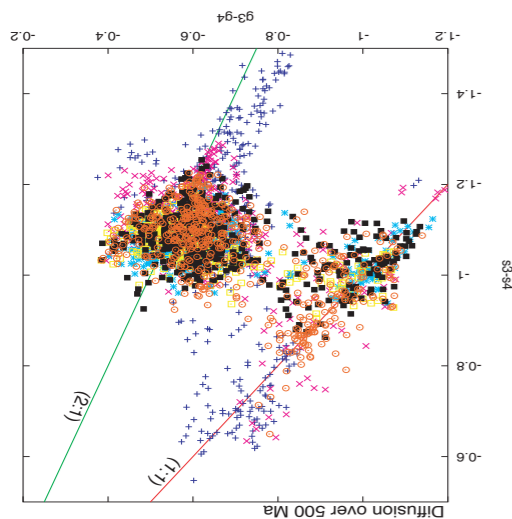
# Origin of CHAOS



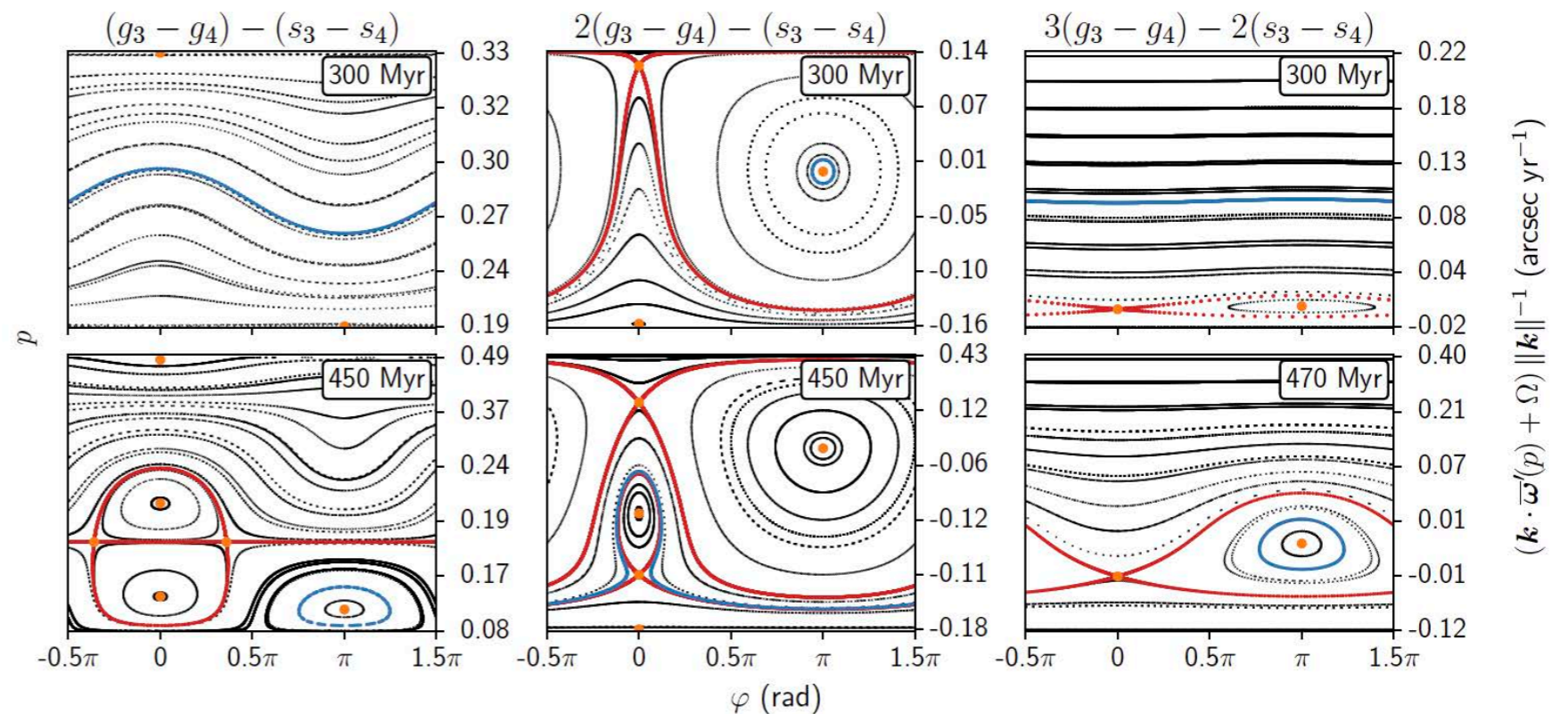
$$\theta_{2:1} = 2(g_4 - g_3) - (s_4 - s_3)$$

$$\theta_{3:2} = (g_4 - g_3) - (s_4 - s_3)$$

$$\theta_{1:1} = (g_4 - g_3) - (s_4 - s_3)$$



Laskar, 2000?



**ICARUS 88, 266–291 (1990)**

**The Chaotic Motion of the Solar System: A Numerical Estimate of  
the Size of the Chaotic Zones**

**J. LASKAR**

**Measure of the chaotic  
diffusion in all directions  
in a  
32 dimensional  
phase space**

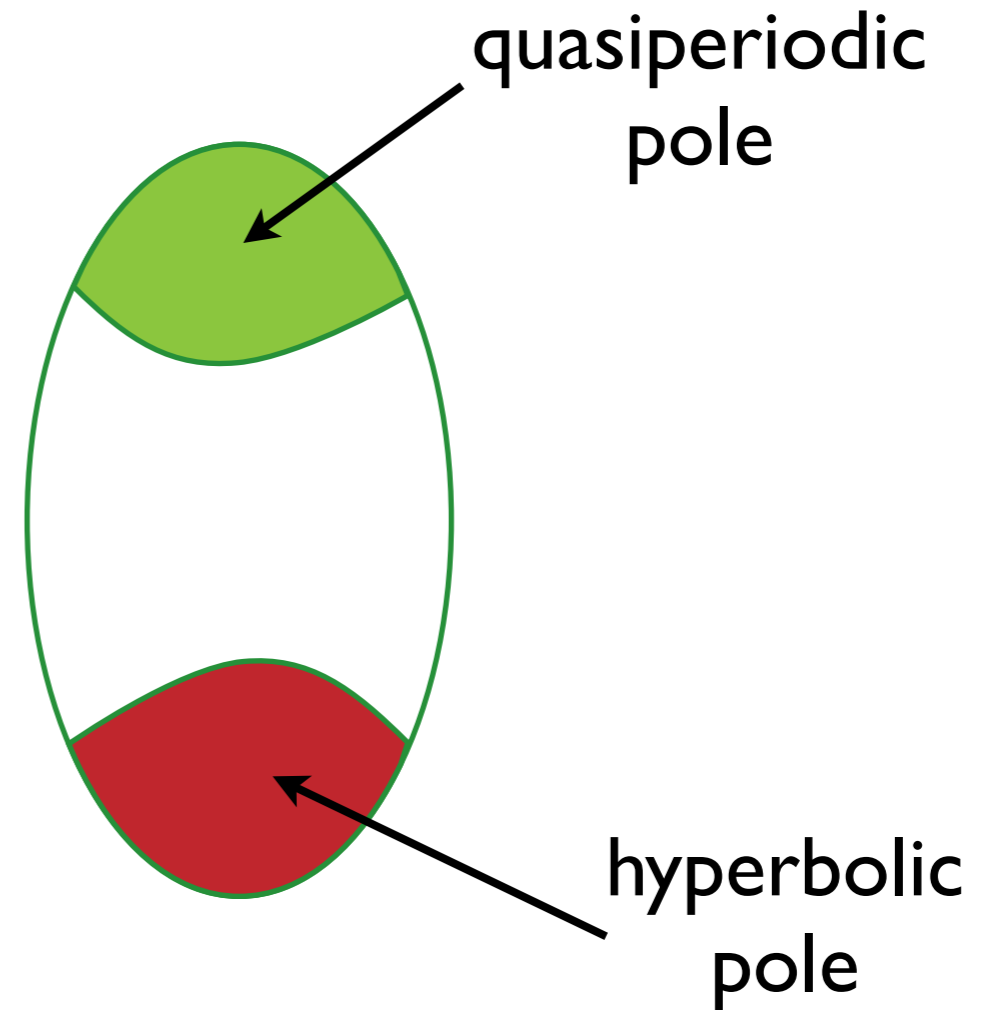
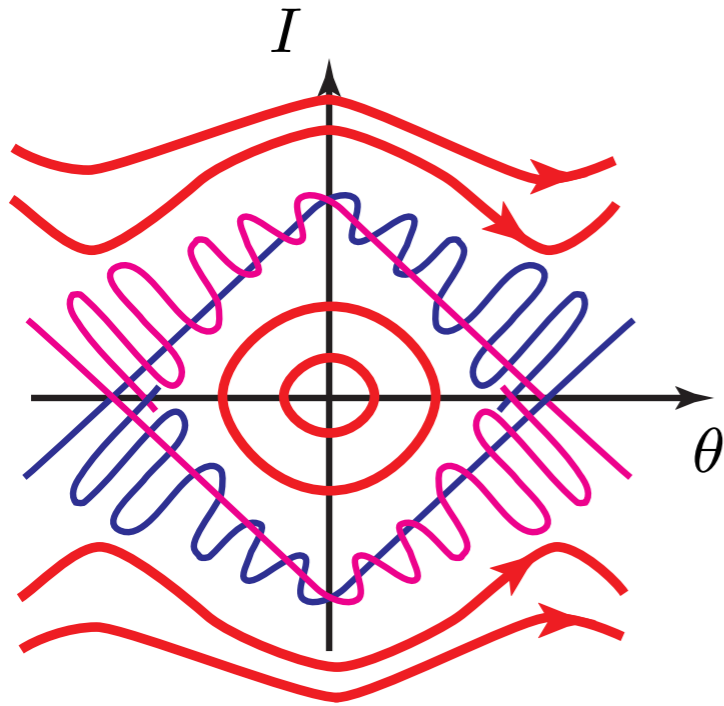
**(Laskar, 1990)**

**Frequency MAP**



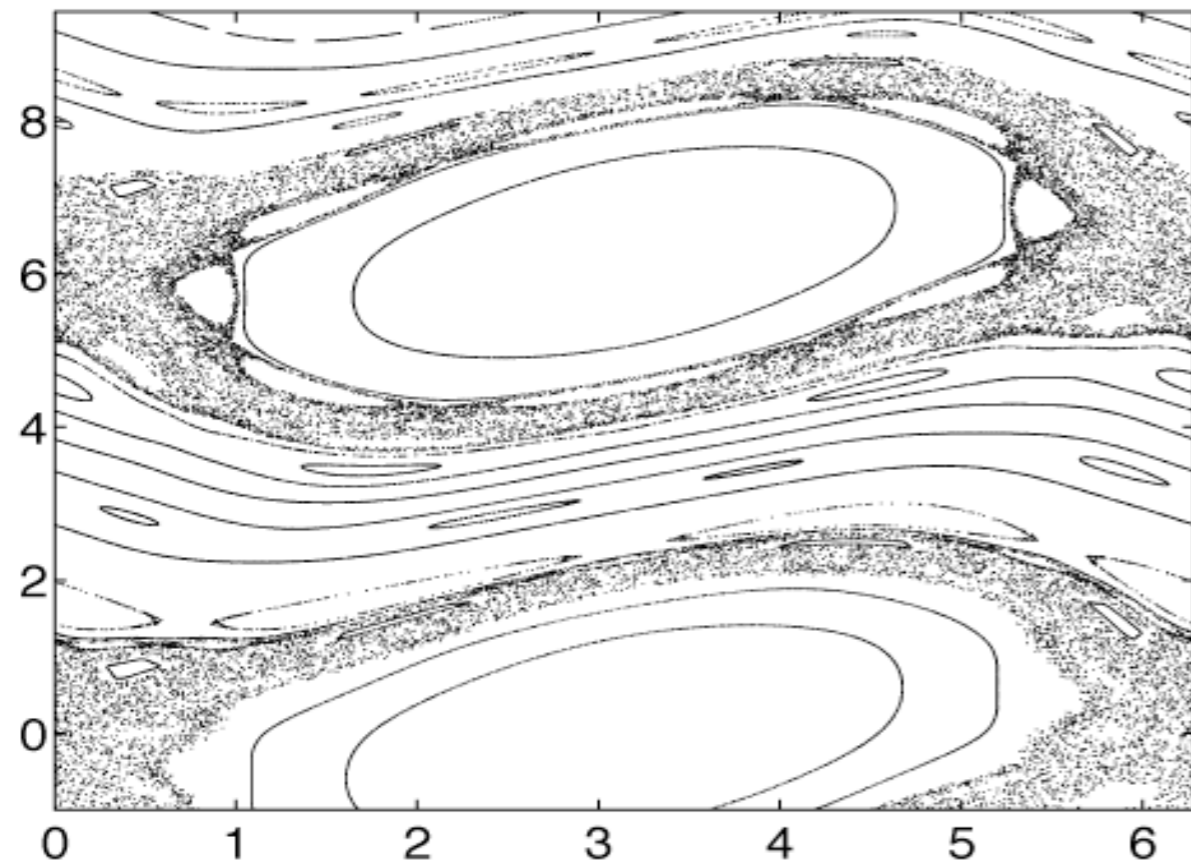
# Non-quasiperiodic Motion

(Poincaré, Smale,...)



chaotic : non-quasiperiodic

**Frequency MAP**



## Frequency Maps

$$H(I, \theta) = H_0(I) + \varepsilon H_1(I, \theta) \quad (I, \theta) \in \mathbb{B}^n \times \mathbb{T}^n$$

$$\varepsilon = 0$$

$$\dot{I}_j = 0 \quad , \quad \dot{\theta}_j = \frac{\partial H_0(I)}{\partial I_j} = \nu_j(I) \quad ;$$

$$I_j = I_{j0} \quad \theta_j(t) = \theta_{j0} + \nu_j t$$

nondegenerate

$$\left| \frac{\partial \nu(I)}{\partial I} \right| = \left| \frac{\partial^2 H_0(I)}{\partial I^2} \right| \neq 0$$

frequency map

$$\begin{aligned} F : \mathbb{B}^n &\longrightarrow \mathbb{R}^n \\ (I) &\longrightarrow (\nu) \end{aligned}$$

diffeomorphism on  $F(\mathbb{B}^n) = \Omega$

**Frequency MAP**

# Frequency MAP

$$\varepsilon \neq 0$$

**KAM theorem** (Kolmogorov 1954, Arnold 1963, Moser 1963)

$$\exists \Omega_\varepsilon \subset \Omega \quad \text{Cantor set} \quad |\langle k, \nu \rangle| > \frac{\kappa_\varepsilon}{|k|^p}$$

$(\nu) \in \Omega_\varepsilon \Rightarrow$  quasiperiodic solution

**Pöschel (1982)**, there exists a diffeomorphism

$$\begin{aligned} \Psi : \mathbb{T}^n \times \Omega &\longrightarrow \mathbb{T}^n \times \mathbb{B}^n \\ (\varphi, \nu) &\longrightarrow (\theta, I) \end{aligned}$$

analytical  $/\varphi$  and  $C^\infty/\nu$  on  $\mathbb{T}^n \times \Omega_\varepsilon$  transforms the equations into

$$\dot{\nu}_j = 0, \quad \dot{\varphi}_j = \nu_j;$$

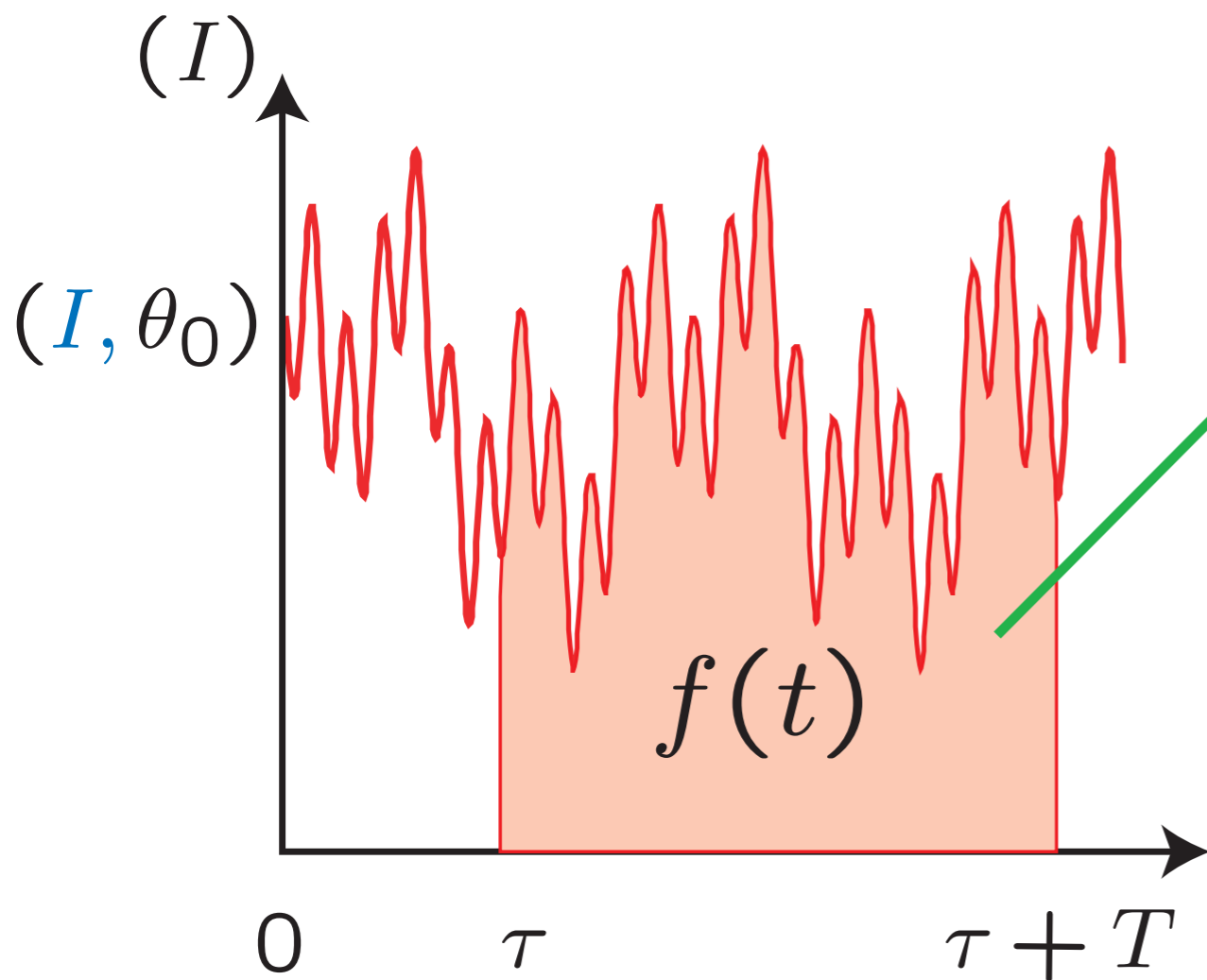
thus, if  $(\nu) \in \Omega_\varepsilon$ ,

$$z_j = I_j e^{i\theta_j},$$

$$z_j(t) = z_{j0} e^{i\nu_j t} + \sum_m a_m(\nu) e^{i\langle m, \nu \rangle t}$$

# Frequency MAP

$$\theta = \theta_0$$



# Numerical Frequency Map

$$f(t) = \sum a_k e^{i\omega_k t}$$

$$f(t) = \sum a_k e^{i\langle k, \nu \rangle t}$$

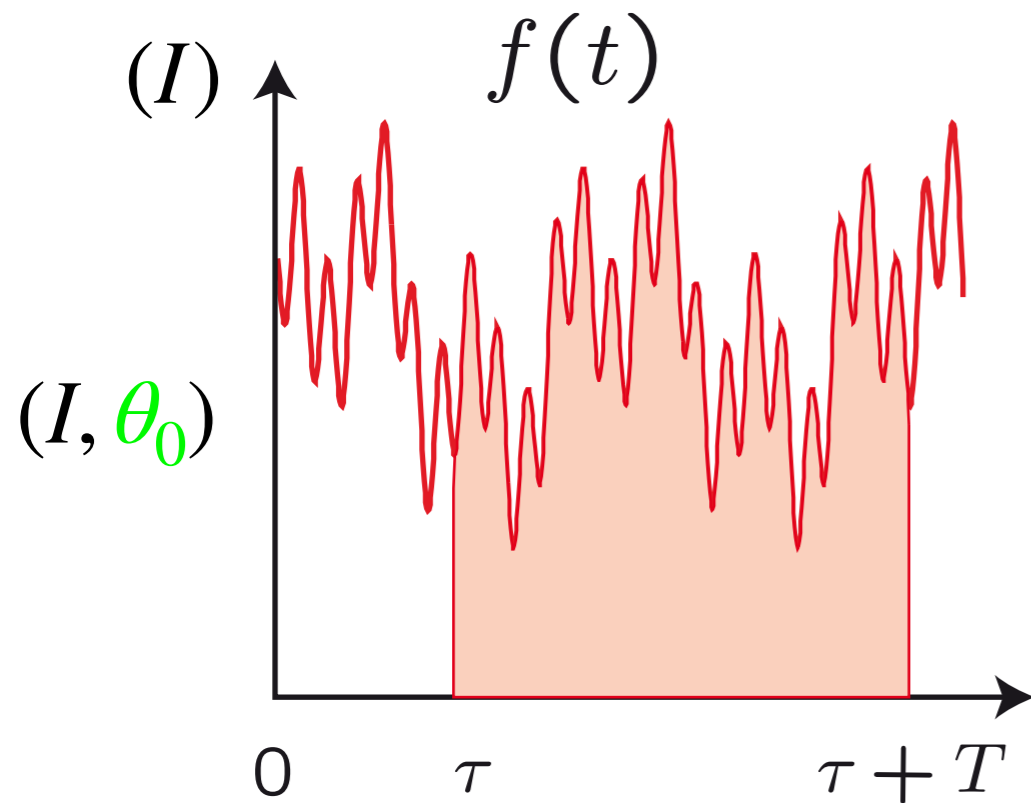
$$(\nu_1, \nu_2, \dots, \nu_n)$$

$$F_{\theta_0}^T : \mathbb{R}^n \longrightarrow \mathbb{R}^n$$

$$(I) \longrightarrow (\nu_1, \nu_2, \dots, \nu_n)$$

# Frequency MAP

$$\theta = \theta_0$$

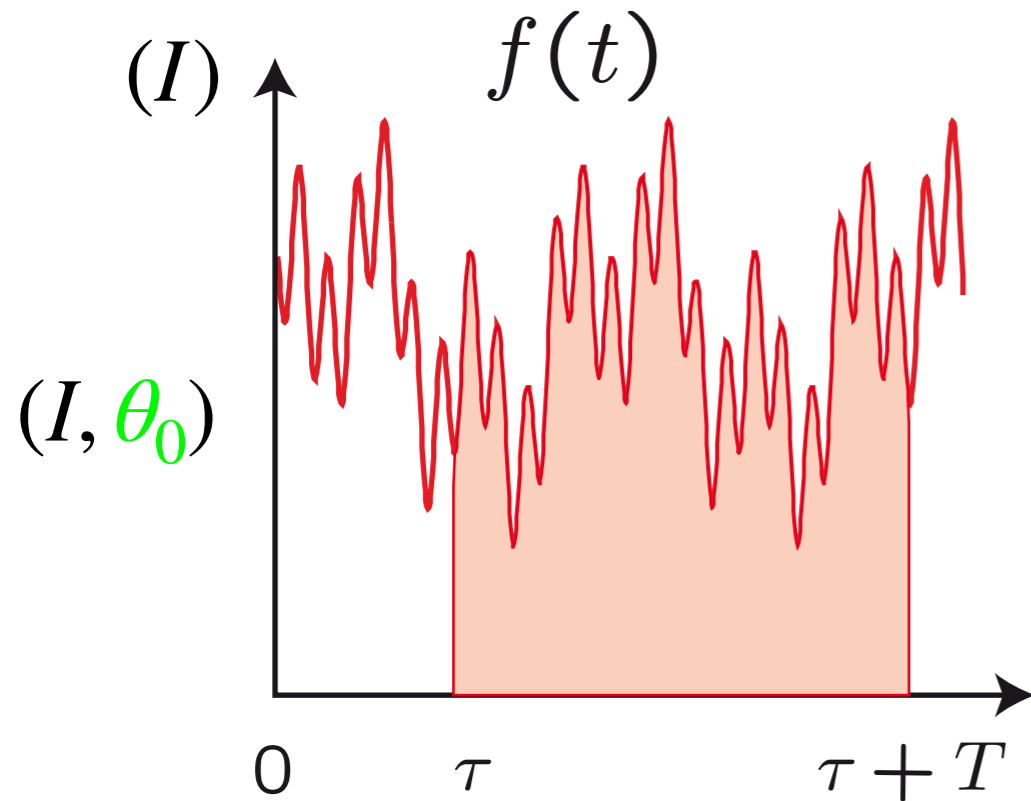


$$F_{\theta_0}^T : \mathbb{R} \times \mathbb{R}^n \longrightarrow \mathbb{R}^n$$
$$(\tau, I) \longrightarrow (\nu)$$



# Frequency MAP

$$\theta = \theta_0$$

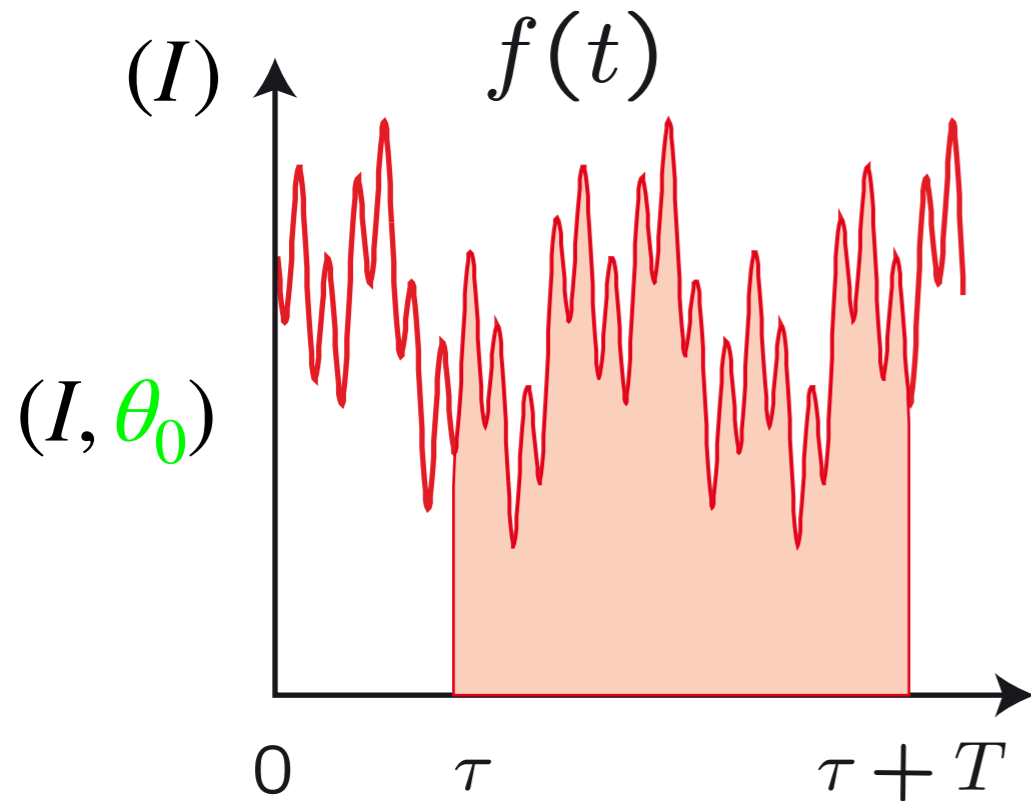


$$F_{\theta_0}^T : \mathbb{R} \times \mathbb{R}^n \longrightarrow \mathbb{R}^n$$
$$(\tau, I) \longrightarrow (\nu)$$

Thus : on the set of KAM tori,

# Frequency MAP

$$\theta = \theta_0$$



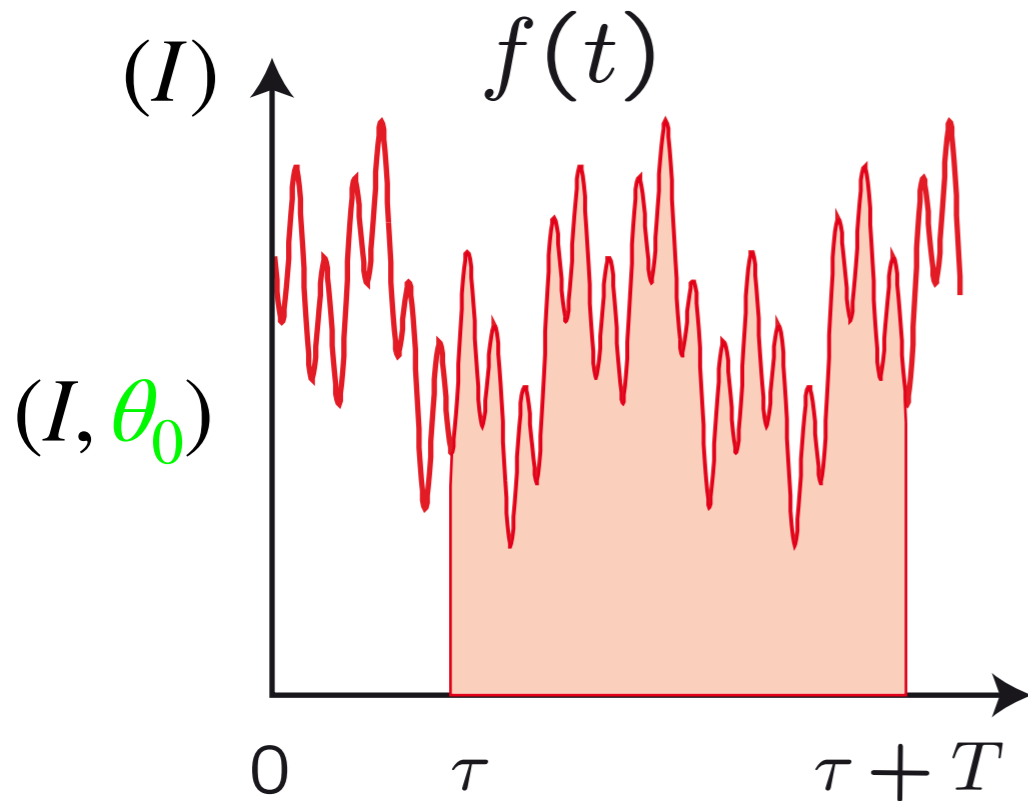
$$F_{\theta_0}^T : \mathbb{R} \times \mathbb{R}^n \longrightarrow \mathbb{R}^n$$
$$(\tau, I) \longrightarrow (\nu)$$

Thus : on the set of KAM tori,

$$F_{\theta_0}^T \text{ is constant } / \tau$$

# Frequency MAP

$$\theta = \theta_0$$



$$F_{\theta_0}^T : \mathbb{R} \times \mathbb{R}^n \longrightarrow \mathbb{R}^n$$
$$(\tau, I) \longrightarrow (\nu)$$

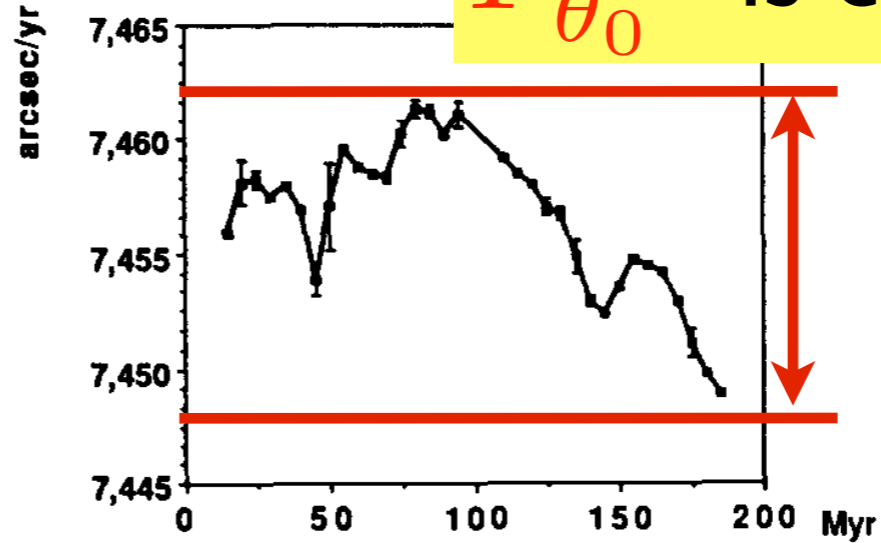
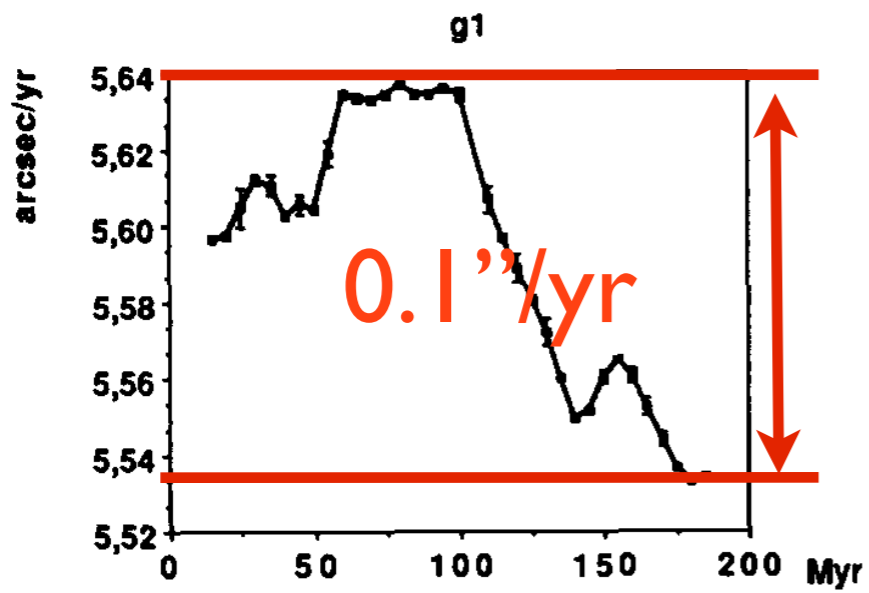
Thus : on the set of KAM tori,

$F_{\theta_0}^T$  is constant  $/\tau$

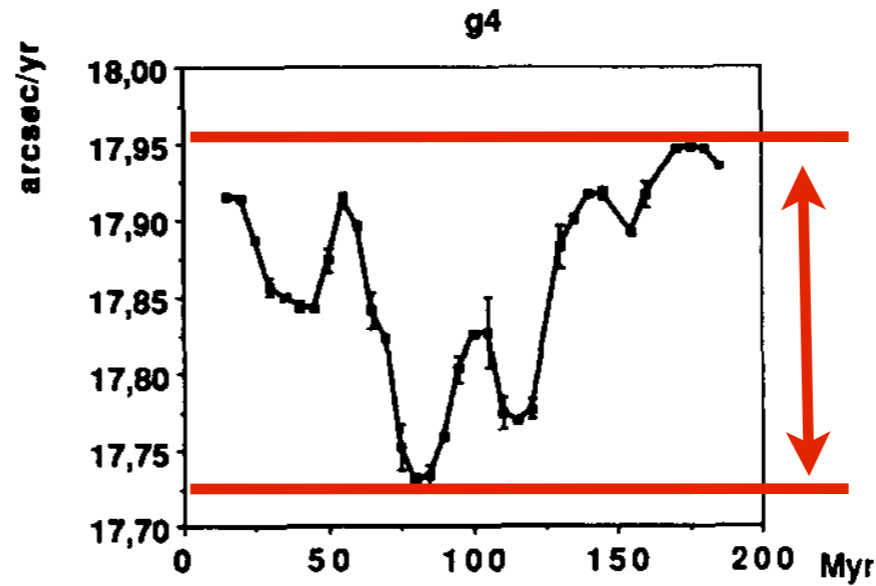
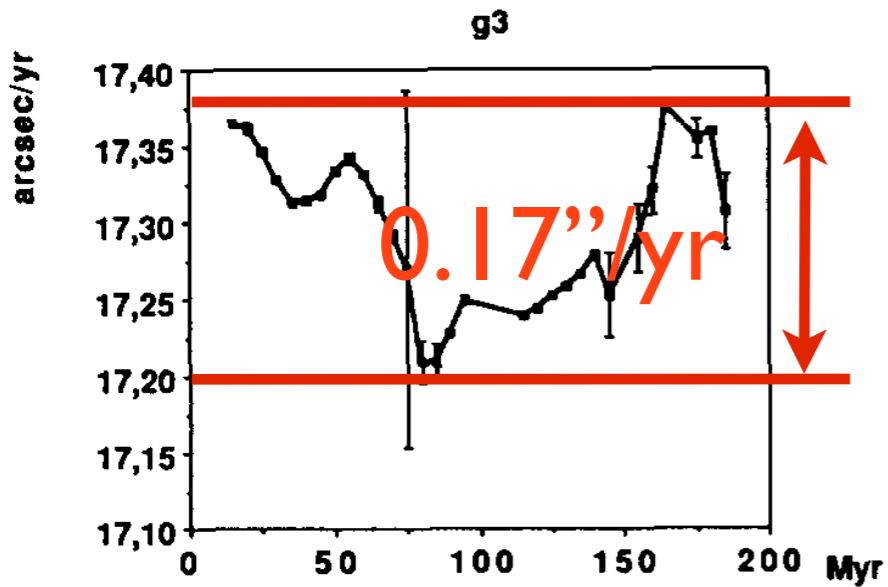
$F_{\theta_0}^T$  is a smooth diffeomorphism

(Laskar+, 1992, 1993)

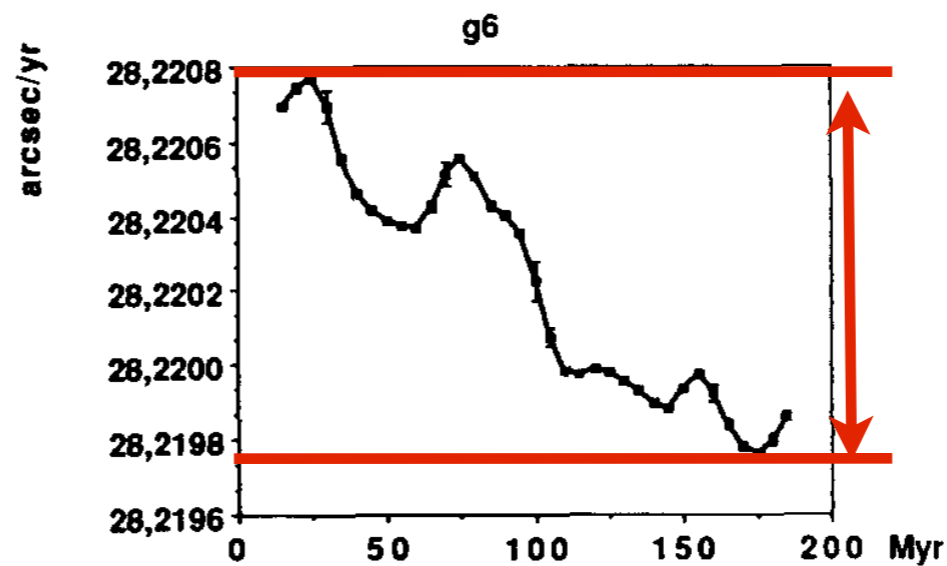
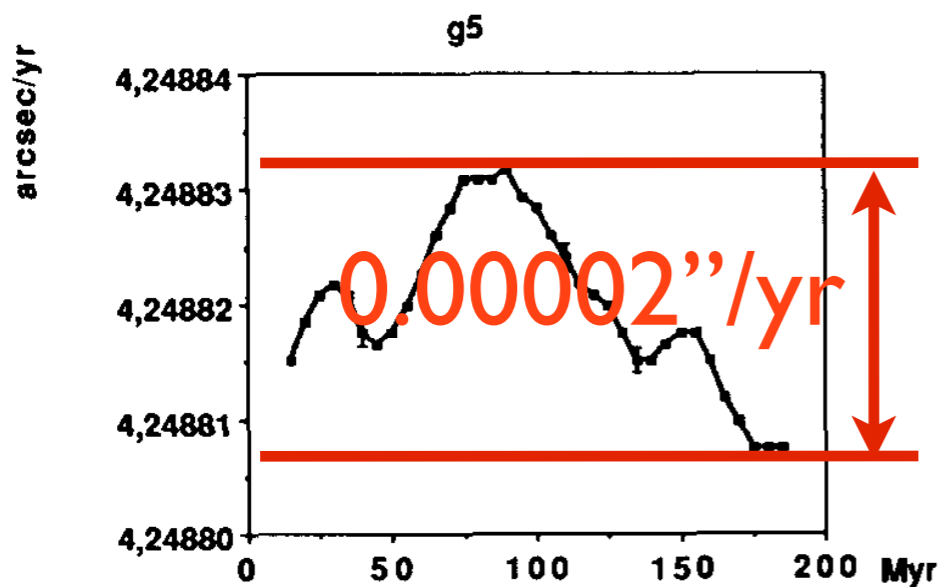
$F_{\theta_0}^T$  is constant  $/\tau$



0.013''/yr



0.2''/yr

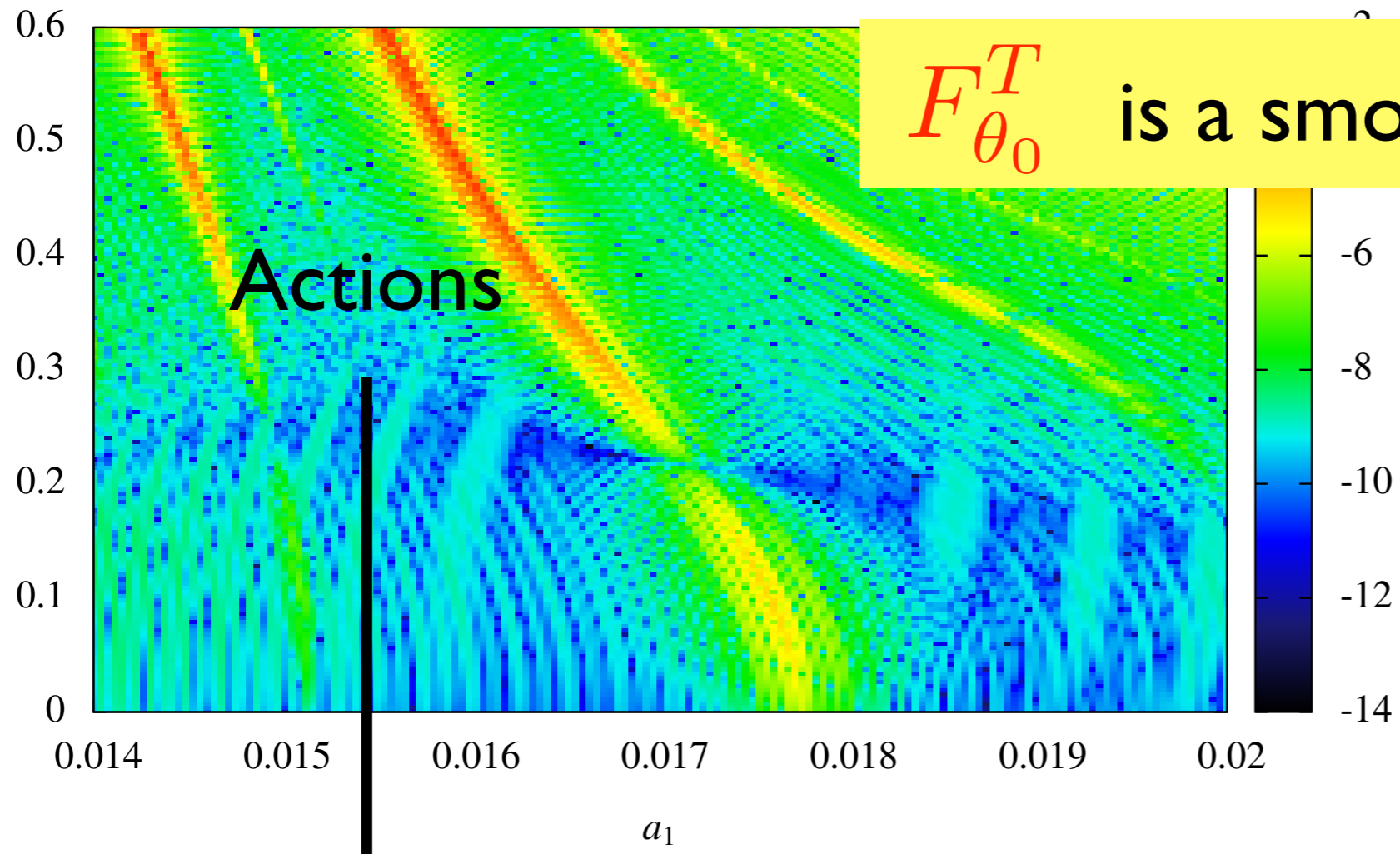


0.001''/yr

$$F_{\theta_0}^T$$

is a smooth diffeomorphism

Actions



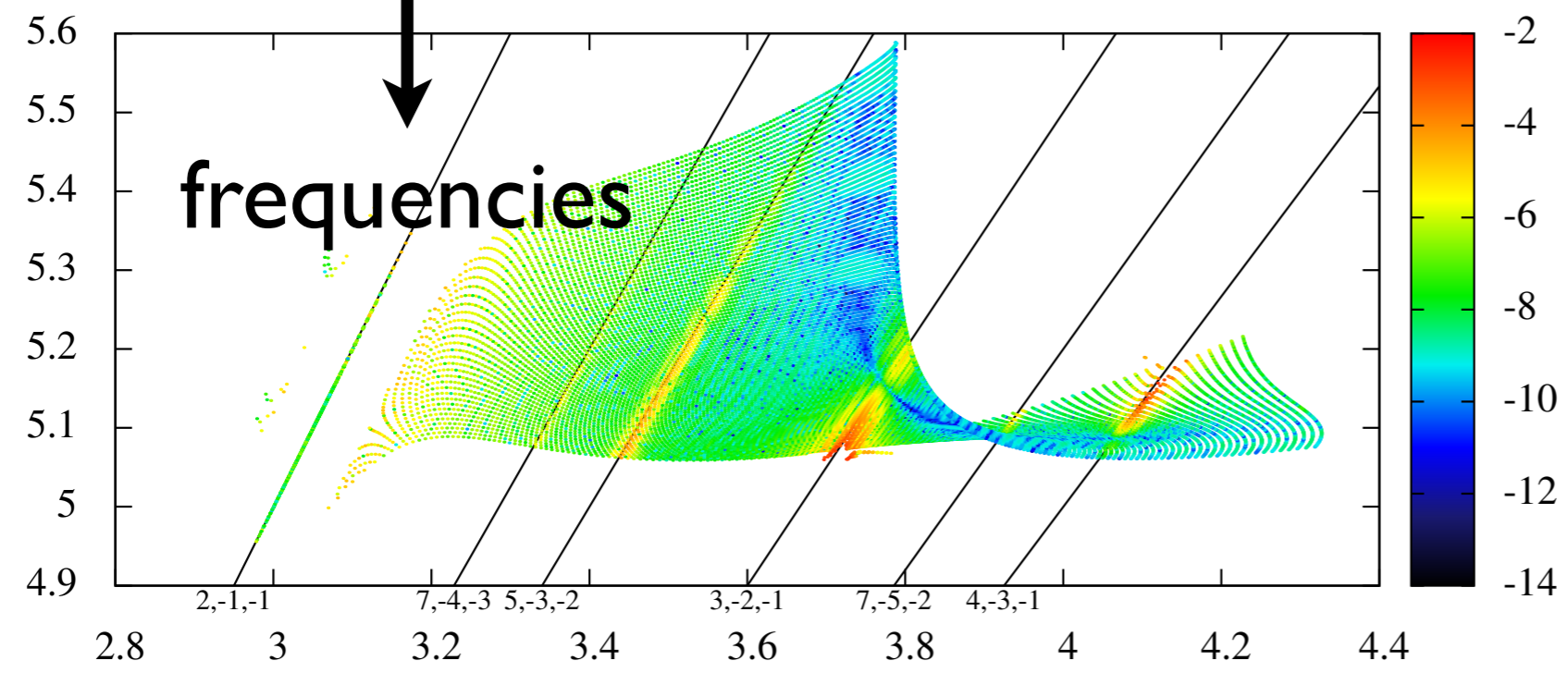
Frequency Map

of an

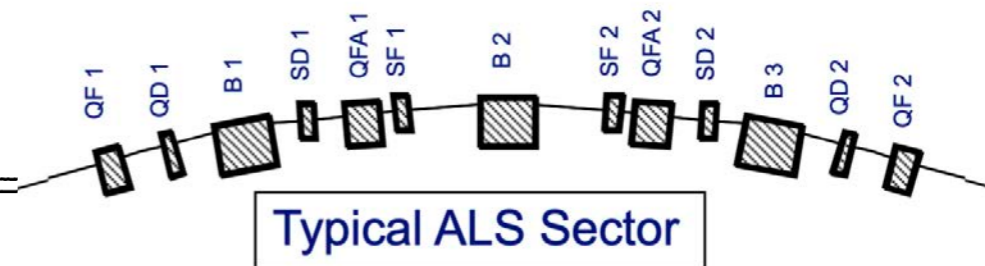
extrasolar planetary system

$$F_{\theta_0}^T : \mathbb{R}^n \longrightarrow \mathbb{R}^n$$
$$(I) \longrightarrow (\nu_1, \nu_2, \dots, \nu_n)$$

frequencies



(with JB Delisle, 2013)



## Global Dynamics and Long-Time Stability in Hamiltonian Systems via Numerical Frequency Analysis

H. S. Dumas

*Department of Mathematical Sciences, University of Cincinnati, Cincinnati, Ohio 45221-0025*

J. Laskar

*Astronomie et Systèmes Dynamiques, Bureau des Longitudes, 77 av. Denfert-Rochereau, 75014 Paris, France*

(Received 18 November 1992)

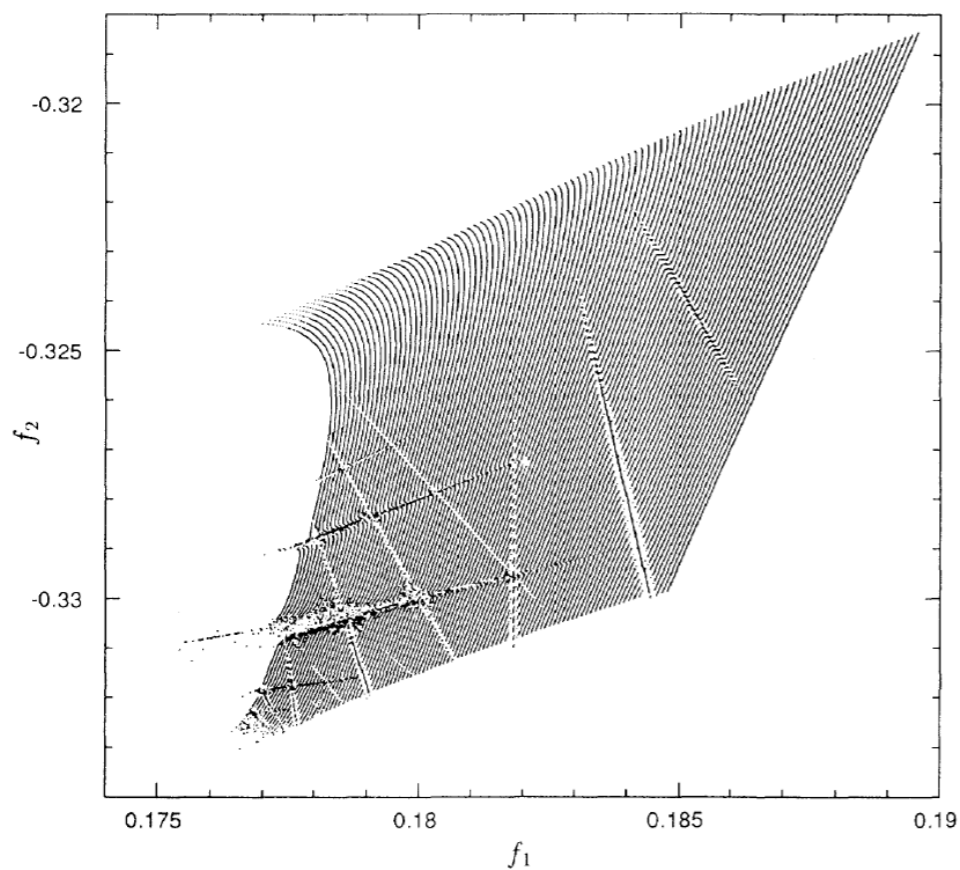


FIG. 1. Image in the frequency plane (“tune space”)  $(f_1, f_2)$  of the square sector  $0 \leq I_1, I_2 \leq 10^{-5}$ , obtained using frequency analysis over 4052 turns.

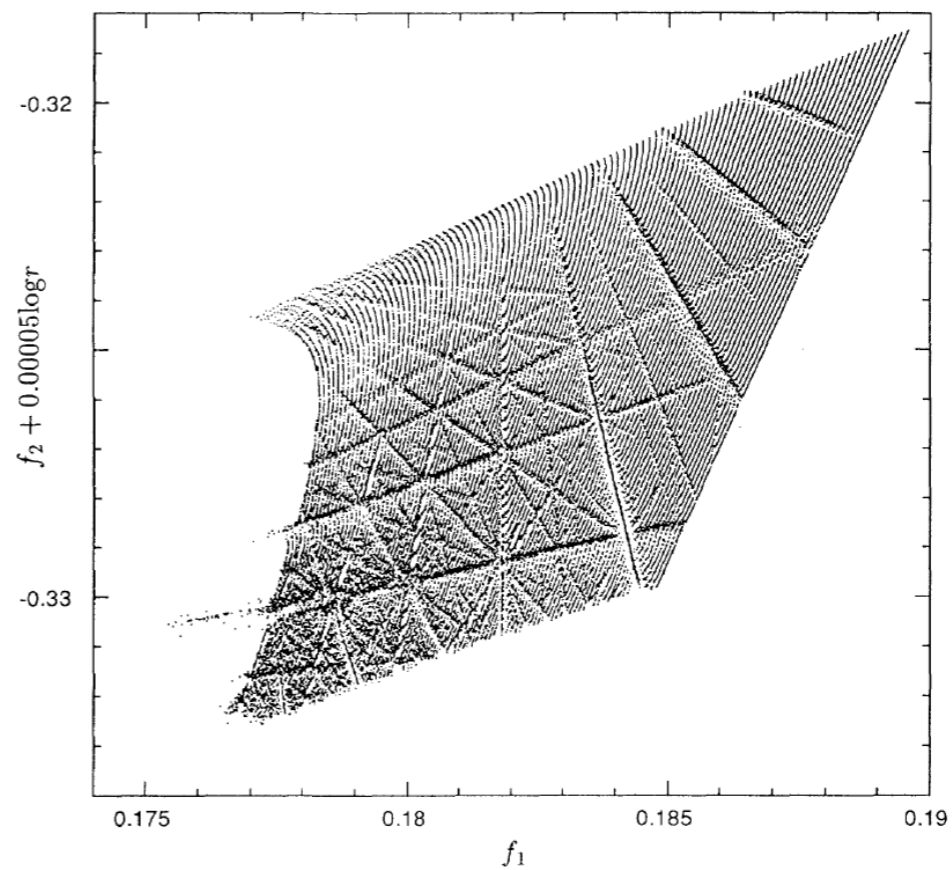
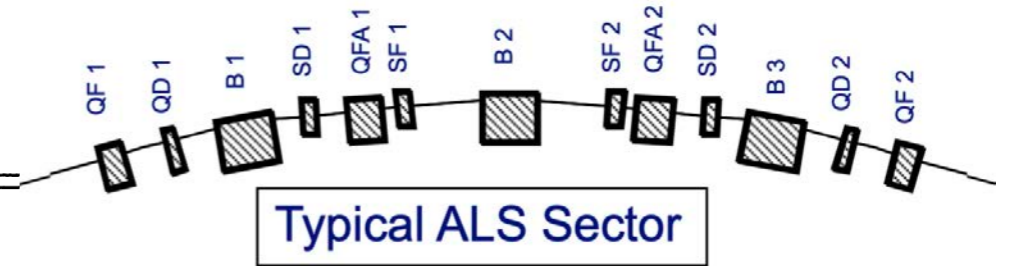


FIG. 2. Transport rates in the frequency plane. The speed and location of local transport phenomena are visualized by plotting  $f_2 + 0.00005 \log(r)$  against  $f_1$  for the same data as in Fig. 1, where  $r$  is the estimated local rate of transport (for  $r$  above a given threshold).





## Global Dynamics and Long-Time Stability in Hamiltonian Systems via Numerical Frequency Analysis

H. S. Dumas

*Department of Mathematical Sciences, University of Cincinnati, Cincinnati, Ohio 45221-0025*

J. Laskar

*Astronomie et Systèmes Dynamiques, Bureau des Longitudes, 77 av. Denfert-Rochereau, 75014 Paris, France*

(Received 18 November 1992)

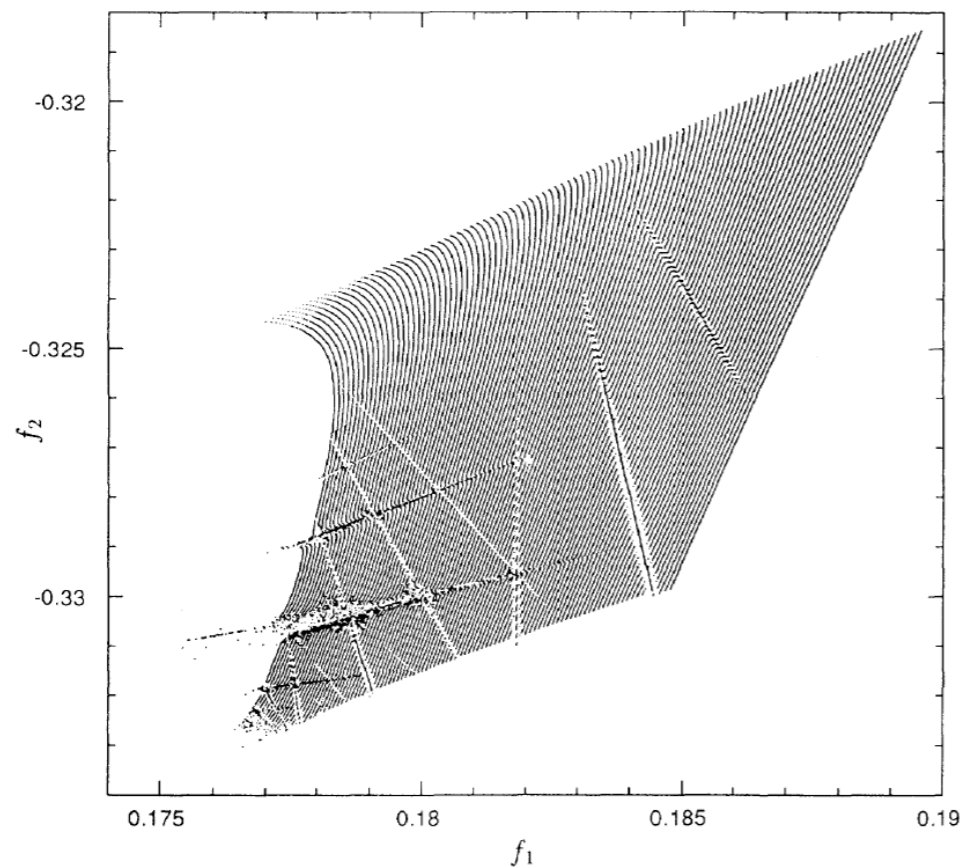


FIG. 1. Image in the frequency plane (“tune space”)  $(f_1, f_2)$  of the square sector  $0 \leq I_1, I_2 \leq 10^{-5}$ , obtained using frequency analysis over 4052 turns.

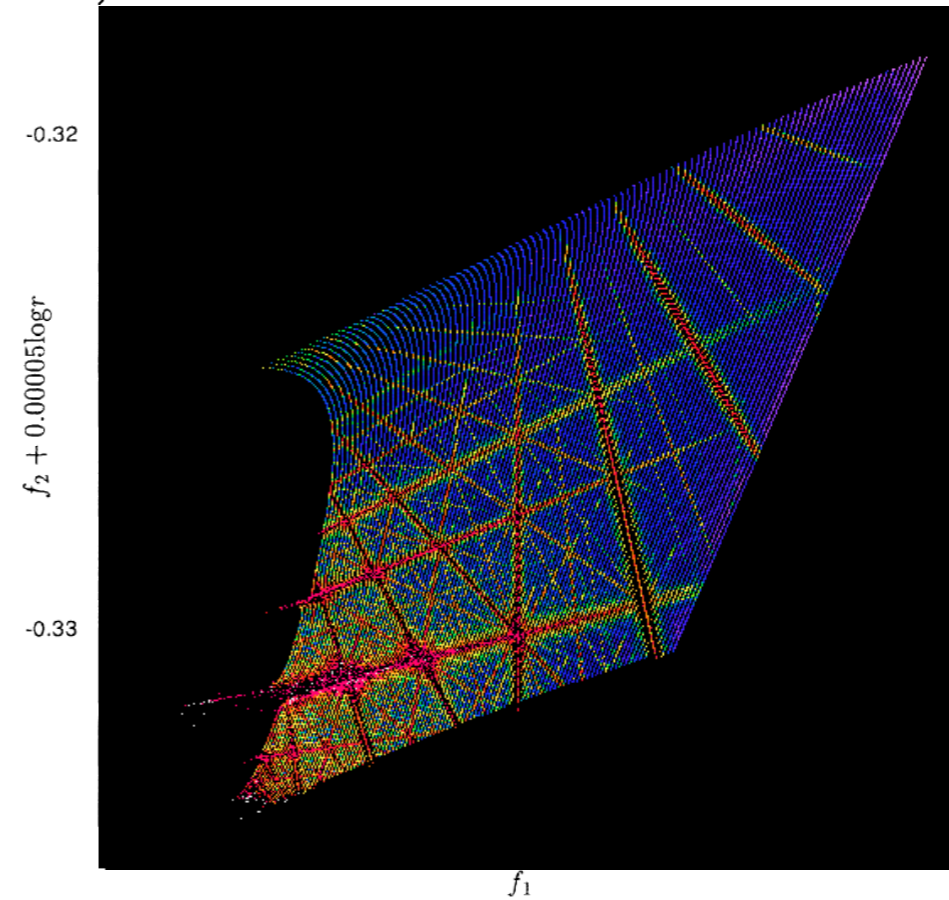


FIG. 2. Transport rates in the frequency plane. The speed and location of local transport phenomena are visualized by plotting  $f_2 + 0.00005 \log(r)$  against  $f_1$  for the same data as in Fig. 1, where  $r$  is the estimated local rate of transport (for  $r$  above a given threshold).

# Example : Superbend Upgrade

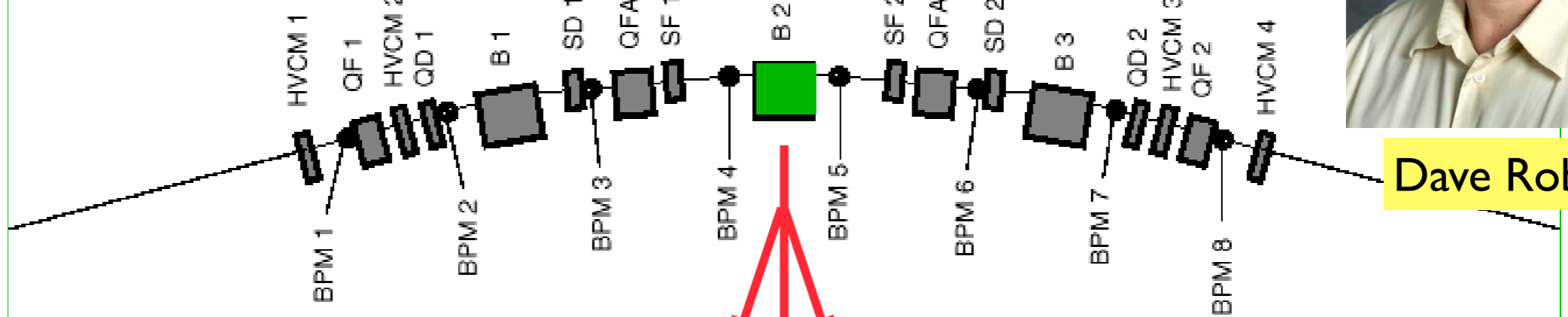
## In three of the twelve ALS Sectors

- Replaced the central **combined function dipole** with a **Superbend** and **two quadrupoles**

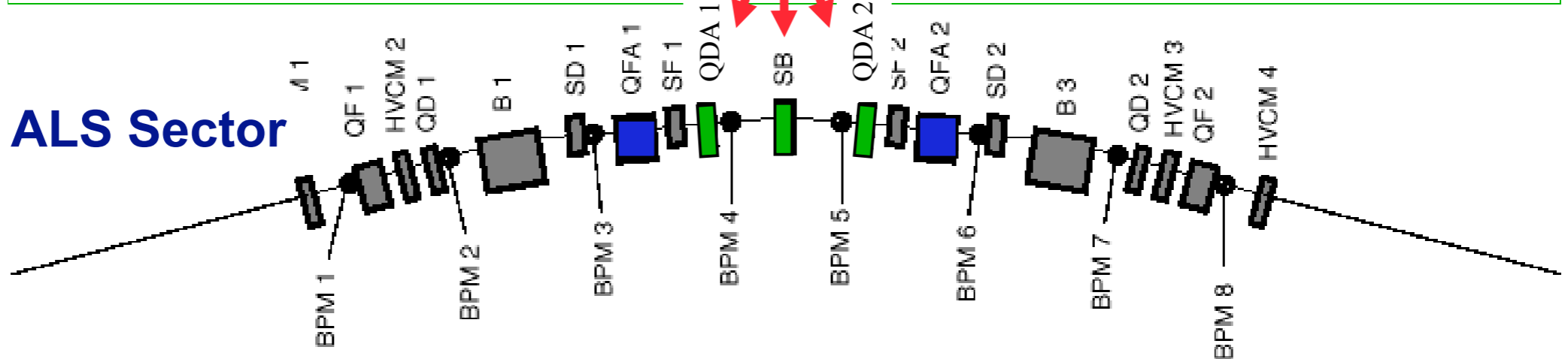


Dave Robin

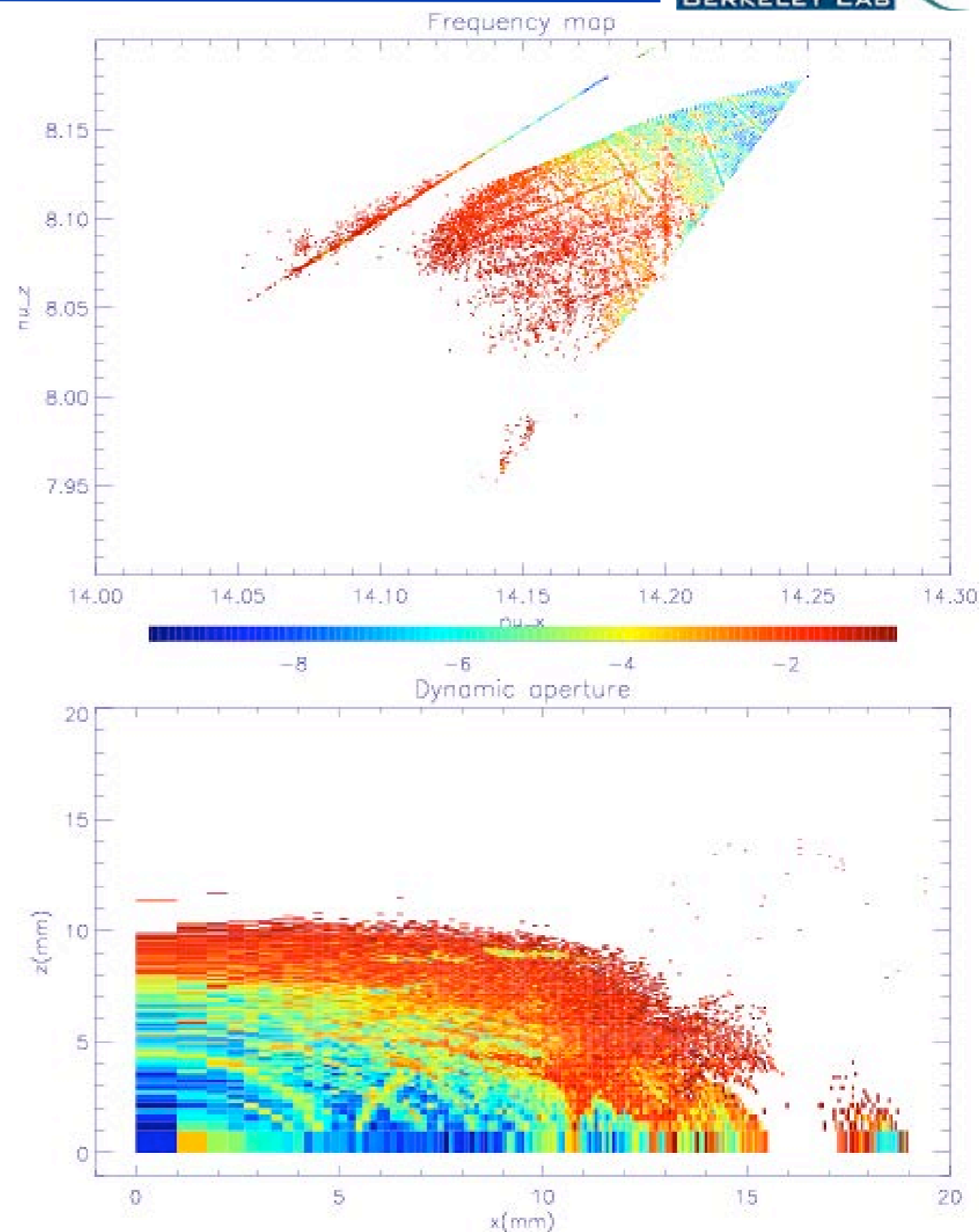
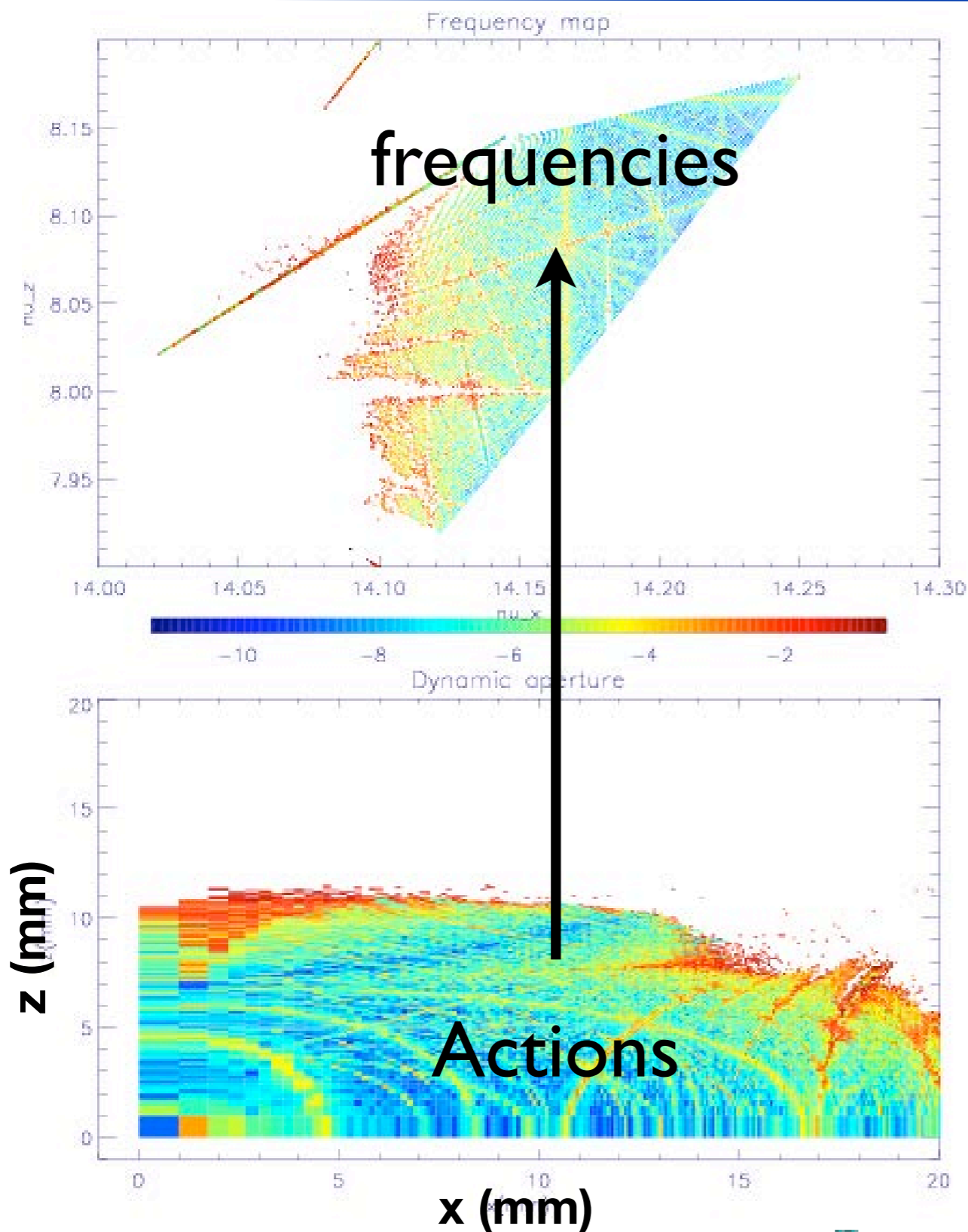
### Normal ALS Sector



### Modified ALS Sector

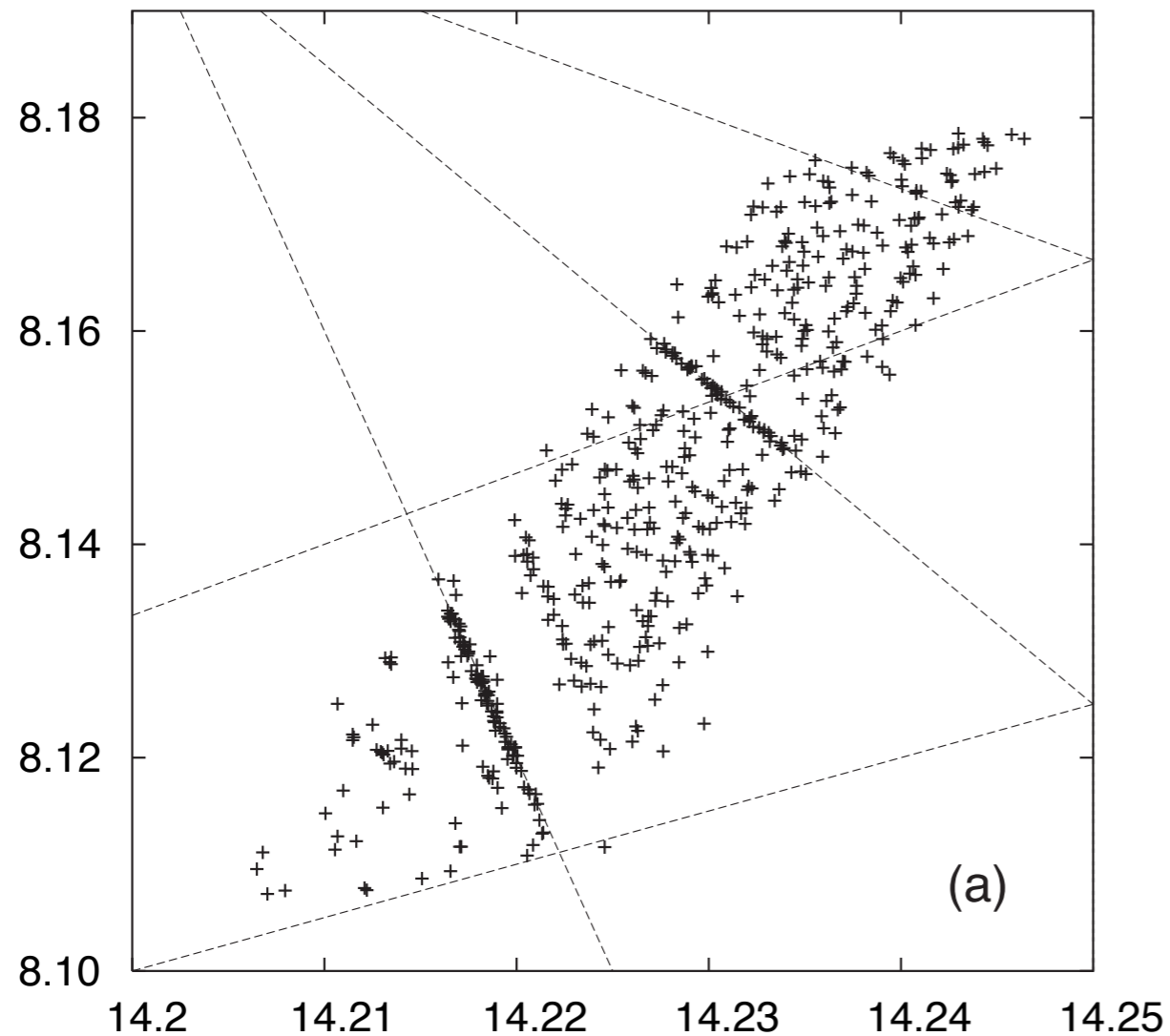


# ALS : Ideal Lattice versus Calibrated Model

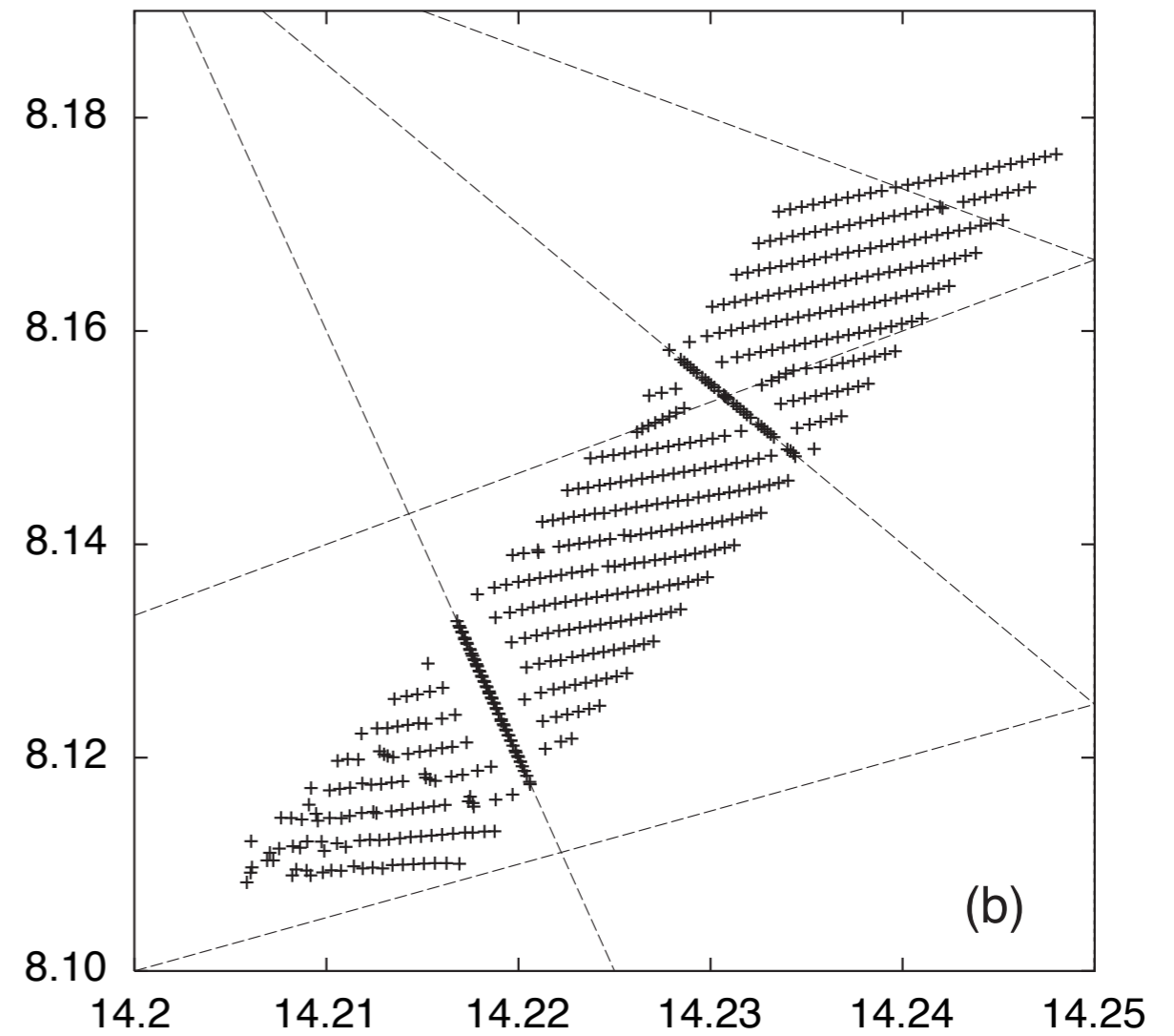


# Experimental Frequency Map at ALS

## Experiment



## Numerical model





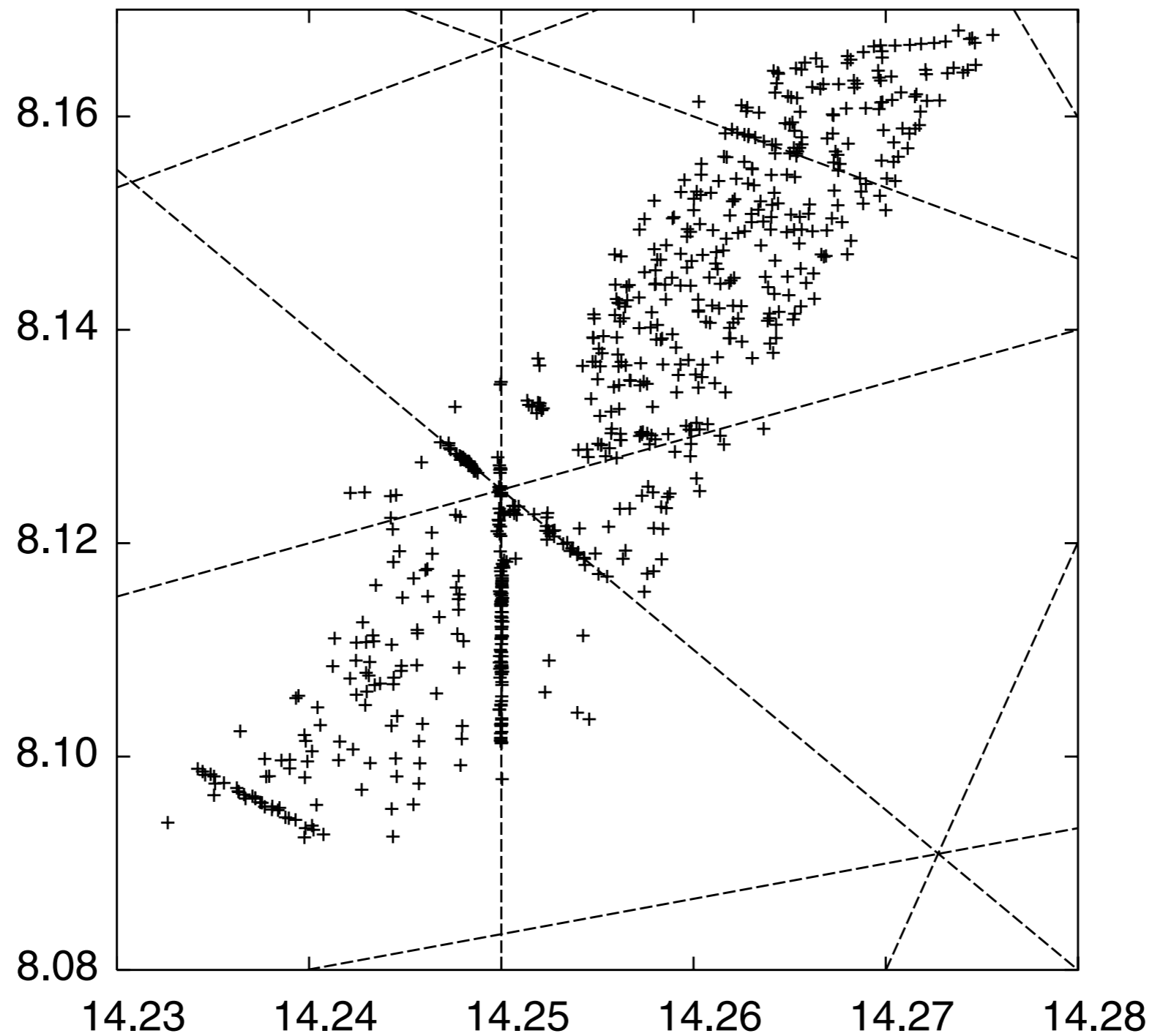


FIG. 4. Experimental frequency map for a previous setting of the ALS.

# Mapping chaos in particle revolutions

Over the past decade the technique of frequency map analysis, developed to study astronomical systems, has shown its value in an increasing number of areas, including the analysis of particle orbits in accelerators.

At first glance, any close association between the planets of the solar system – huge masses of rock, liquid and gas gently guided by gravity through the vast emptiness of space – and the mad traffic of tightly bunched particles in a circular accelerator, crushed together by fierce radiofrequency and magnetic fields, could hardly seem less likely.

Nonetheless, the dynamics of planets moving through our solar system and particles moving in accelerators do share many similar features. Both demand an analysis of the evolution of a dynamic system over a very long time – up to 1 billion revolutions for both the



*Part of the ALS storage ring at the Lawrence Berkeley National Laboratory. Frequency mapping was first applied to measured rather than simulated electron trajectories at the ALS.*

trajectories in a storage ring, at the Advanced Light Source (ALS) at the Lawrence Berkeley National Laboratory. The aim was to reveal the dynamics of an actual particle beam.

## **Chaotic motion**

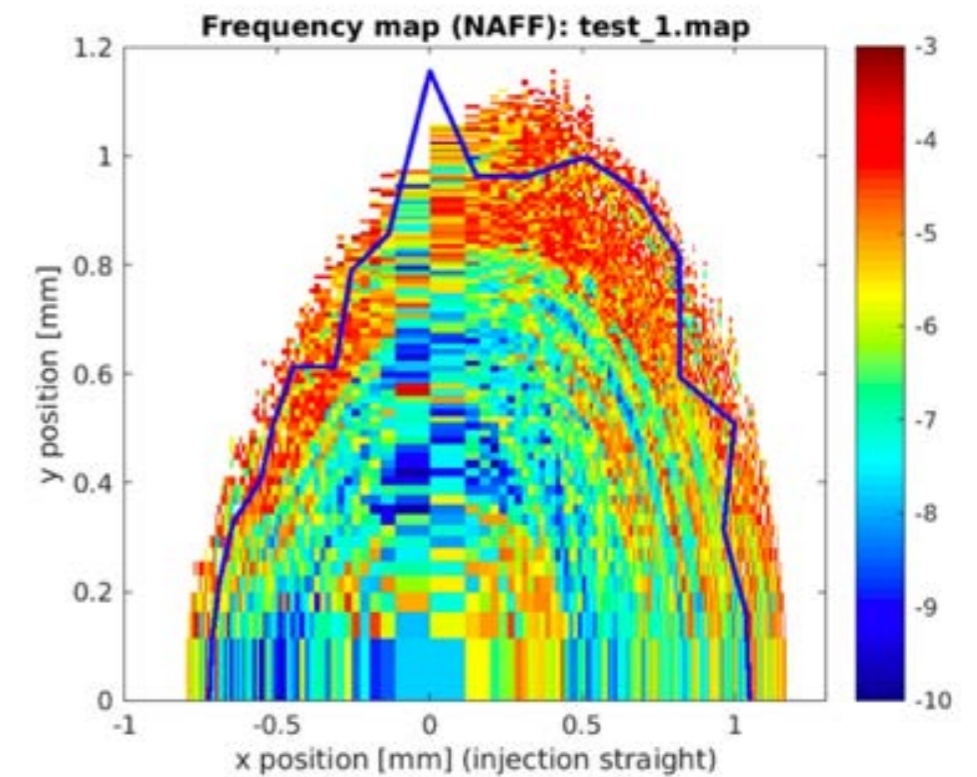
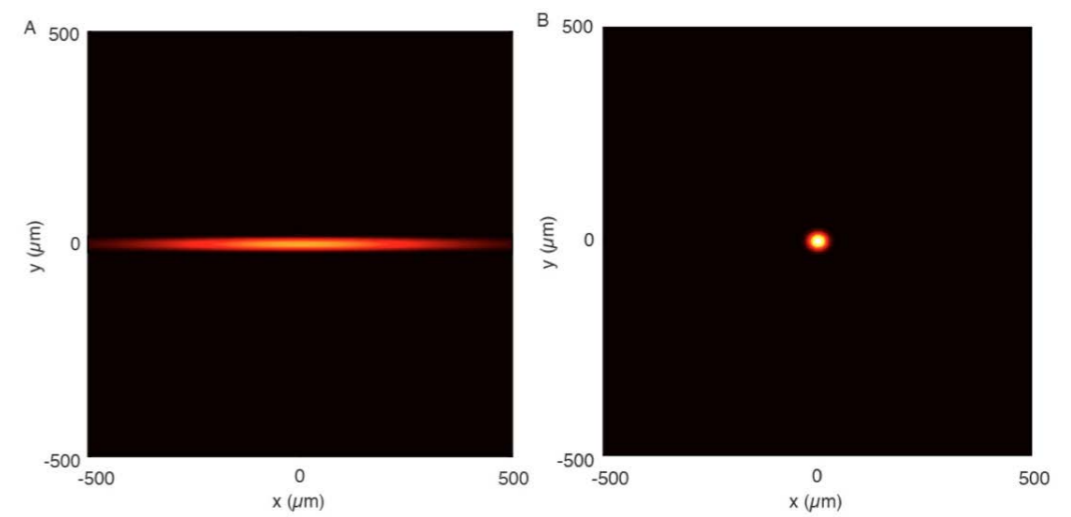
The story of frequency map analysis began in 1989 when Jacques Laskar (Bureau des Longitudes, Paris) demonstrated that the motion of the solar system is chaotic (Laskar 1989). He showed that the separation between two orbits with similar initial conditions will diverge exponentially over time (e.g. the distance between the orbits will increase



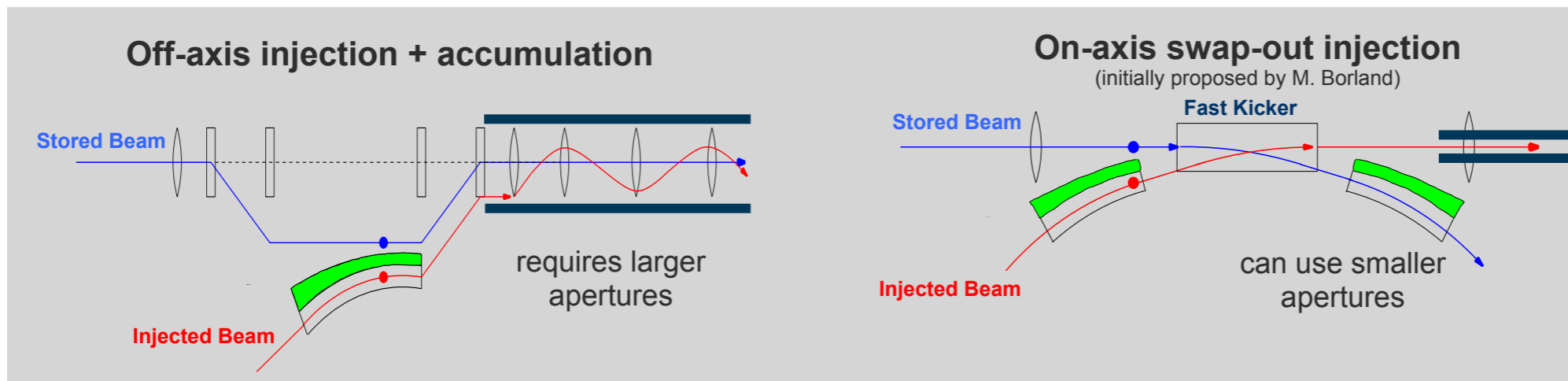
# Project Director Dave Robin Announces ALS-U Project Beamlines

JANUARY 29, 2019

Over the past year, a process involving ALS and ALS-U staff, the ALS user community, and external advisory committees has been ongoing to select the insertion-device beamlines that will be built and upgraded within the scope of the ALS-U Project. These beamlines will join existing ALS beamlines to form the full complement of capabilities that will be available at the upgraded ALS in several years. I am delighted to inform you that the selection process is now complete and to announce the result.



## ALS-U will reach soft x-ray diffraction limit up to 1.5 keV



C. Steier /ALS



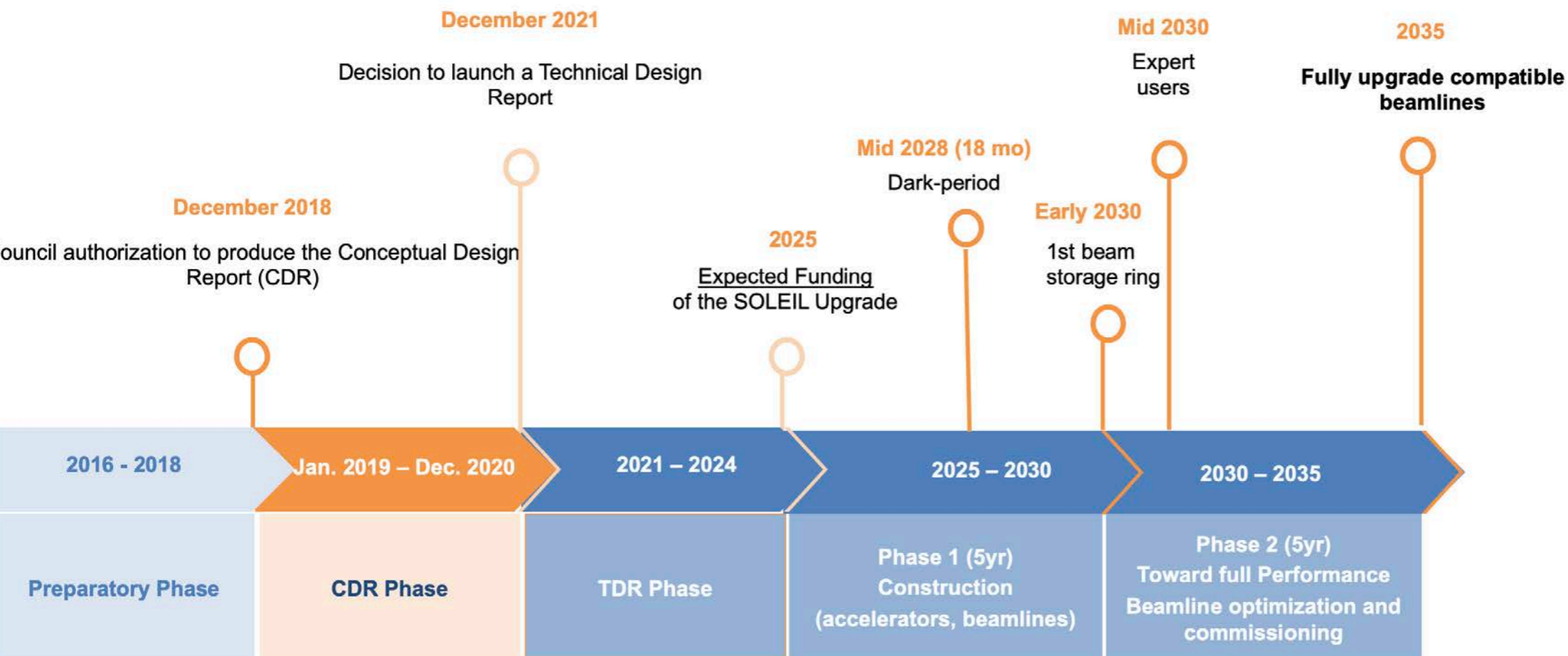


# Laurent S. Nadolski

Senior Accelerator Physicist  
Accelerators Coordinator  
Synchrotron SOLEIL, France

- Ph.D., (2001).
- “**Application of Frequency Map Analysis to the Study of Beam Dynamics**” (J. Laskar’s supervision).
- Former President of Accelerator Sect. of the French Physical Society
- SOLEIL II: nonlinear beam dynamics, robustness studies, storage ring coordination (collimation, radiation safety, machine protection interlock).

## Present SOLEIL II Timeline





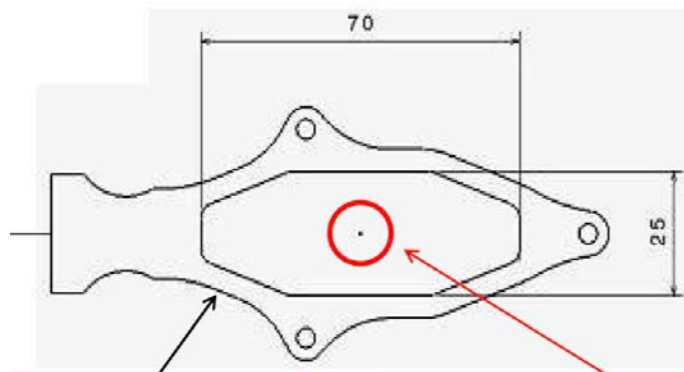
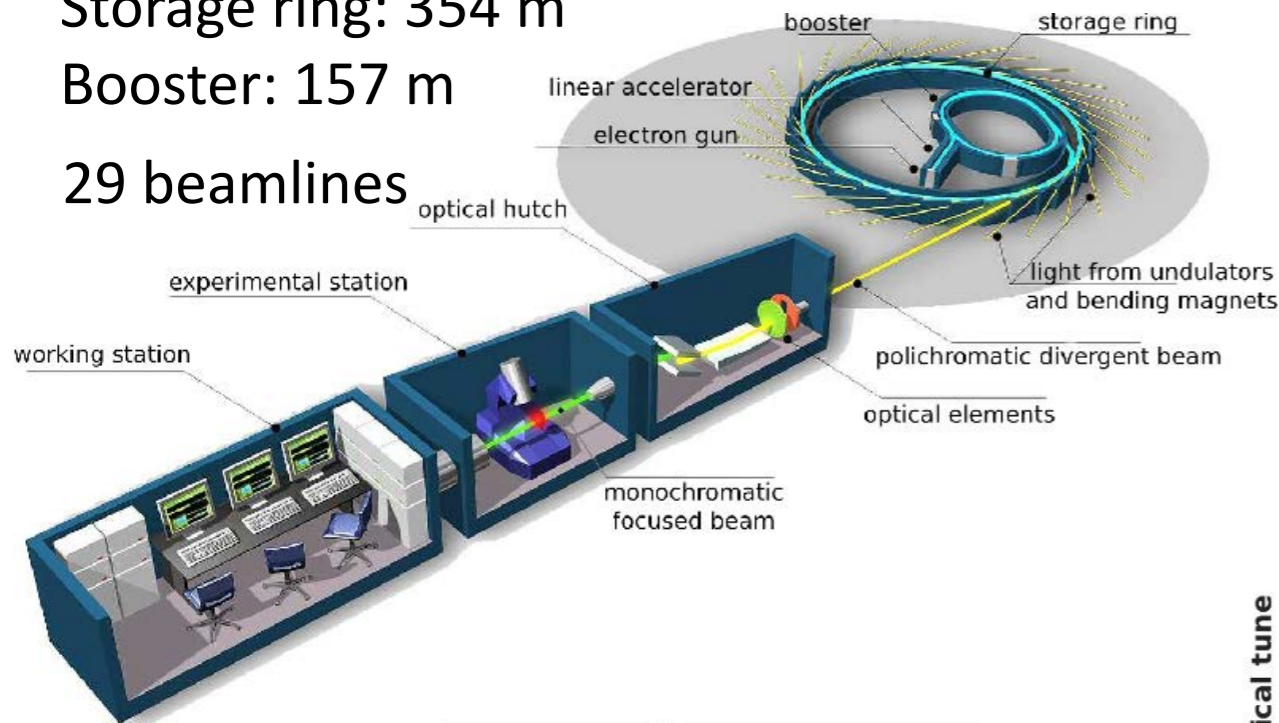


# SOLEIL II: a 4<sup>th</sup> GENERATION SYNCHROTRON LIGHT SOURCE for the Science of Tomorrow

An electron beam 40 times smaller and circular  
Photon beams at least 100 times brighter and more coherent in the X-ray range.

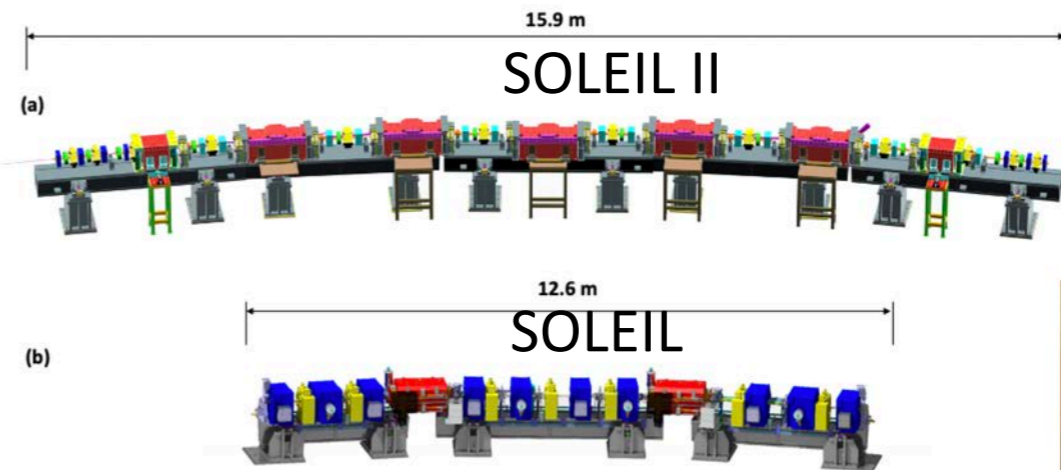
Obtaining a very compact layout:  
 Lifting of technological barriers, with the miniaturization of the vacuum chambers where the electrons circulate and of the magnets that guide them.

Storage ring: 354 m  
 Booster: 157 m  
 29 beamlines

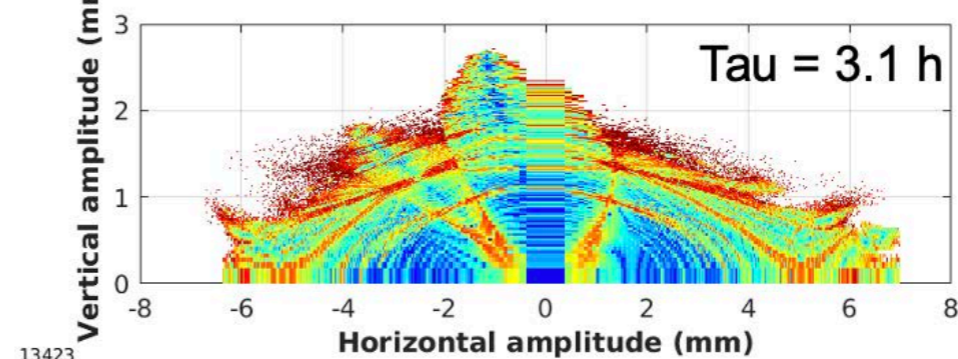
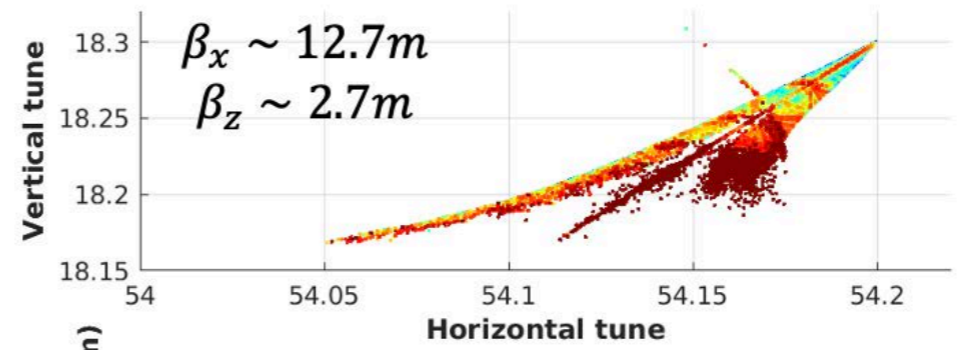


**SOLEIL today**  
 Standard vac. Chamber  
 Qpole, Spole

**SOLEIL UPGRADE project**  
 center achromat  
 ø 10 mm internal diameter

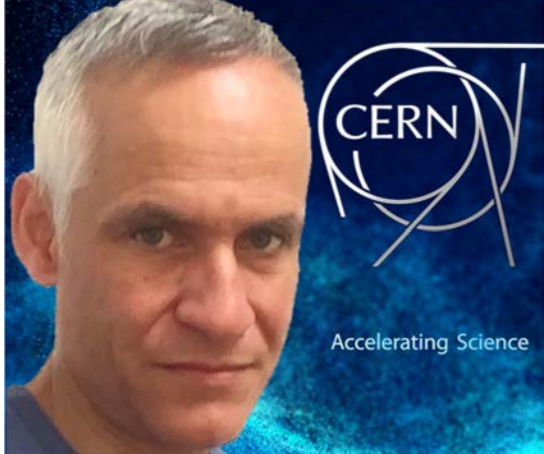


Permanent magnet quadrupole prototype (top) for SOLEIL II and Electromagnet quadrupole for SOLEIL



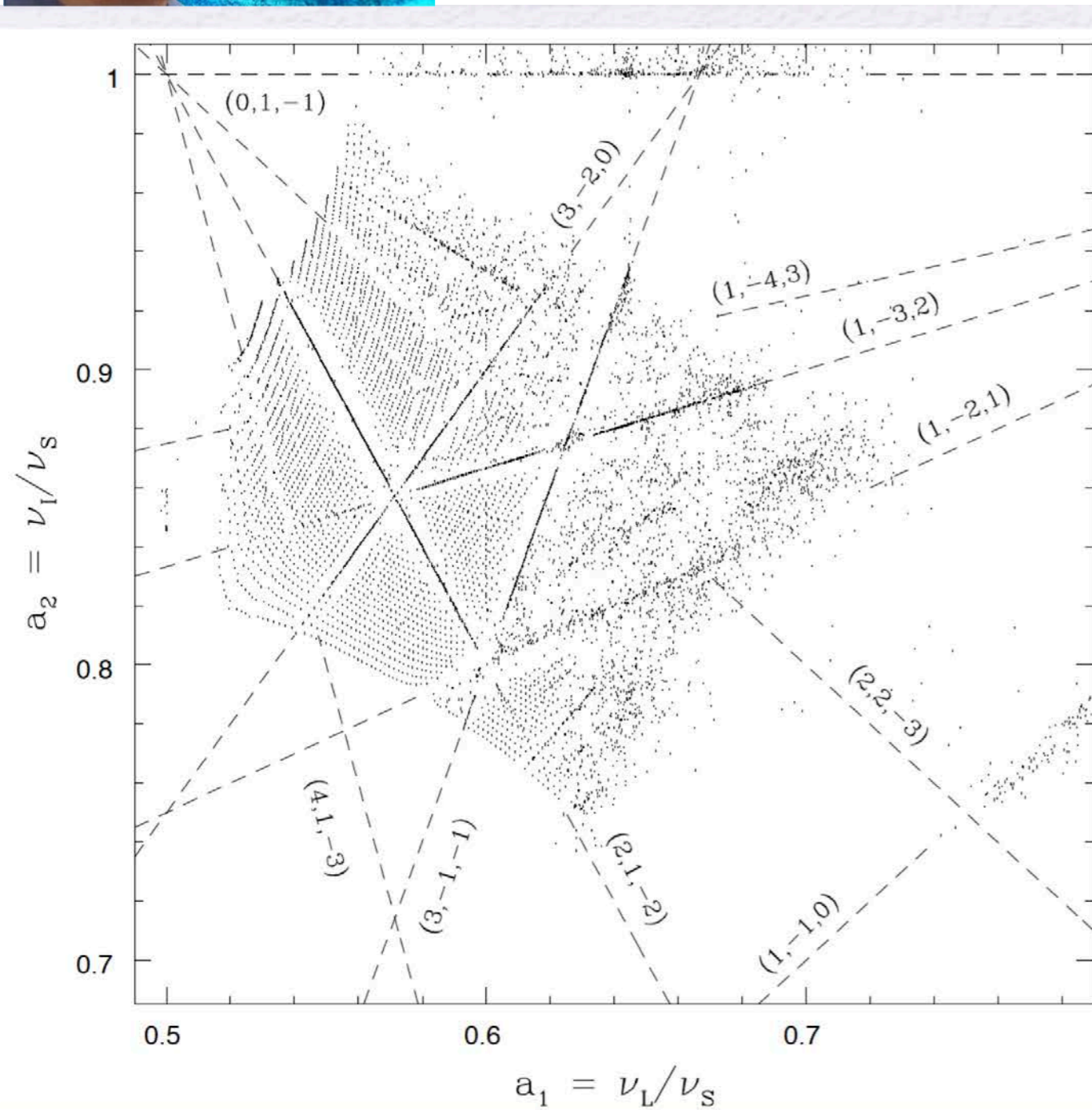
BPM prototypes for SOLEIL (bottom) and SOLEIL II (top)





Yannis Papaphilippou

PhD (1997) Application of the Frequency Map Analysis Method in Galactic Dynamics



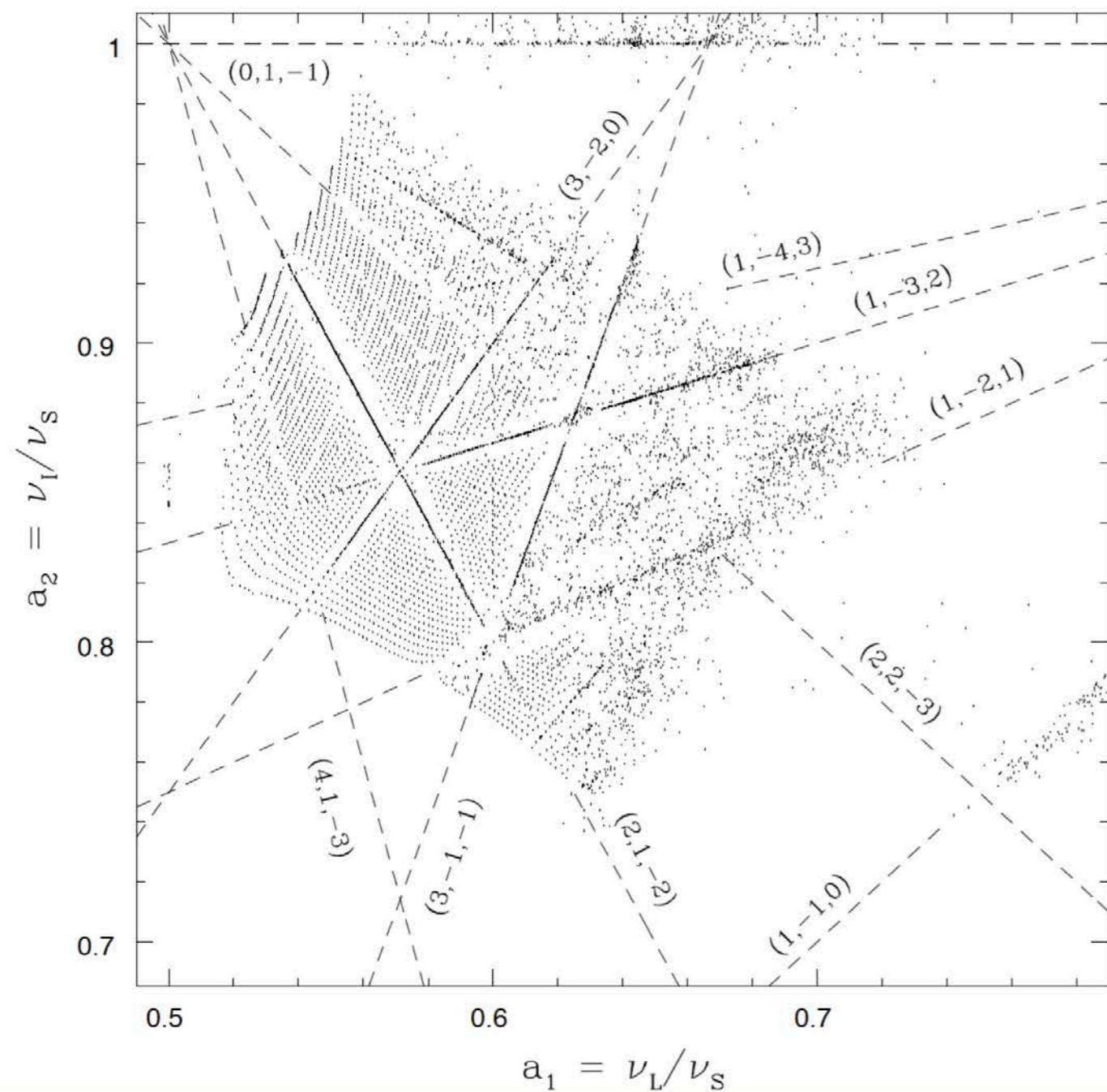
Galactic model



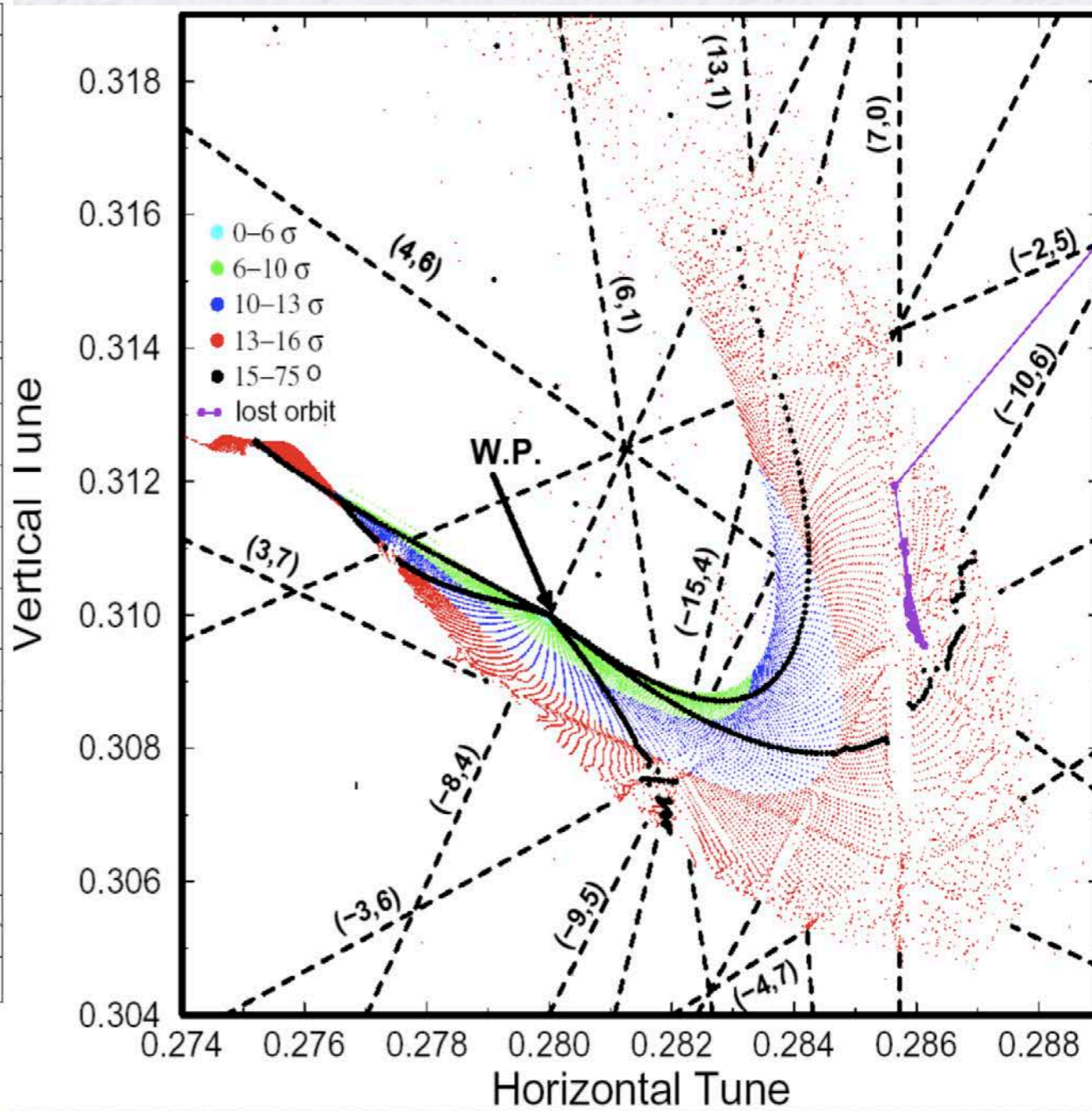


Yannis Papaphilippou

PhD (1997) Application of the Frequency Map Analysis Method in Galactic Dynamics



Galactic model



The LHC



# ABP @ CERN organisation

ABP  
Accelerators & Beam Physics  
GL: **Y. Papaphilippou**  
DGL: R. Scrivens

GAO  
S. Palluel

ABP Computing Panel  
Ch: G. Iadarola

CEI  
Coherent Effects &  
Impedances  
SL: G. Rumolo

N. Biancacci  
X. Buffat  
G. Iadarola  
L. Mether  
E. Metral  
N. Mounet  
C. Zannini  
D. Amorim (FELL)  
L. Giacomel (FELL)  
S. Lopaciuk (FELL)  
K. Paraschou (FELL)  
C. Antuono (DOCT)  
E. De La Fuente Garcia (DOCT)  
L. Giacomel (DOCT)  
S. Johannesson (DOCT)  
S. Joly (DOCT)  
C. Lannoy (DOCT)  
L. Sabato (COAS)  
L. Sito (DOCT)  
R. Soos (DOCT)  
E. Vik (TECH)

HSL  
Hadron Sources & Linacs  
SL: A. Lombardi

G. Bellodi  
S. Bertolo  
F. Di Lorenzo  
D. Kuchler  
J.-B. Lallement  
J. Lettry  
E. Mahner  
C. Mastrostefano  
M. O'Neil  
E. Sargsyan  
F. Wenander  
M. Koopmans (FELL)  
A. Mamaras (DOCT)  
E. Pasino (DOCT)  
J. Thiboud (FSU)  
N. Van Woudenberg (TECH)

INC  
Incoherent Effects  
SL: H. Bartosik

F. Asvesta  
S. Kostoglou  
I. Efthymiopoulos  
D. Gamba  
G. Sterbini  
D. Colas (FELL)  
T. Prebibaj (FELL)  
G. Russo (FELL)  
P. Belanzer (COAS)  
M. Bozatzis (TECH)  
A. Fornara (COAS)  
H. Huttunen (TECH)  
M. Krasny (PJAS)  
P. Kruyt (DOCT)  
E. Lamb (DOCT)  
I. Mases Sole (DOCT)  
A. Radoslavova (TECH)  
M. Rufolo (TECH)  
E. Waagaard (DOCT)  
D. Zeitz (TECH)

LAF  
Lepton Accelerators &  
Facilities  
SL: E. Gschwendtner

C. Carli  
R. Corsini  
W. Farabolini  
B. Holzer  
A. Latina  
G. Roy  
D. Schulte  
M. Turner  
F. Zimmermann  
K. Andre (FELL)  
V. Cilento (FELL)  
E. Fol (FELL)  
M. Hofer (FELL)  
A. Malyzhenkov (FELL)  
A. Pastushenko (FELL)  
K. Skoufaris (FELL)  
L. Verra (FELL)  
Y. Zhao (FELL)  
A. Aksoy (PJAS)  
P. Desire Valdor (TECH)  
J. Farmer (COAS)  
S. Jagabathuni (DOCT)  
P. Korysko (COAS)  
V. Mussat (DOCT)  
K. Oide (COAS)  
J. Olivares Herrador (DOCT)  
F. Pannell (COAS)  
P. Raimondi (SASS)  
V. Rieker (DOCT)  
J. Salvesen (DOCT)  
B. Stechauner (DOCT)  
N. Van Gils (DOCT)  
T. Von Witzleben (DOCT)  
G. Zevi Della Porta (PJAS)

LNO  
Linear & Non-linear Optics  
SL: R. Tomas

F. Carlier  
R. De Maria  
L. Deniau  
S. Fartoukh  
E. Maclean  
J. Dilly (FELL)  
J. Keintzel (FELL)  
A. Wegscheider (FELL)  
I. Angelis (DOCT)  
A. Borjesson Carazzo (TECH)  
F. Chuboda (TECH)  
V. Ferrentino (DOCT)  
C. Garcia Jaimes (COAS)  
J. Gray (TECH)  
S. Horney (DOCT)  
S. Lampaki (TECH)  
M. Le Garreg (DOCT)  
E. Manosperti (DOCT)  
T. Nissinen (TECH)  
G. Simon (DOCT)  
W. Van Goethem (DOCT)  
L. Van Riesen-Haupt (COAS)

NDC  
Non-linear Dynamics &  
Collimation  
SL: S. Redaelli

R. Alemany Fernandez  
R. Bruce  
M. Giovannozzi  
P. Hermes  
F. Van Der Veken  
A. Abramov (FELL)  
M. D'Andrea (FELL)  
K. Dewhurst (FELL)  
B. Lindstorm (FELL)  
G. Perez Segurana (FELL)  
T. Pugnati (FELL)  
M. Slupecki (FELL)  
N. Triantafyllou (FELL)  
C. Beaubis (COAS)  
G. Broggi (DOCT)  
R. Cai (DOCT)  
D. Di Croce (COAS)  
C. Montanari (PJAS)  
M. Rakic (DOCT)  
D. Veres (DOCT)  
S. Wang (COAS)

~50 Staff,

~30 Fellows

~50 Students

~20 Associates

~80 Visitors and  
External collaborators





# Goal of High-Luminosity LHC



*Y. Papaphilippou*

# Goal of High-Luminosity LHC

Prepare machine for operation beyond 2025 and up to **2035**

# Goal of High-Luminosity LHC

Prepare machine for operation beyond 2025 and up to **2035**

Devise beam parameters and operation scenarios for enabling at total integrated luminosity of **3000 fb<sup>-1</sup>**

# Goal of High-Luminosity LHC

Prepare machine for operation beyond 2025 and up to **2035**

Devise beam parameters and operation scenarios for enabling at total integrated luminosity of **3000 fb<sup>-1</sup>**

→ 10 times the luminosity reach over first 10 years of LHC operation

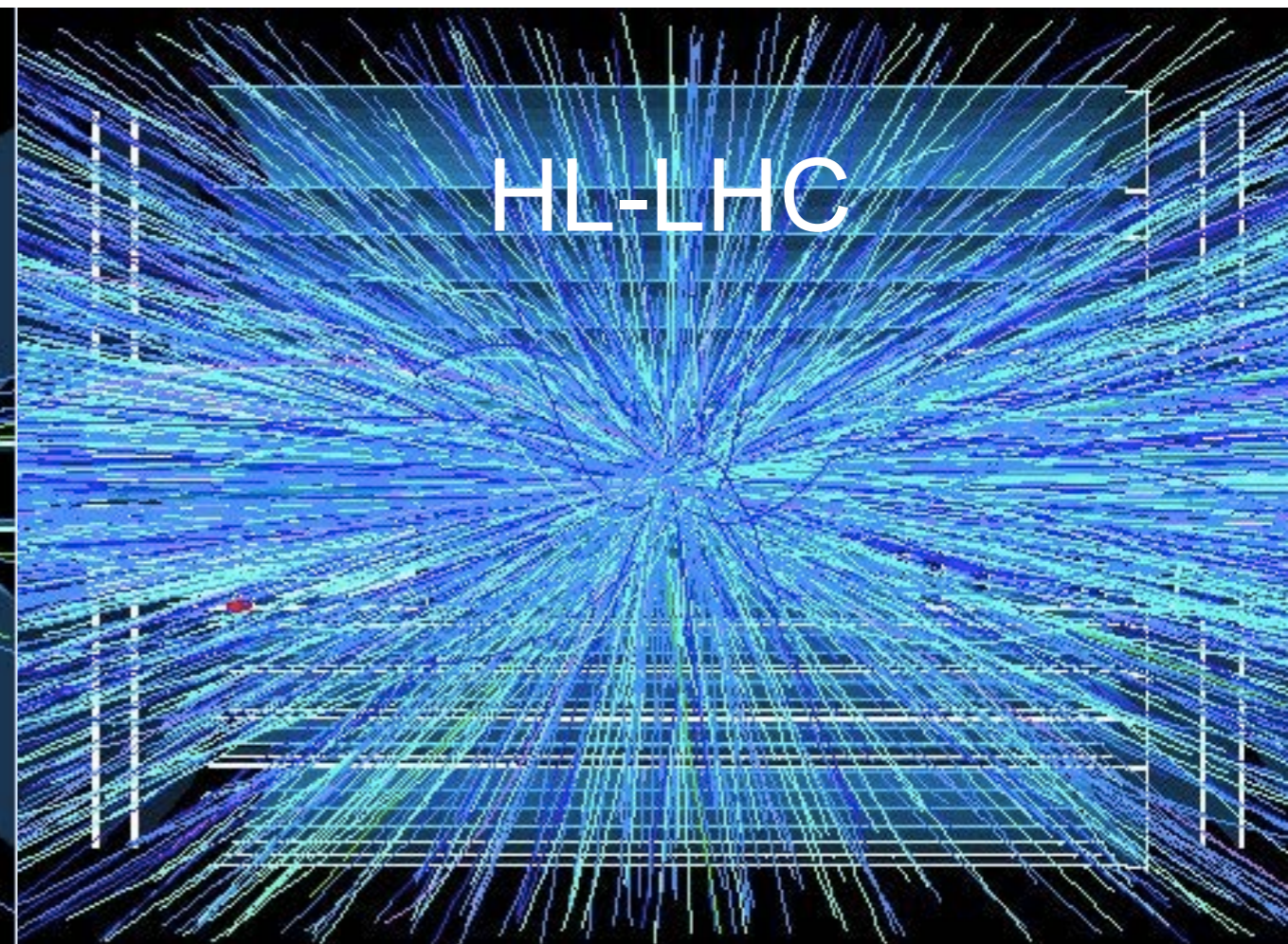
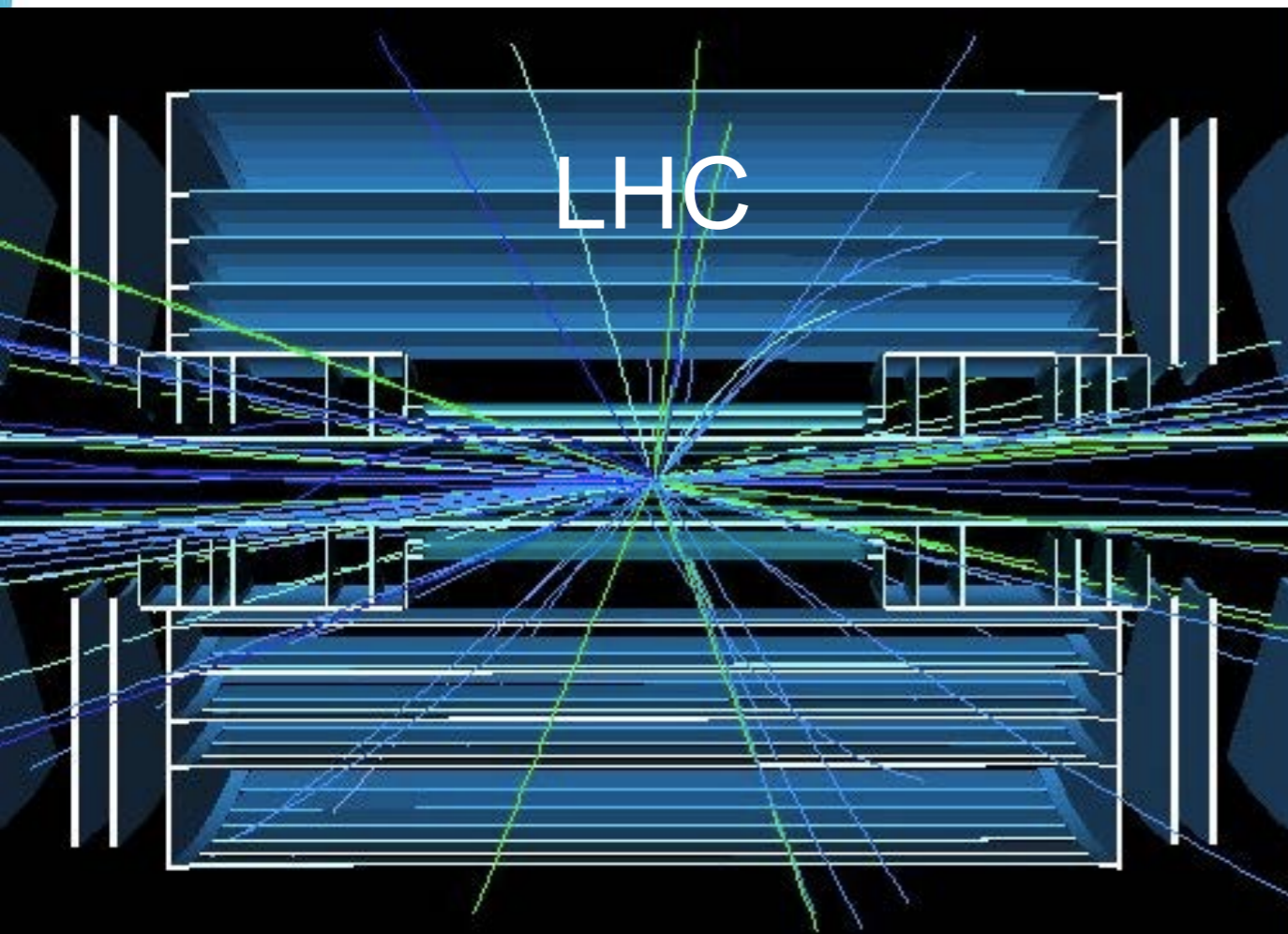


# Goal of High-Luminosity LHC

Prepare machine for operation beyond 2025 and up to **2035**

Devise beam parameters and operation scenarios for enabling at total integrated luminosity of **3000 fb<sup>-1</sup>**

→ 10 times the luminosity reach over first 10 years of LHC operation





# Beam-Beam interaction

Variable	Symbol	Value
Beam energy	$E$	7 TeV
Particle species	...	protons
Full crossing angle	$\theta_c$	300 $\mu$ rad
rms beam divergence	$\sigma_x^l$	31.7 $\mu$ rad
rms beam size	$\sigma_x$	15.9 $\mu$ m
Normalized transv. rms emittance	$\gamma\varepsilon$	3.75 $\mu$ m
IP beta function	$\beta^*$	0.5 m
Bunch charge	$N_b$	$(1 \times 10^{11} - 2 \times 10^{12})$
Betatron tune	$Q_0$	0.31

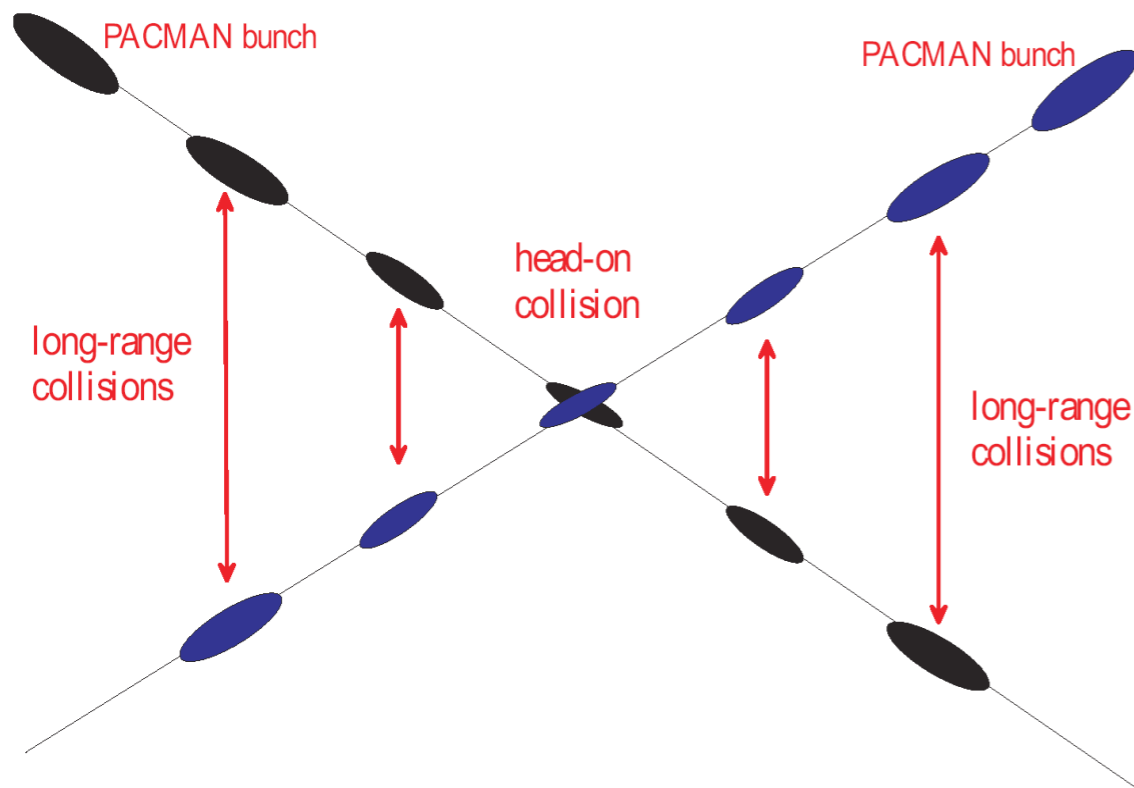
- Long range beam-beam interaction represented by a 4D kick-map

$$\Delta x = -n_{par} \frac{2r_p N_b}{\gamma} \left[ \frac{x' + \theta_c}{\theta_t^2} \left( 1 - e^{-\frac{\theta_t^2}{2\theta_{x,y}^2}} \right) - \frac{1}{\theta_c} \left( 1 - e^{-\frac{\theta_c^2}{2\theta_{x,y}^2}} \right) \right]$$

$$\Delta y = -n_{par} \frac{2r_p N_b}{\gamma} \frac{y'}{\theta_t^2} \left( 1 - e^{-\frac{\theta_t^2}{2\theta_{x,y}^2}} \right)$$

with

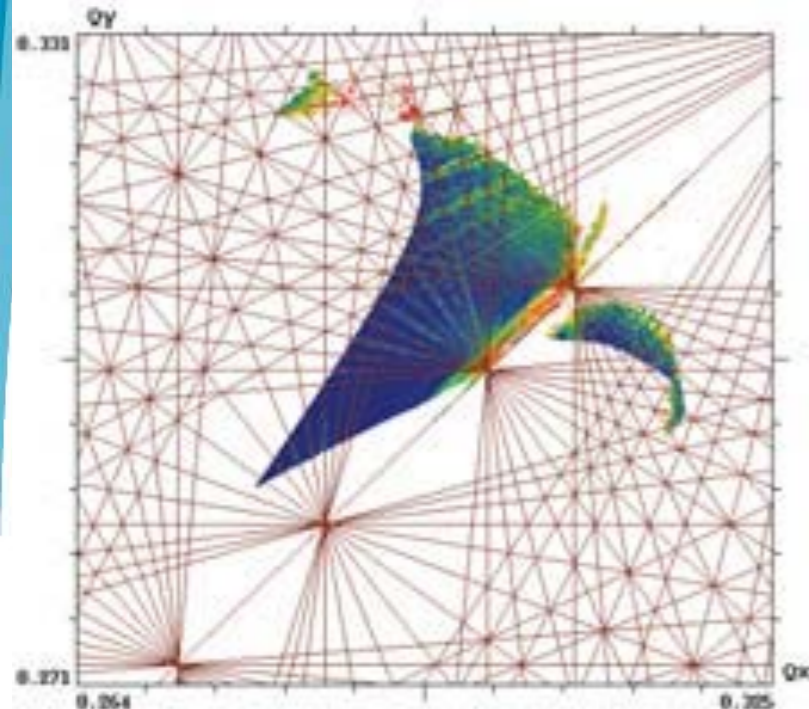
$$\theta_t \equiv \left( (x' + \theta_c)^2 + y'^2 \right)^{1/2}$$



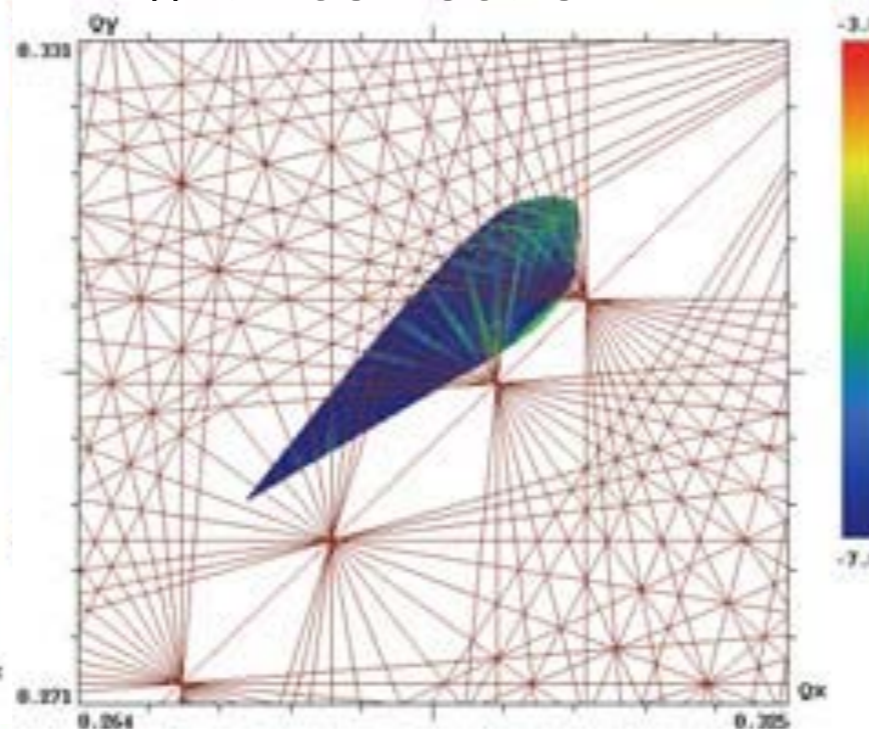


# Wire compensation

Without correction



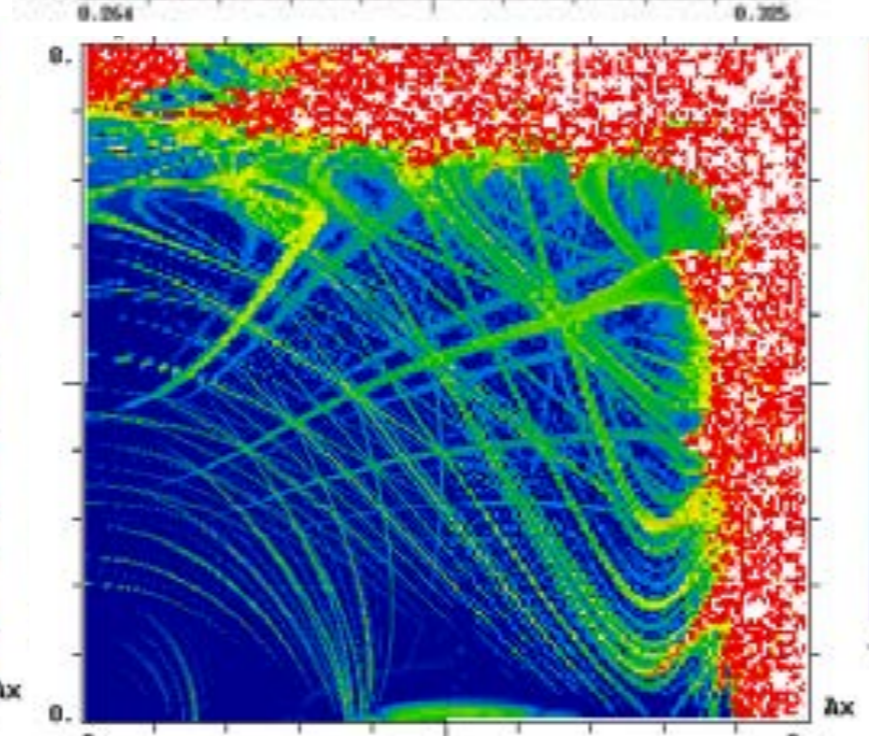
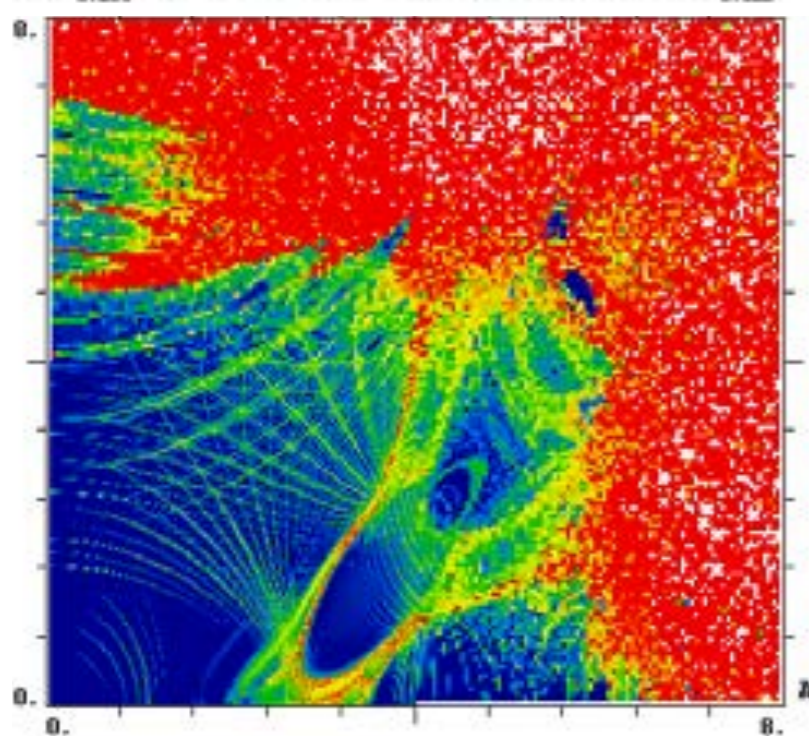
With correction



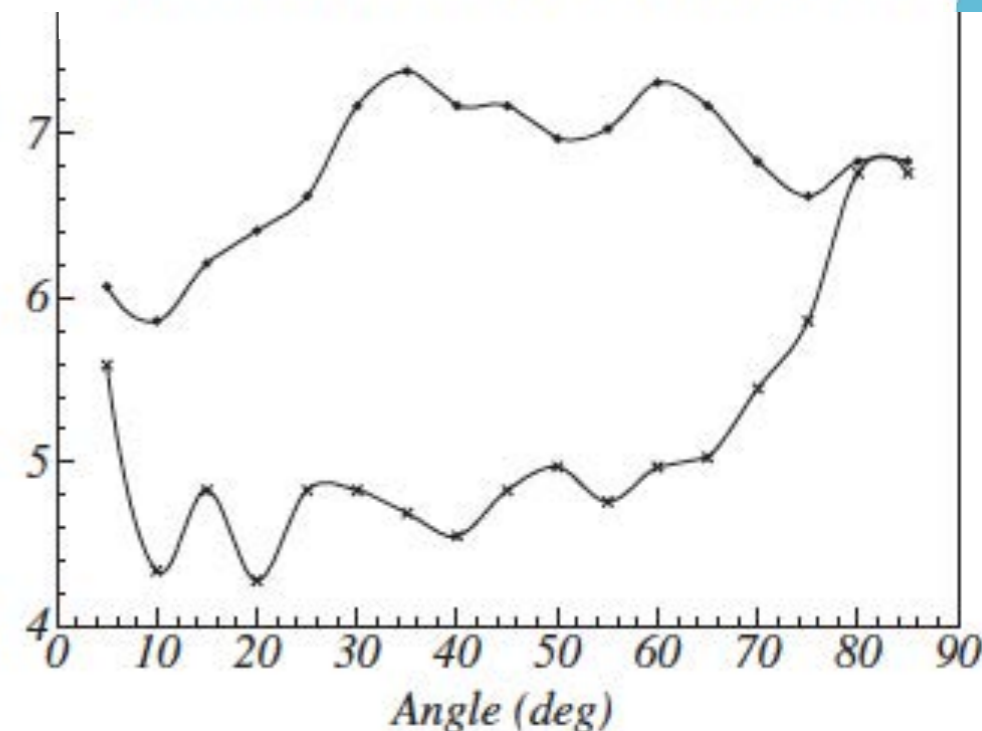
- Current baring wire can **improve DA by 1-2  $\sigma$**
- Tests in the LHC during 2017-2018

Reduced crossing angle of  $450\mu\text{rad}$  @ 15cm

S. Fartoukh, al., PRSTAB, 2015



- Nominal bunches with wire correction
- Nominal bunches without wire correction

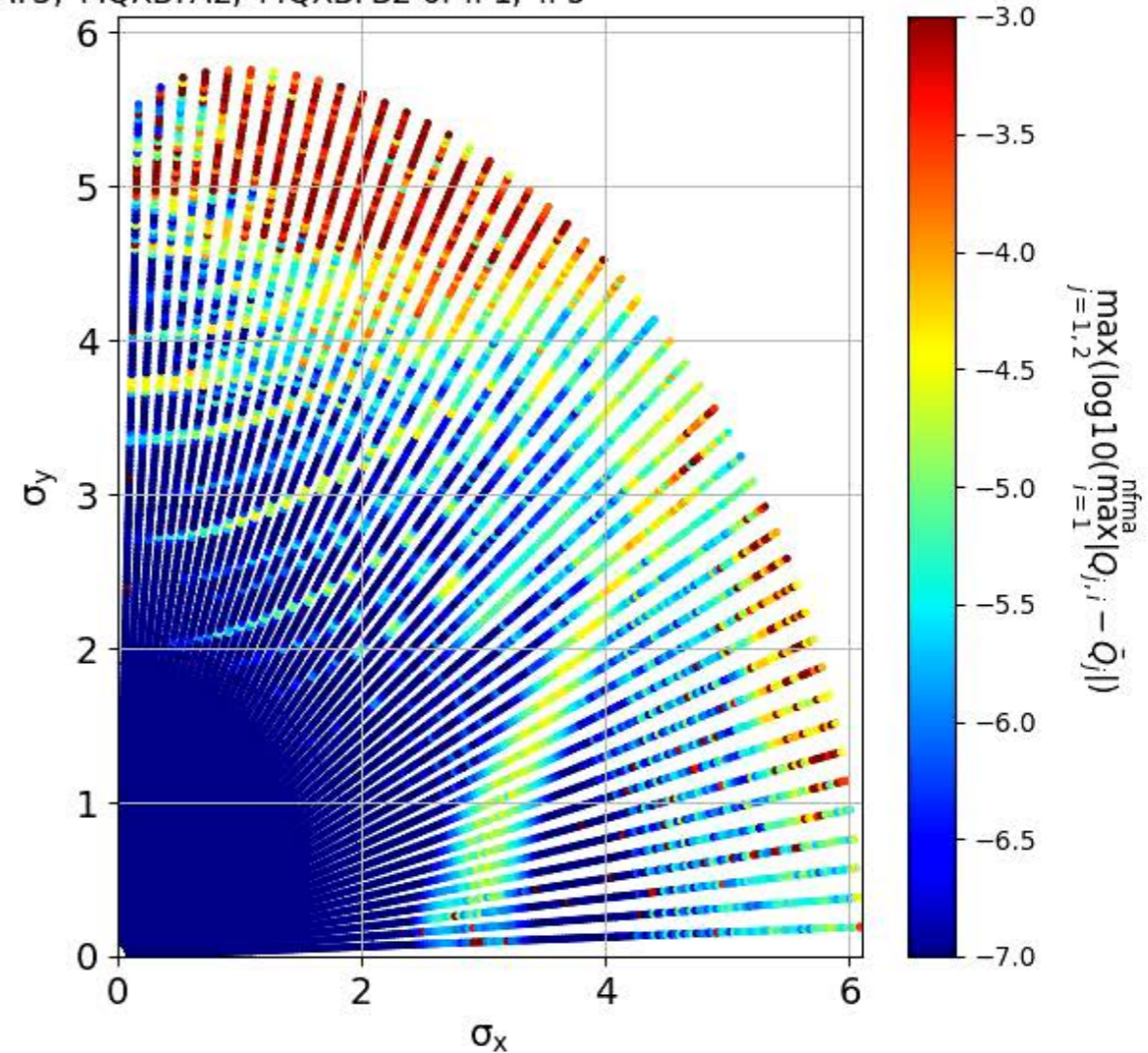
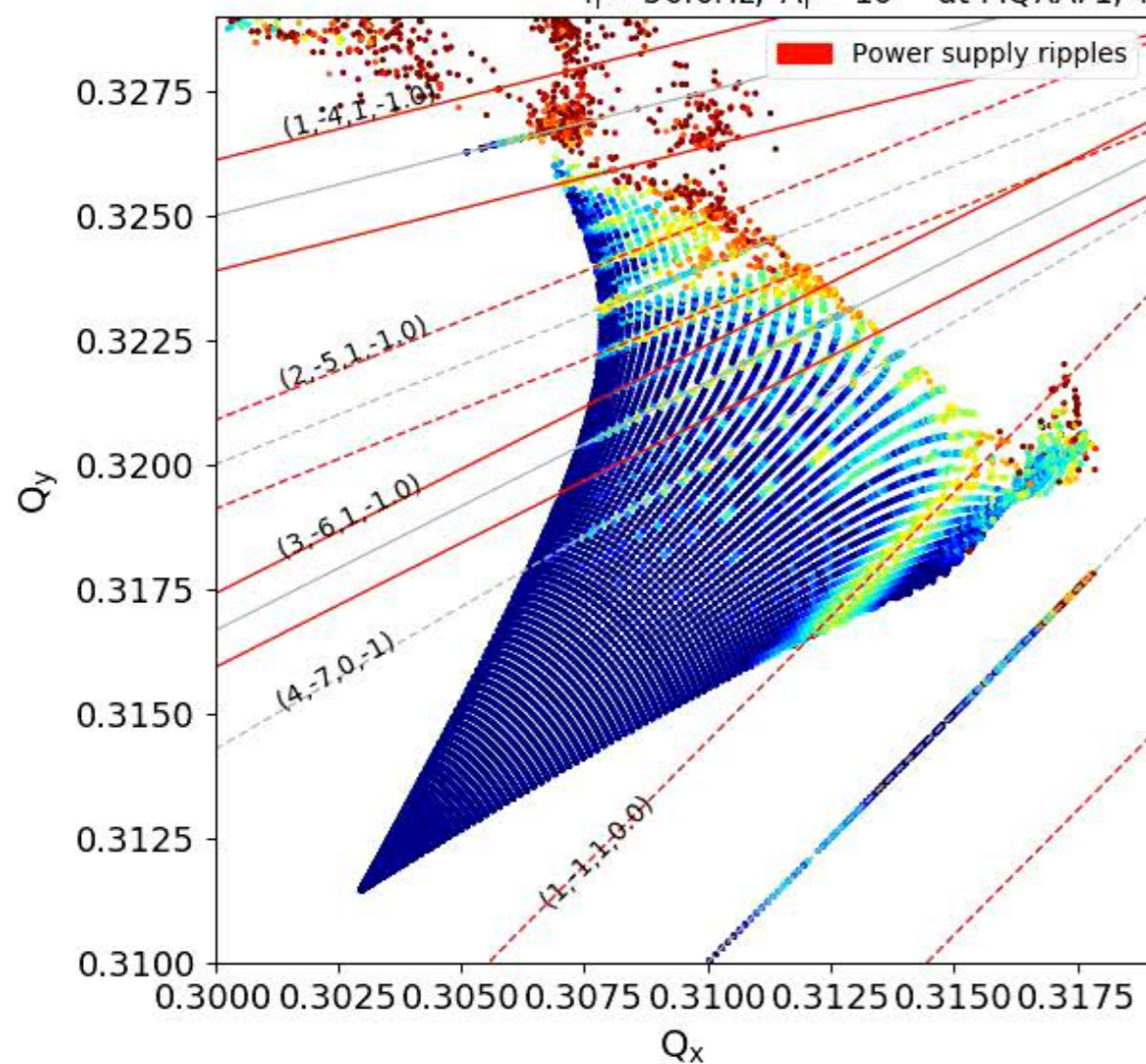




# LHC: Power supply ripples (5D)

□ Scan of different ripple frequencies **(50-900 Hz)**

5D,  $E = 6.5\text{TeV}$ ,  $I_{\text{oct}} = 510\text{A}$ , Beam – beam ON,  $\epsilon_n = 2.5\mu\text{m}$ ,  $\beta^* = 40\text{cm}$ ,  $q = 15$   
 $(Q_x, Q_y) = (62.31, 60.32)$ ,  $V_{\text{RF}}$  OFF,  $\delta p = 27e - 5$ , 49 angles,  $0.1 - 6.1 \sigma$ , sliding NAFF  
 $f_r = 50.0\text{Hz}$ ,  $A_r = 10^{-7}$  at MQXA. 1, MQXA. 3, MQXB. A2, MQXB. B2 of IP1, IP5

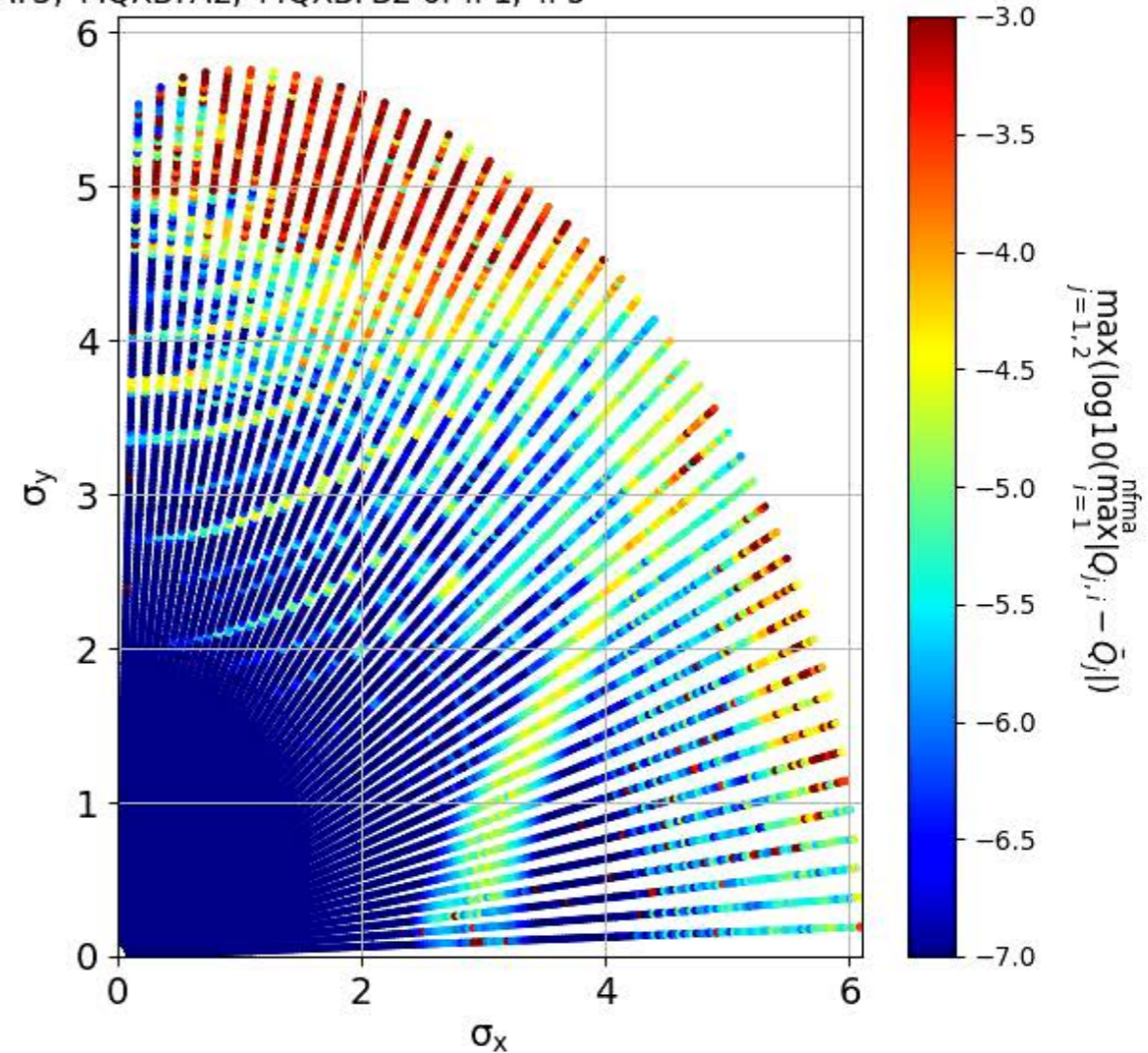
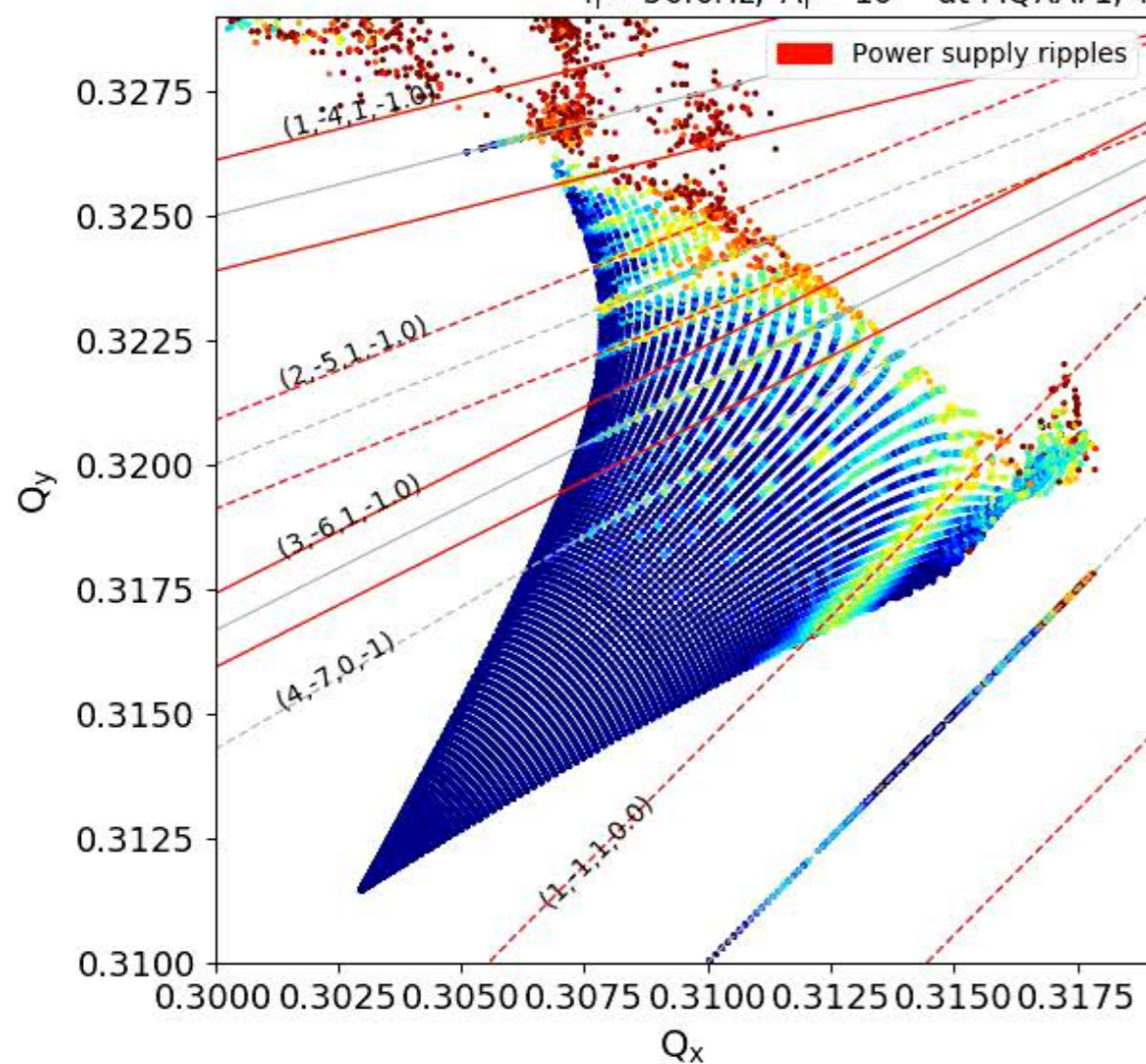




# LHC: Power supply ripples (5D)

□ Scan of different ripple frequencies **(50-900 Hz)**

5D,  $E = 6.5\text{TeV}$ ,  $I_{\text{oct}} = 510\text{A}$ , Beam – beam ON,  $\epsilon_n = 2.5\mu\text{m}$ ,  $\beta^* = 40\text{cm}$ ,  $q = 15$   
 $(Q_x, Q_y) = (62.31, 60.32)$ ,  $V_{\text{RF}}$  OFF,  $\delta p = 27e - 5$ , 49 angles,  $0.1 - 6.1 \sigma$ , sliding NAFF  
 $f_r = 50.0\text{Hz}$ ,  $A_r = 10^{-7}$  at MQXA. 1, MQXA. 3, MQXB. A2, MQXB. B2 of IP1, IP5

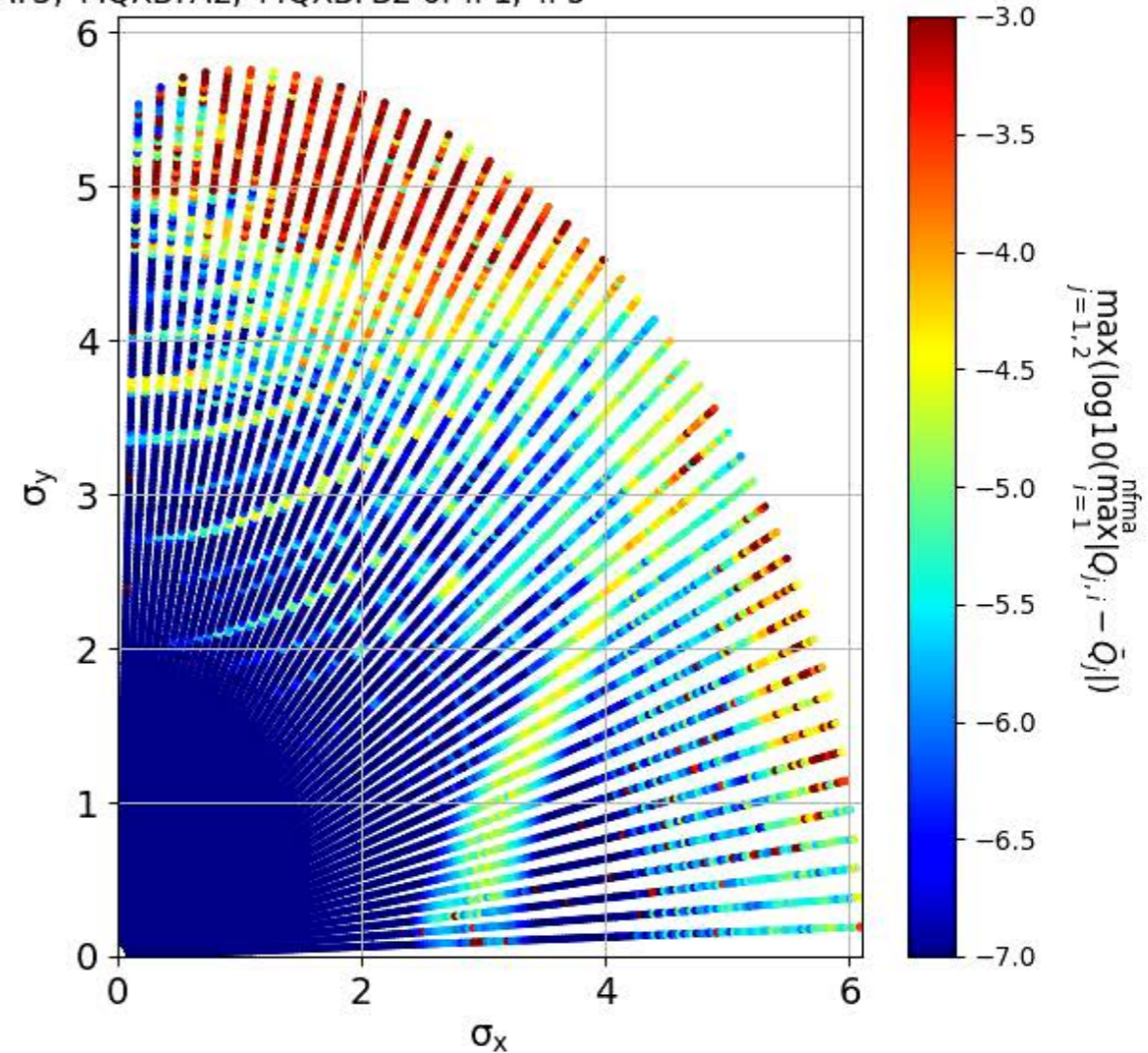
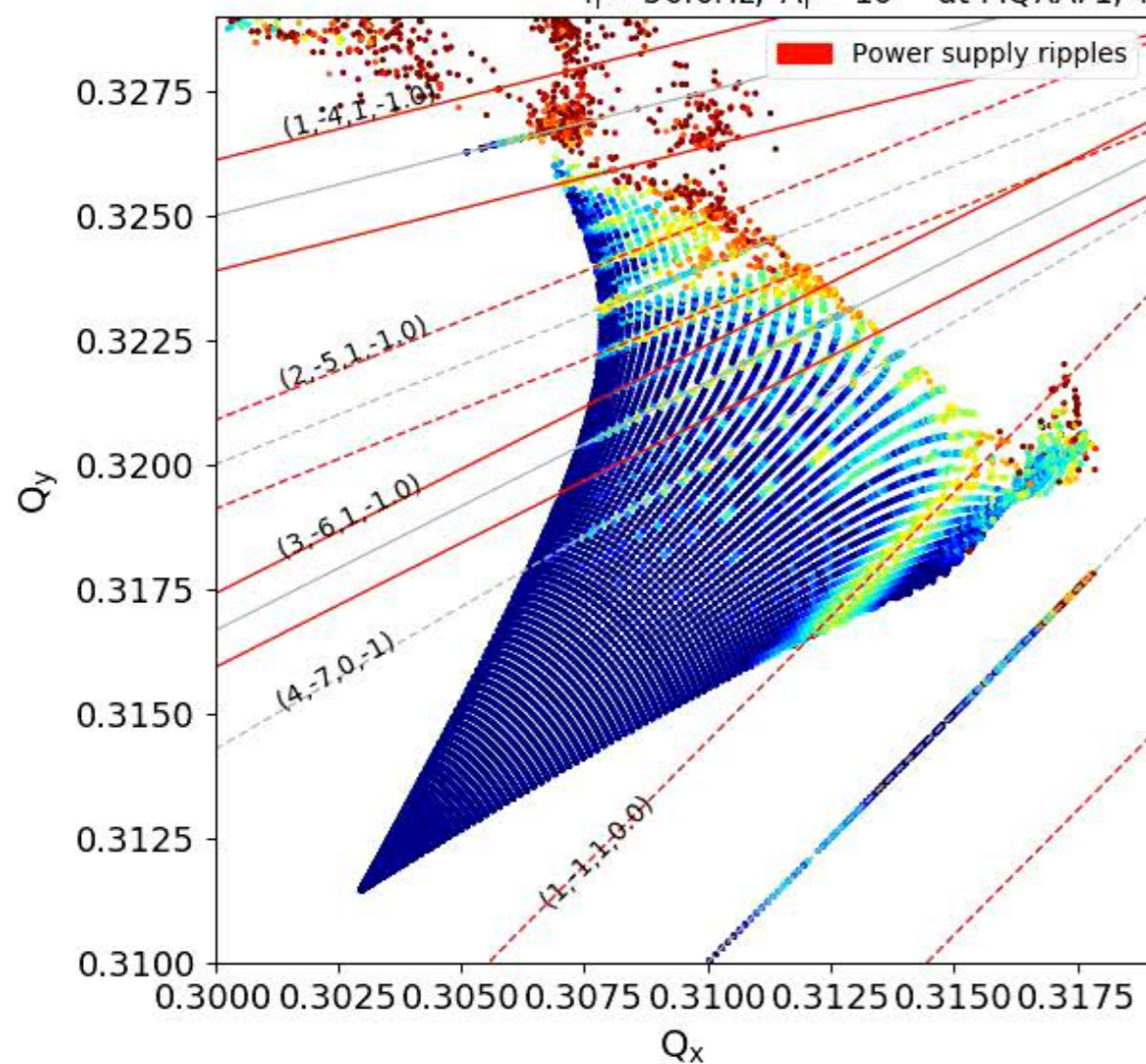




# LHC: Power supply ripples (5D)

□ Scan of different ripple frequencies **(50-900 Hz)**

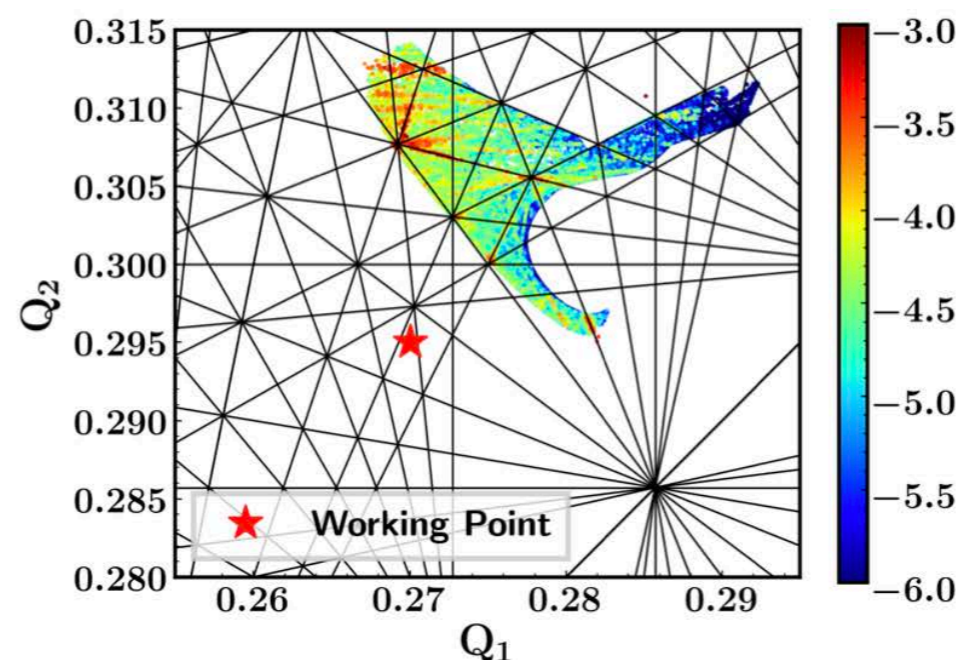
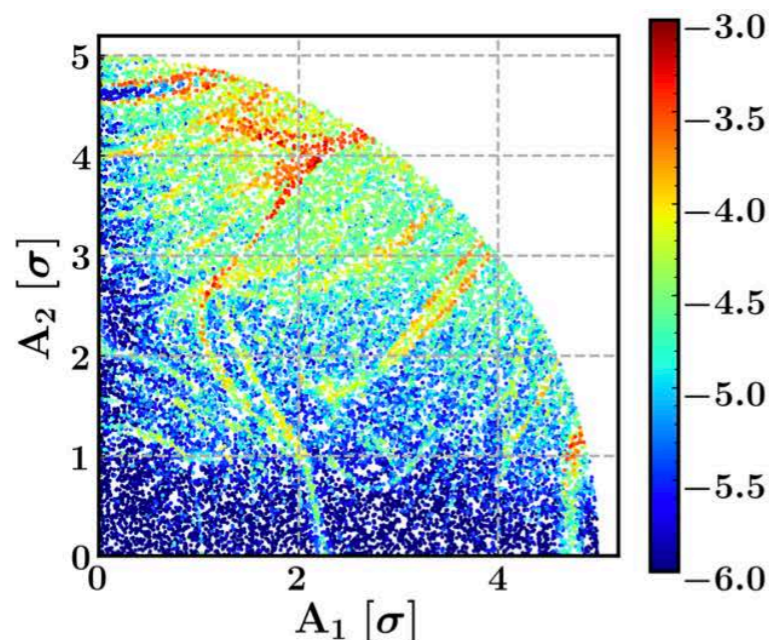
5D,  $E = 6.5\text{TeV}$ ,  $I_{\text{oct}} = 510\text{A}$ , Beam – beam ON,  $\epsilon_n = 2.5\mu\text{m}$ ,  $\beta^* = 40\text{cm}$ ,  $q = 15$   
 $(Q_x, Q_y) = (62.31, 60.32)$ ,  $V_{\text{RF}}$  OFF,  $\delta p = 27e - 5$ , 49 angles,  $0.1 - 6.1 \sigma$ , sliding NAFF  
 $f_r = 50.0\text{Hz}$ ,  $A_r = 10^{-7}$  at MQXA.1, MQXA.3, MQXB.A2, MQXB.B2 of IP1, IP5





# Incoherent e-cloud effects at (HL-)LHC

- Analysis of experimental data from the LHC shows a slow beam degradation due to e-cloud both at injection and in collisions
- A development effort was launched to acquire the ability of simulating the effect of e-cloud forces within a symplectic tracking code over the required long timescales (10M turns). The development included:
  - Theoretical framework
  - Tricubic interpolator in sixtracklib tracking code to apply forces from a recorded pinch in a symplectic way
  - Software infrastructure to simulate and condition the electron pinches and setup the simulation from the MAD-X description of the machine
- Presently capable of simulating 10 M turns (15 minutes of beam time) by exploiting the computational power of GPUs





When you tackle difficult problems,  
you need to invent new methods  
that may be of general use

## Some references

[The chaotic motion of the solar system: A numerical estimate of the size of the chaotic zones](#)

J Laskar  
Icarus 88 (2), 266-291

[Frequency analysis for multi-dimensional systems. Global dynamics and diffusion](#)

J Laskar  
Physica D: Nonlinear Phenomena 67 (1-3), 257-281

[The measure of chaos by the numerical analysis of the fundamental frequencies. Application to the standard mapping](#)

J Laskar, C Froeschlé, A Celletti  
Physica D: Nonlinear Phenomena 56 (2-3), 253-269

[Existence of collisional trajectories of Mercury, Mars and Venus with the Earth](#)

J Laskar, M Gastineau  
Nature 459 (7248), 817-819

[Frequency map analysis and particle accelerators](#)

J Laskar  
Proceedings of the 2003 Particle Accelerator Conference 1, 378-382

[Measuring and optimizing the momentum aperture in a particle accelerator](#)

C Steier, D Robin, L Nadolski, W Decking, Y Wu, J Laskar  
Physical Review E 65 (5), 056506

[Review of single particle dynamics for third generation light sources through frequency map analysis](#)

L Nadolski, J Laskar  
Physical Review Special Topics-Accelerators and Beams 6 (11), 114801

[Global dynamics and long-time stability in Hamiltonian systems via numerical frequency analysis](#)

HS Dumas, J Laskar  
Physical review letters 70 (20), 2975

[Understanding the nonlinear beam dynamics of the advanced light source](#)

D Robin, J Laskar  
AIP Conference Proceedings 391 (1), 15-20